Catalytic reactive distillation for the esterification of propionic acid with n-butanol: Experimental and simulation studies

A Thesis Submitted
to
NATIONAL INSTITUTE OF TECHNOLOGY WARANGAL
For the award of the degree of

DOCTOR OF PHILOSOPHY

in

CHEMICAL ENGINEERING

By

Raju Kalakuntala
Roll No. 701630

Under the guidance of

Dr.S.SRINATH
Associate Professor

DEPARTMENT OF CHEMICAL ENGINEERING
NATIONAL INSTITUTE OF TECHNOLOGY
WARANGAL - 506004, TELANGANA, INDIA.

June-2022.

DECLARATION

I declare that this written submission represents my ideas in my own words and where others' ideas or words have been included, I have adequately cited and referenced the original sources. I also declare that I have adhered to all principles of academic honesty and integrity and have not misrepresented or fabricated or falsified any idea/data/fact/source in my submission. I understand that any violation of the above will be a cause for disciplinary action by the institute and can also evoke penal action from the sources which have thus not been properly cited or from whom proper permission has not been taken when needed.

Raju Kalakuntala
Roll No. 701630

Date:20-06-2022

NATIONAL INSTITUTE OF TECHNOLOGY- WARANGAL

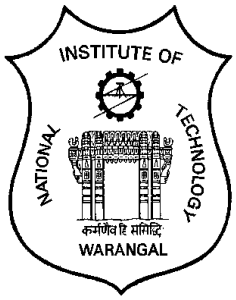

CERTIFICATE

This is to certify that the thesis entitled "Catalytic reactive distillation for the esterification of propionic acid with n-butanol: Experimental and simulation studies" Being submitted by Mr. Raju Kalakuntala for the award of the degree of Doctor of Philosophy (Ph.D) in Chemical Engineering to the National Institute of Technology, Warangal, India is a record of the bonafide research work carried out by her under my supervision. The thesis has fulfilled the requirements according to the regulations of this Institute and in our opinion has reached the standards for submission. The results embodied in the thesis have not been submitted to any other University or Institute for the award of any degree or diploma.

(Dr. S. Srinath)
Supervisor
Associate Professor& HOD
Department of Chemical Engineering,
National Institute of Technology, Warangal.

Date : 20 -06-2022

ACKNOWLEDGEMENT

First and foremost I want to thank my supervisor Dr. S. Srinath. It has been honor to be, his Ph.D. student. He cultivated seed of the research in me and inspired to apply this knowledge not only in laboratories but also in the personal life. His invaluable contributions of time and ideas provides by him during my Ph.D. stay made me wealthy in experiences, which is productive and stimulating in all aspects. He provided me an excellent platform to nourish and grow my professional as well as personal life.

I wish to sincerely thank university authorities, Prof. N.V. Ramana Rao, Director, National Institute of Technology, Warangal and other top officials who gave me an opportunity to carry out research work.

I wish to express my sincere and whole hearted thanks and gratitude to my doctoral scrutiny committee (DSC) members professor Dr. K. Anand kishore, Dr.A.Shirish H Sonawane, professor, Dr. G. Uday baskar Babu, Assistant Professor, Department of Chemical Engineering and, Dr. SrinivasaCharya Professor Department of Mathematics, National Institute of Technology, Warangal for their kind help, encouragement and valuable suggestions for successful completion of research work.

I would like to extend my thanks to all the faculty members in Department of Chemical Engineering for their valuable suggestions and encouragement.

I am also thankful to all the supporting and technical staff of Department of Chemical Engineering who has directly or indirectly helped during the course of my work.

I am thankful to all my fellow research scholars who helped me directly and indirectly to boost my confidence to during my Ph.D.

I take this opportunity to sincerely acknowledge the MHRD Government of India for providing the financial assistance in the form of stipend.

Last but not the least, I would like to thank my Family, who are surely the happiest to see me complete this endeavor. To them, I owe all my accomplishments.

Raju Kalakuntala

ABSTRACT

In any production process for a chemical, the steps involved are reaction, separation, and purification. Reactive distillation is an energy-efficient technology wherein reactions and separations occur simultaneously in a single column. In addition, catalytic reactive distillation technology reduces capital costs and production costs by reducing the number of process units and the direct heat integration between the reaction and distillation process in the presence of a catalyst.

The present study involves the production of butyl propionate over different catalysts in a catalytic reactive distillation column. The performance of selected commercially available cation exchange resins was evaluated in a batch reactor for maximum yield of the desired product, i.e., butyl propionate. The obtained results were compared with the activity of a newly synthesized catalyst to select the best suitable catalyst for maximum conversion of reactants and higher yield of the desired product. The kinetic study is carried out to find a better kinetic model that can be applied in the catalytic reactive distillation process simulation. The kinetic analysis is made in homogeneous catalysts, i.e., P-toluene sulfonic acid and solid cation exchange resin catalysts; Amberlite IR-120 , Indion- 190 and Indion -180 . The kinetic models based on concentration and activity were developed from the first principles for the homogeneous catalyst.

Pseudo homogeneous and adsorption-based kinetic models were developed for the butyl propionate synthesis over prepared solid catalyst. In addition, a novel evaporation rate-based model is developed and applied to model batch reactive distillation. Experiments are conducted in a packed bed batch reactive distillation column under various operating conditions. The simulation results from the evaporation-based model agree with the experimental results.

The present study aims to understand and develop a model for designing catalytic reactive distillation columns by considering the proposed esterification reaction's suitable, accurate kinetic models. First, the developed kinetic model was applied to simulate a continuous reactive distillation column using the robust RADFRAC model in ASPEN PLUS software. Further, the same kinetic model was applied to simulate a new configuration of the reactive distillation column, i.e., reactive divided wall column, to establish optimum parameters for achieving maximum purity and high productivity with minimum energy requirement.

Table of contents

List of Figures

List of Tables

Chapter 1

Introduction

1. Introduction

1.1 Background

Esters can be found in a variety of products, including food, medications, and cosmetics. In 1848, German scientist Leopold Gmelin coined the term "ester," which was most likely derived from the German Essigather, which means "acetic ether"[1]. Each ester compound has a characteristic odour, flavour, and/or scent. As a result, ester compounds are widely employed in food, pharmaceutical (medicine), cosmetic (especially scent) items, solvents, lubricants, plasticizers, and coatings. Hundreds of companies work in the ester compound industry, either through chemical synthesis or natural source recovery [2]. Thousands of different varieties of esters are produced commercially for a range of uses. The simplest and most common method for creating organic esters is the direct esterification reaction between carboxylic acids and alcohols in the presence of a homogeneous or heterogeneous catalyst.

The reaction of acids and alcohols to produce ester and water is known as esterification. A wide range of ester compounds can be derived from a variety of abundant and renewable natural sources, including fruits, vegetables, and plants, making them a low-cost raw material for ester compounds [3]. Natural ester products are frequently much more expensive on the market than synthetic ester goods. Esters produced from natural sources are often acquired by the extraction method, which has drawbacks such as high process costs, periodic supply shortages, and geographical variation in taste quality and quantity[4]. Researchers and businesses have been drawn to the manufacture of esters using an appropriate technique in this scenario. Furthermore, retrieving ester compounds from natural sources is a reasonable solution in terms of cost. Natural-source esters are often found in very low amounts, typically in the parts per million (ppm) range. A solvent is used in extraction to attract the component that has to be separated, and then it must be separated to remove the desired component from the solvent. The solvent will contaminate the final product if the later separation is not done properly, potentially producing substantial toxicity[5]. Distillation is another procedure that is both costly and unsuitable with heat-sensitive items due to its high energy consumption. The inherent characteristics of ester compounds are destroyed at high working temperatures, resulting in oxidation and the conversion of the ester into other molecules. These difficulties motivate and inspire the creation of a safer and more cost-effective approach.

From the manufacture of highly specialised esters in a chemical laboratory to the manufacture of millions of tonnes of commercial ester products, the esterification process has a wide range of uses. These commercial items are produced in either a batch or continuous process. The batch

method employs a single pot reactor that contains the acid and alcohol as reactants. As the reaction progresses, the acid catalyst is added, and the water is withdrawn. This method is primarily used by chemists in the lab, but in a few cases, it is also used in industry to generate huge quantities of esters. This batch approach frequently needs reactors with enormous reactant volumes. Butyl acetate is made from butanol and acetic acid using this method[6]. The continuous synthesis of esters technology was initially invented in 1921 and is currently widely utilised in large-scale ester production. This approach entails mixing streams of reactants into a reaction chamber while simultaneously extracting the result. Continuous esterification has the advantage of manufacturing huge quantities of goods in a short length of time. This process can go on for days or weeks without stopping, but it requires specific equipment and chemical engineering considerations. Continuous esterification is used in industry to produce methyl acetate from acetic acid and methanol, as well as ethyl acetate from acetic acid and ethanol[7]. In the pharmaceutical business, the alternative method of generating esters by reacting an alcohol with an anhydride is critical. An acid is produced as a by-product of this action.

Process intensification is becoming increasingly popular, as it leads to the creation of smaller, cleaner, more energy-efficient technology. Reactive distillation is a good example of process intensification because it combines reaction and separation in one unit. Traditional chemical processing systems that integrate reaction and distillation in a sequential manner are replaced by reactive distillation. Reactive distillation can save capital investment and production costs by reducing the number of process units and allowing direct heat integration between reaction and distillation[8]. Reactive distillation constantly eliminates products from the reaction zone when reactions are equilibrium controlled, significantly increasing overall conversion. By continuously removing products from the reactant mixture, this approach may increase selectivity in some competitive reaction systems. Reactive distillation is an interesting alternative to conventional distillation because of its reduced capital investment, lower energy usage, higher product yields, and purity[9]. Nonvolatile and heat-sensitive chemicals are not suitable for reactive distillation. Fine chemicals and medicinal items are examples of RD products. Despite the fact that the first patent for the reactive separation technique was issued in 1920, little progress was made in the field until 1980. Following this, research into the reactive distillation process has taken the place of traditional reaction-separation unit operations.

The steps involved in any chemical production process are reaction, separation, and purification. One of the separating procedures is distillation. The process of distillation liquid components into desired components consumes a large amount of thermal energy. A reaction,

which requires heat energy, is commonly used to create the combination. If the reaction and distillation procedures are carried out concurrently, the total energy consumption for the reaction and distillation operations can be reduced. The use of catalysts in the distillation apparatus itself can help to intensify the process, which is known as catalytic reactive distillation[10]. The reaction and separation occur concurrently in a packed column containing a solid catalyst, referred to as the reaction section, in a catalytic reactive distillation unit. A rectifying section is located above the reaction area, while a stripping section is located below it.

Reactive distillation equipment is a single column that combines a reactor and a distillation column to conduct several reaction and separation operations by converting reactants into products. The catalytic reactive segment is represented by the presence of the packed solid catalyst in the column[11]. The feed is injected into the column above or below the reactive section, depending on the volatilities of the compound. The products are taken from the column's top or bottom. It avoids the need for further purification or recycling by continuously removing the product. All of these advantages lead to lower energy and capital costs as well as higher conversion rates.

The catalyst should be less volatile in general if a homogeneous catalyst is used. The reactive section of the column is the section of the column below the catalyst feed location when a liquid catalyst is used. When a solid catalyst is employed in the reactive section, it is deposited on trays in tray columns or immobilized in packed columns using various forms of packing. As a result, the reactive zone is defined as the catalyst that is fixed on trays or in immobilized packing's[12]. Incorporating in situ operation into reactive distillation results in complicated interactions between vapor-liquid equilibrium, vapor-liquid mass transfer rates, diffusion limits in the case of heterogeneous catalysts, and chemical reaction kinetics, making design challenging. According to the literature, the reactive distillation technique cannot be employed for endothermic reactions because the vapors inside the reactive zone can condense. When endothermic reactions are used, however, there are no constraints on reactive distillation, which necessitates higher reboiler duty and increases the process' energy demand[13].

One of the example systems considered for this study is the production of butyl propionate through reactive distillation. Butyl propionate is a highly sought-after chemical. It's often used as a thinner in adhesives and as a solvent in paints, dyes, printing inks, and nail polish removers. Butyl propionate is made by esterifying propionic acid and butanol in the presence of liquid or solid catalysts in a liquid state[14]. Some of the most often used liquid catalysts include HCl, HBr, HI, and H2SO4. Amberlyst 15, Amberlyst 16, Amberlyst 35, Amberlyst 36, Indion 130, and Indion

190 are examples of cat-ion-exchange resins used in reactive distillation. In this study, another new catalyst, TI SBA-15, is used. The reaction of propionic acid with n-butanol is shown schematically below.

Propionic acid produces H+, which reacts with OH- to make water. Butyl propionate is formed when the remaining species mix. The esterification reaction is a reversible liquid phase reaction. The equilibrium criterion, which is when the rate of forward reaction equals the rate of backward reaction, determines the maximum conversion of reactants[15]. Without a catalyst, the esterification reaction is very sluggish and takes many days to reach equilibrium. The addition of a catalyst speeds up the reaction rate, allowing the system to reach equilibrium in just a few hours. H+ ions are usually liberated by the catalyst, which catalyze the esterification reaction.

Understanding the behavior of the reactive distillation process would require a mathematical model. However, due of the complex relationship between reaction and distillation, designing, modelling, and controlling reactive distillation is difficult. For the integration of response and separation in a single unit, perfect matching of diverse effects is necessary. It has been observed that if the appropriate processing parameters are chosen, the process can depart from the targeted operation, lowering its efficiency. In order to obtain high conversion and purity, the kinetic rate expression of the reaction, as well as the mass transfer rate between vapour and liquid, are crucial in modelling the reactive distillation process. In the presence of the liquid and solid catalyst, a number of reaction pathways for butyl propionate synthesis have been proposed in the literature.

For the integration of response and separation in a single unit, perfect matching of diverse effects is necessary. It has been observed that if the appropriate processing parameters are chosen, the process can depart from the targeted operation, lowering its efficiency. In order to obtain high conversion and purity, the kinetic rate expression of the reaction, as well as the mass transfer rate between vapour and liquid, are crucial in modelling the reactive distillation process. In the presence of the liquid and solid catalyst, a number of reaction pathways for butyl propionate synthesis have been proposed in the literature. For simultaneous reactive distillation, an evaporation rate based model is created. Experiments are carried out in a reactive distillation column with a packed bed under varied operating conditions. Using the data obtained from the experiments RDWC simulations studies[16].

1.2 Esterification reactions

The esterification process has a wide range of uses, from the generation of highly specialised esters in the laboratory to the manufacturing of millions of tonnes of commercial ester products. These commercial items are made using a batch or continuous technique. The batch approach makes use of a single pot reactor with the acid and alcohol as reactants. The acid catalyst is supplied as the reaction continues, and the water is removed. This approach is often employed by chemists in the lab, but it is also utilised in industry to produce large quantities of esters in a few circumstances. This batch method often necessitates reactors with extraordinarily large reactant contents. Butyl acetate is made from butanol and acetic acid using this method. The continuous synthesis of esters was initially patented in 1921 and is now widely used in large-scale ester production[18]. Mixing streams of reactants into a reaction chamber while simultaneously withdrawing the result is what this method implies. The continuous esterification method has the advantage of being able to manufacture large quantities of goods quickly. This process can continue without interruption for days or weeks, but it necessitates specialised equipment and chemical engineering considerations. In industry, the continuous esterification technique is used to make methyl acetate from acetic acid and methanol, and ethyl acetate from acetic acid and ethanol. The alternate method of producing esters by reacting an alcohol with an anhydride is crucial in the pharmaceutical industry. As a by-product of this process, an acid is formed.

1.3 Heat & mass transfer effects

The amount of reactants transferred from bulk fluid to the surface of catalyst particles is determined by the concentration difference, which is influenced by the velocity pattern of the fluid at the catalyst surface, the fluid's physical qualities, and the intrinsic rate of chemical reactions. While fluid parameters influence mass transfer between the catalyst surface and the fluid, the intrinsic rate is determined by the catalyst characteristics and condition. When it comes to determining the kinetics of a reaction, the diffusion of reactants into the catalyst is crucial. Prior to kinetic studies, it's required to look into reactant diffusion from the bulk phase to the catalyst particle surface, and then from the surface to the particle's interior[19]. The rate at which reactants transfer to heterogeneous catalysts is influenced by external and internal diffusion.

1.4 Mass transfer limitations

The rate of reaction in heterogeneous catalytic reactions is influenced by gas diffusion from the bulk to the catalyst surface (External diffusion) and from the surface to the catalyst interior (Internal diffusion). These diffusion mechanisms operate as resistances, affecting reaction rates, and should not be overlooked. The stages in a porous catalytic particle are depicted in the diagram below[20].

1.5 Significance of reactive distillation (RD)

Chemical reactions and product purification operations are often carried out in sequential order in the chemical industry. Many commercially essential technologies are based on reversible processes that are equilibrium constrained. These equilibrium constrained methods restrict the highest degree of transformation of the reactants into the intended products. The untransformed reactants must be recovered using the appropriate separation technique, and the product must be purified simultaneously. If the degree of transformation in the response stage is smaller, the capital and operating expenses are greater. Economic factors are key motivators in improving chemical processes and facilities. The processes must be strengthened to get high-quality goods, increase output, reduce byproduct production in the process, and reduce energy consumption. To improve the efficiency of the process, extra attention must be paid to developing new unit operations that merge the many activities and units into one. These systems are commonly referred to as hybrid systems, and they are distinguished by lower costs and increasing process complexity. One system is reactive distillation, where reaction and product purification occurs simultaneously. The major benefits of the reactive distillation are as follow:

- The combination of the separation system with the reactor results in capital cost reductions.
- The conversion of reactant is reaching %. This improvement in conversion results in lower recycling costs.
- Side reactions can be prevented by eliminating one of the products from the reaction mixture or maintaining a low concentration of one of the reactants. As a result, the targeted product's selectivity improves.
- For the same amount of conversion, the catalyst required for the process is dramatically lowered.
- When reactants and products produce numerous Azeotropes with each other, reactive distillation proves useful.
- Product production is minimised by immediately removing goods from the reactive zone.
- When the process is exothermic, the heat of reaction can be used to vaporize the components within the column, reducing reboiler duty.
- In reactive distillation, hot spots and runaways may be avoided.

There are several constraints and difficulties, which are listed below.

Reactants and products should have appropriate relative volatilities to maintain high reactant concentrations and low product concentrations in the reaction zone.

Temperature and pressure parameters in the reactor and distillation must be acceptable; otherwise,

improved yield and conversion of the target product cannot be obtained.
If the residence period for the reaction is considerable, large column size and big tray hold-ups are necessary; therefore, using a reactor-separator configuration may be more expensive.
Because of the liquid distribution issue, designing a catalyst-packed reactive distillation column with a high input flow rate is difficult.

1.5.1 Catalytic reactive distillation

Although reactive distillation is not new, it has been used for some notable applications in recent years, and as a result, various aspects of it are being investigated around the world. In particular, continuous reactive distillation processes as an alternative to conventional processes are receiving increasing attention [23]. As a result, a number of strategies for modelling reactive multistage continuous columns have been developed.

The majority of data-driven distillation synthesis investigations have focused on multi-component non-ideal mixtures. The ability to complete equilibrium-limited chemical reactions and the simultaneous separation of reaction products in only one unit are the key advantages of this technique over conventional alternatives. Reactor and recycle costs are reduced or eliminated as a result. The value of reactive distillation processes has increased in process design. They are cost-effective in many circumstances, and they provide a viable alternative to traditional reaction separation procedures.

Chemical reactivity differences between the isomers are exploited in reactive distillation. Because reaction products are continuously removed from the reaction zone, conversion can be improved for beyond chemical equilibrium conversion, especially for equilibrium limited reactions like esterification and ester hydrolysis. It's proven to be a viable process alternative to the traditional reactor-separate setup. In reactive distillation, the chemical reaction usually takes place in the liquid phase or at the surface of the solid catalyst in constant contact with the liquid phase [24].

Designing equipment is challenging for the heterogeneous catalytic packed bed reactive distillation columns. The catalysts used in the process are 0.5-3 mm. large size of the catalyst particles leads to internal diffusion limitation. On the other hand, if the small-sized particles are used, the column may be flooded due to the small void size. So the catalyst particles should be immobilized in the column using the wire gauge envelopes. All the catalyst envelopes are to be packed inside the column. Different kinds of catalyst envelopes are available.

1. The porous spheres are filled with the catalyst inside of the sphere
2. Cylindrical shape envelopes catalyst inside of the cylindrical shape

3. Wire gauge envelopes with different shapes, spheres, tablets, and doughnuts.
4. Horizontally disposed of wire gauge cutters and wire gauge tubes that contain catalyst

1.5.2 Continuous reactive distillation operation

Continuous reactive distillation is a technique that combines continuous distillation with a chemical reaction in one unit. Two important advantages of this technique over conventional alternatives are the capacity to complete equilibrium limited chemical operations and the simultaneous separation of reaction products in only one unit [25]. Reactor and recycle costs are reduced or eliminated as a result. In modern process design, the calculation of reactive distillation has become increasingly significant. A chemical reaction and distillation take place at the same time in reactive distillation, with the chemical reaction taking place in the liquid phase. Reactive distillation is frequently used to separate a close-boiling or azeotropic mixture.

1.5.3 Reactive divided wall column

Reactive dividing wall distillation column (RDWC) is a highly integrated and energy efficient technology. This technology is the outcome of the integration of two integrated technology namely reactive distillation (Integration of Reaction-Separation) and the dividing wall distillation column (Integration of Separation-Separation). The important element that allows such integration of two columns into one single unit is the identical pressure and temperature conditions in the stand-alone columns[26]. The reactive dividing wall distillation column (RDWC) comprises of one condenser, one reboiler, a reactive zone, a pre-fractionator, and the main column in a single shell distillation arrangement. The advantages of RDWC are given as follows:

- Increases yield by reducing the chemical and thermodynamic limitations.
- Increases selectivity by suppressing the undesired consecutive reactions.
- Reduces energy consumption by integrating heat generated in case of exothermic reaction
- With reboiler duty and integrating heat required in case of endothermic reaction with heat released in condenser and this is the goal of the process intensification.
- Reduces the possibility of formation of hot-spots by simultaneous liquid evaporation
- Increases the ability to separate close boiling components by reactions.
- Gives high purity for all the three product streams in one single column.
- Gives thermodynamic efficiency than that for serial column sequence because of the reduced remixing effects with respect to the middle component.
- Shows a reduction in capital and energy cost by reducing the number of equipment units

1.6 Problem statement

This thesis draws attention to the intensification of esterification reaction as its general topic. In this thesis, most of the studies on esterification reaction have focused on the kinetics of reaction. Aside from economic considerations, there are a number of crucial aspects to consider, some of which are interrelated, in order for the esterification reaction to take place. Considering that the esterification reaction is chemically and thermodynamically limited. In addition to addressing the kinetics of esterification reaction, this thesis work attempt to optimize the process conditions of esterification reaction, catalyst development and process intensification by catalytic reactive distillation. The work discussed includes both experimental and modeling studies. In the experimental study, a series of experimental runs of esterification reaction is carried out. The esterification reaction is performed using commercial homogeneous catalyst and commercial heterogeneous catalyst. Subsequently, the development of low cost catalyst for the esterification reaction is attempted. Later to that, the process intensification of esterification reaction by employing catalytic reactive distillation is being carried out. The optimization of process conditions of the esterification reaction using response surface methods is examined in the modelling section. The kinetics of the esterification reaction is then examined at optimal process conditions. With time, the effort became more focused on areas where there were evident process difficulties that might be improved with good chemical engineering application. The esterification experiments were performed at several process variables which include reaction temperature, catalyst loading, molar ratio and reaction time because they have significant effect on esterification reaction. Low cost catalyst is prepared and selected to develop the heterogeneous catalyst for the esterification reaction. The modeling study deals with the process parameters which significantly affect the esterification reaction. In addition, the kinetic modeling is provided to study the kinetics for the esterification reaction.

1.7 Structure of the thesis

The various chapters in the thesis are arranged based on the research objectives achieved in this work. Therefore, this thesis conforms to the "integrated article" format as outlined in the Thesis Regulation Guide by the National Institute of Technology Warangal (NITW).

The introduction, given in **Chapter 1** describes the motivation for the research topic, problems statement, and research objectives. The theoretical background related to the general esterification process (including applications of esterification compounds, selection of acids and alcohols, process variables, selection of catalytic material, reactive catalytic distillation, Continuous reactive distillation, and RDWC) is provided.

A literature review on homogeneous/heterogeneously catalyzed esterification reaction and process intensification of reactive batch distillation is provided in **Chapter 2**.

Chapter 3 presents the materials and methods of the esterification reaction and the reactive batch distillation using the different catalysts. The preparation of the catalyst and its analysis are discussed.

Chapter 4 presents experimental studies in the batch reactor for the esterification reaction and the reactive batch distillation. Kinetic studies for the esterification reaction catalyzed by different catalysts. This chapter is divided into five sections.

In the first section, the experimental study of the activity of selected commercial ion exchange resins for esterification kinetics of propionic acid with n-butanol in a batch reactor.

The second section of the chapter discusses the performance evaluation of synthesis mesoporous catalyst (Ti SBA-15@SO3H) and evaluates the performance of the esterification process.

The third section of the chapter discusses the development of kinetic models for the best suitable catalyst using experimental data from a batch reactor.

The fourth section of the chapter discusses the Experimental and simulation studies of catalytic batch reactive distillation for esterification of propionic acid with n-butanol. Using the mesoporous catalyst (Ti SBA-15@SO3H)

The fifth section of the chapter discusses the Modelling and simulation of continuous reactive distillation and reactive divided wall column for esterification of propionic acid with n-butanol over mesoporous catalyst.

Chapter 5 summarizes the principal conclusions of this thesis and provides recommendations for future research directions based on the findings of this research.

References:

[1] R. Taylor, R. Krishna, Modelling reactive distillation, Chem. Eng. Sci. 55 (2000) 5183–5229. https://doi.org/10.1016/S0009-2509(00)00120-2.

[2] P. Meena, R.K. Dohare, K. Singh, V.P. Singh, S. Upadhyaya, M. Agarwal, A review: control of reactive diviMeena, Priyanka, et al. "A Review: Control of Reactive Divided Wall Distillation Column." International Journal of Advanced Technology and Engineering Exploration, vol. 4, no. 27, 2016, pp. 28–36, doi:10.19101/ijatee.2017, Int. J. Adv. Technol. Eng. Explor. 4 (2016) 28–36.

[3] B.A.N.N. Bamunusingha, E.C.L. de Silva, M.Y. Gunasekera, Performance of ion exchange resin as solid catalyst for the esterification of acetic acid with ethanol, J. Natl. Sci. Found. Sri Lanka. 44 (2016) 83–93. https://doi.org/10.4038/jnsfsr.v44i1.7985.

[4] S. Hernández, J.G. Segovia-Hernández, L. Juárez-Trujillo, J.E. Estrada-Pacheco, R. Maya-Yescas, Design study of the control of a reactive thermally coupled distillation sequence for the esterification of fatty organic acids, Chem. Eng. Commun. 198 (2011) 1–18. https://doi.org/10.1080/00986445.2010.493102.

[5] H. Sciences, 済無No Title No Title No Title, Chem. Eng. Sci. 4 (2016) 1–23.

[6] Y. Li, S. Han, L. Zhang, W. Li, W. Xing, Fabrication and modeling of catalytic membrane for removing water in esterification, J. Memb. Sci. 579 (2019) 120–130. https://doi.org/10.1016/j.memsci.2019.02.063.

[7] N. Redondo, M.L. Dieuzeide, N. Amadeo, ACID REMOVAL FROM CRUDE OILS BY CATALYTIC ESTERIFICATION NAPHTHENIC ACID CATALIZE BY Mg/Al HYDROTALCITE, Catal. Today. (2019) 0–1. https://doi.org/10.1016/j.cattod.2019.09.051.

[8] K. Raju, G.U.B. Babu, S. Surnanai, Heat and Mass Transfer Limitations in Esterification of Propionic Acid Over Ion Exchange Resin, Proc. Acad. 16th Int. Conf. (2018) 4–7.

[9] M. Banchero, R.D. Kusumaningtyas, G. Gozzelino, Reactive distillation in the intensification of oleic acid esterification with methanol - A simulation case-study, J. Ind. Eng. Chem. 20 (2014) 4242–4249. https://doi.org/10.1016/j.jiec.2014.01.027.

[10] M. Mallaiah, G.V. Reddy, Kinetic Study of Esterification of Acetic Acid with Methanol Over Indion 190 Acidic Solid Catalyst, Кинетика И Катализ. 56 (2015) 421–429. https://doi.org/10.7868/s0453881115040127.

[11] N. Asiedu, D. Hildebrandt, D. Glasser, Experimental Simulation of Three-Dimensional Attainable Region for the Synthesis of Exothermic Reversible Reaction: Ethyl Acetate Synthesis Case Study, Ind. Eng. Chem. Res. 54 (2015) 2619–2626.

https://doi.org/10.1021/ie503276s.

[12] V.S. Chandane, A.P. Rathod, K.L. Wasewar, P.G. Jadhav, Response Surface Methodology and Artificial Neural Networks for Optimization of Catalytic Esterification of Lactic Acid, Chem. Eng. Technol. 43 (2020) 2315–2324. https://doi.org/10.1002/ceat.202000041.

[13] Y. Cho, B. Kim, D. Kim, M. Han, [doi 10.1109_2Ficcas.2008.4694294] Youngmin Cho, _ Bokyung Kim, _ Dongpil Kim, _ Myungwan Han, -- [IEEE 2008 International Conference on Control, Automation and Systems (ICCAS) - Seoul, South Korea (2.pdf, (2008) 2596–2599.

[14] D. Seth, A. Sarkar, F.T.T. Ng, G.L. Rempel, Uncertainties in the simulation of catalytic distillation process: A systematic grid refinement study, Chem. Eng. Sci. 60 (2005) 5445–5457. https://doi.org/10.1016/j.ces.2005.04.036.

[15] F. Aiouache, S. Goto, Reactive distillation-pervaporation hybrid column for tert-amyl alcohol etherification with ethanol, Chem. Eng. Sci. 58 (2003) 2465–2477. https://doi.org/10.1016/S0009-2509(03)00116-7.

[16] S. Hernández, R. Sandoval-Vergara, F.O. Barroso-Muñoz, R. Murrieta-Dueñas, H. Hernández-Escoto, J.G. Segovia-Hernández, V. Rico-Ramirez, Reactive dividing wall distillation columns: Simulation and implementation in a pilot plant, Chem. Eng. Process. Process Intensif. 48 (2009) 250–258. https://doi.org/10.1016/j.cep.2008.03.015.

[17] P.A. Turhanen, J. Leppanen, J.J. Vepsalaïnen, Green and efficient esterification method using dried Dowex H+/NAI approach, ACS Omega. 4 (2019) 8974–8984. https://doi.org/10.1021/acsomega.9b00790.

[18] W.T. Liu, C.S. Tan, Liquid-phase esterification of propionic acid with n-butanol, Ind. Eng. Chem. Res. 40 (2001) 3281–3286. https://doi.org/10.1021/ie001059h.

[19] M.-J. Lee, J.-Y. Chiu, H. Lin, Kinetics of Catalytic Esterification of Propionic Acid and n -Butanol over Amberlyst 35 , Ind. Eng. Chem. Res. 41 (2002) 2882–2887. https://doi.org/10.1021/ie0105472.

[20] M. Mekala, V.R. Goli, Kinetics of esterification of methanol and acetic acid with mineral homogeneous acid catalyst, Chinese J. Chem. Eng. 23 (2015) 100–105. https://doi.org/10.1016/j.cjche.2013.08.002.

[21] A. Shahid, Y. Jamal, S.J. Khan, J.A. Khan, B. Boulanger, Esterification Reaction Kinetics of Acetic and Oleic Acids with Ethanol in the Presence of Amberlyst 15, Arab. J. Sci. Eng. 43 (2018) 5701–5709. https://doi.org/10.1007/s13369-017-2927-y.

[22] M. Weerasinghe, J. Wilkie, D.A. Mammant, A. Diez-Lazaro, M.L. Hitchman, Modelling and Simulation of a Laboratory Scale Esterification Process, IFAC Proc. Vol. 33 (2000) 1037–1042. https://doi.org/10.1016/s1474-6670(17)38677-9.

[23] C.E. Transactions, Simulation of Middle Vessel Batch Reactive Distillation Column : Application to Hydrolysis of Methyl Lactate Simulation of Middle Vessel Batch Reactive Distillation Column : Application to Hydrolysis of Methyl Lactate, (2015). https://doi.org/10.3303/CET1229100.

[24] D.Y. Aqar, N. Rahmanian, I.M. Mujtaba, Feasibility of integrated batch reactive distillation columns for the optimal synthesis of ethyl benzoate, Chem. Eng. Process. Process Intensif. 122 (2017) 10–20. https://doi.org/10.1016/j.cep.2017.08.012.

[25] A. Niesbach, N. Fink, P. Lutze, A. Górak, Design of reactive distillation processes for the production of butyl acrylate: Impact of bio-based raw materials, Chinese J. Chem. Eng. 23 (2015) 1840–1850. https://doi.org/10.1016/j.cjche.2015.08.019.

[26] I. Dejanović, L. Matijašević, Ž. Olujić, Dividing wall column-A breakthrough towards sustainable distilling, Chem. Eng. Process. Process Intensif. 49 (2010) 559–580. https://doi.org/10.1016/j.cep.2010.04.001.

Chapter 2

Literature Survey

2. Literature Survey

A literature review on homogeneous/heterogeneously catalyzed esterification reaction and process intensification of reactive batch distillation is presented.

2.1 Reaction kinetics

At higher temperatures, the esterification of organic acid and alcohol is slower without a catalyst. The presence of the catalyst frequently speeds up the reaction. The reactions could take place with either homogeneous or heterogeneous catalysts present. Mineral acid catalysts such as HI, HCl, HBr, and H2SO4 are homogeneous catalysts. These catalysts accelerate the acid-alcohol reaction, causing an ester to develop. Solid catalysts for esterification, etherification, alkylation, metathesis, and trans-esterification processes are ion-exchange resin catalysts.

2.1.1 The kinetics of esterification of the propionic acid and n-butanol in the presence of solid catalysts

Johanna Lilja [1] have studied heterogeneous fiber catalyst for esterification reactions. Esterification of the chemical reactions catalyzed employing fiber catalyst was discussed. These catalysts are also used in a few industrially important procedures, according to the authors. In esterification reactions, for example, the polymer-supported sulphonic acid catalyst Smopex-101 (Smoptech Ltd., a Johnson Matthey employer) was used, and the esterification kinetics were studied. Within the presence of these catalysts, the selectivity of a few chemical reactions became progressed.

Sami H.Ali [2] has developed the fee expression for the Dowex 50 catalyst for the esterification reaction of propionic acid. Dowex 50 ion-change resins are used in industrially sizeable chemical techniques. They discussed the significance of each external and internal diffusion boundary at the esterification gadget. They mentioned approximately the specific kinetic fashions and tested with the experimental information. Alime et al [3] have studied the kinetics of the propionic acid with isobutyl alcohol in presence of the heterogeneous catalyst (Amberlyst 36 and Amberlyst 70) in a batch reactor. The results of stirrer pace, reactant awareness and the temperature on the response price were provided.

Angela silva et al.[4] have studied Nb2O5/SBA-15 catalyst for esterification response. The mesoporous catalyzed kinetics for the synthesis of butyl propionate. They synthesized the cost-effective catalyst for the esterification reaction. They experimented at distinctive temperatures and

catalyst concentrations in a batch reactor. Experiments were done to find the equilibrium constants. They look into the potential of SBA-15 supported niobium for the esterification of propionic acid as a version response to evaluate its potential for manufacturing butyl propionate and related structure-feature relationships consisting of butyl propionate and related structure-feature relationships consisting the importance of Bronsted-Lewis individual in dictating activity.Fernando levya et al. [5] studied the response kinetics of liquid esterification of propionic acid and iso-amyl alcohol to synthesize butyl propionate in a batch reactor one after the other. The kinetic parameters have been calculated using statistics from a batch reactor. In addition, the applicability of the derived kinetics was investigated using reactor experimental consequences.

Wen-Tzong Liu et al. [6] explored the kinetics of the liquid-phase esterification of n-butanol with propionic acid catalysed by cation alternative resins, as well as more design records for the reactive distillation system of making n-butyl propionate. They checked out a kinetic model that may be used for any response aggregate beginning composition. The kinetic expression evolved by evaluating experimental data with numerous fashions derived from the Langmuir-Hinshelwood and Eley-Rideal theories' standards. We calculated the equilibrium regular, activation strength, and heat of reaction.

Ming-Jer Lee et al. [7] have studied the catalytic esterification of propionic acid with n-butanol with the aid of Amberlyst 35 as a heterogeneous catalyst inside the temperature range 353.15K-393.15 ok and at atmospheric stress. The kinetic facts of strong catalytic esterification are related to the Q-H, L-H, E-R, and modified L-H patterns in this observation throughout a wide range of temperatures and feed compositions. In the kinetic models, the temperature and feed composition variables are covered.

Over Amberlyst 15, Sami H.Ali [8] was worked on esterification of propionic acid with exceptional alcohols. Using a float-type experimental setup, the kinetics of the reaction between propionic acid and a variety of alcohols (methanol, ethanol, and 1-butanol) were studied under various reaction circumstances. It has been validated that this has a high pastime for the production of various esters. The UNIFAC institution contribution version was applied to account for gadget non-ideality, and the acquired experimental records were suited for P-H, L–H, E–R, and P-P fashions.

Yu-Ting Tsai et al. [9] have performed the experiments on the esterification of propionic acid and methanol for methyl propionate in a packed bed reactor in the presence of the Amberlyst 36

catalyst. The adsorption constants, equilibrium constants, dispersion constants, and reaction constants have been discovered for the reversible response. For the esterification reaction, a pseudo-homogeneous kinetic model was built. They determined that the expected parameters could accurately expect experimental findings from batch and plug glide reactors.

Ajit P.Rathod et al. [10] investigated the use of a homogeneous catalyst to improve the esterification kinetics and chemical equilibrium for the synthesis of butyl propionate in a batch reactor. Experiments with and without pervaporation on the esterification of propionic acid with isopropanol were carried out. The impact of several parameters on the overall performance of the pervaporation reactor, such as the beginning mole ratio of isopropyl alcohol over propionic acid, system temperature, and catalyst concentration, was also investigated.

Ajit P.Rathod et al. [10] have studied to enhance the esterification kinetics and chemical equilibrium for the synthesis of butyl propionate inside the batch reactor using a homogeneous catalyst. Experiments on the esterification of propionic acid with isopropanol with and without pervaporation were executed. Furthermore, the effect of various parameters on the overall performance of the pervaporation reactor became additionally studied, including the starting mole ratio of isopropyl alcohol over propionic acid, system temperature, and catalyst concentration.

Rajendra B Bhandare et al. [12] have studied the synthesis of iso-amyl propionate with the aid of esterification of propionic acid with iso-amyl alcohol using ion trade resin Amberlyst-15. They work on the packed bed to explore the opportunity to apply the packed bed to synthesize isobutyl propionate.

Anurag Tiwari [13] used a solid carbon-based acidic catalyst manufactured from rice husk char, which has a large specific surface area, in combination with a commercial catalyst called Dowex 50Wx8-400 to examine the esterification of propionic acid and ethanol. They studied the influence on temperature, the effect of molar ratio, and the effect of catalyst loading in addition to their homes. The reaction surface method optimization was used to look at the overall results..

Anita Bhatia [14] has studied solid catalysts to synthesize isobutyl propionate from stable waste catalysts from esterification of propionic acid and isobutyl alcohol. Develops a creative support material Fly ash, a solid waste created by electricity flora and high in silica, is used to synthesize NAFA Catalyst, which has an extensive range of packages inside the synthesis of Isobutyl Propionate (RUM), that's used in the meals and beverage sectors. This catalyst can also be utilized to make extra esterification merchandise, including meal preservatives and prescription drugs.

J lilja et al. [15] have mentioned approximately the kinetics of propionic acid esterification with methanol was investigated inside the presence of a fibrous polymer-supported sulphonic acid catalyst in addition to a fashionable resin catalyst. The study reveals that a fibrous polymer-supported sulphonic acid catalyst may be used to esterify propionic acid with methanol and construct a superior kinetic version for the esterification. To compare Amberlyst 15's hobby to Smopex-101, reference studies have been carried out underneath comparable settings with Amberlyst 15. Smopex-101 sturdiness becomes evaluated through re-using it in different assessments.

Beyhan Erdem et al. [16] used Macroporous (Amberlyst-15) and Microporous (Dowex 50 W and Amberlite IR-120) polymeric ion-exchange resins to investigate the esterification of n-amyl alcohol with propionic acid at temperatures ranging from 333 to 348 ok. They investigated the use of Macroporous and gel resins in the esterification of propionic acid and n-amyl alcohol. This esterification reaction was chosen because n-Pentyl propionate is an innocuous evaporating solvent with a linear structure that contributes to excellent viscosity reduction and is employed in meal additives, cleaning fluids, perfume solvents, and printing inks.
The kinetics of the liquid-phase esterification of n-butanol with propionic acid catalysed by cation trade resins, as well as the layout statistics for the reactive distillation approach of generating n-butyl propionate, were explored. They looked into a kinetic model that might be used to simulate any response mixture starting composition. By comparing experimental data to a range of models derived from the Langmuir-Hinshelwood and Eley-Rideal theories, the kinetic expression is enhanced. The steady state equilibrium, activation power, and heat of reaction were all calculated.

S.N Kane et al. [17] investigated the synthesis of propanol. Consistent with GC, IR, and 1H-NMR spectrometers, propionic acid can be esterified with methanol (3:4) using a sulfuric acid catalyst to produce methyl propionate as a prime factor with a yield of seventy five%. In addition, the sodium metal was found to convert methyl propionate to methanol and 1-propanol.

2.1.2 Reactive distillation column

Reaction kinetics are important in column modeling and design in reactive distillation. There are various kinetic models for modeling reactive distillation processes in the literature. Reactive distillation processes require detailed models that can predict process behavior. To obtain experimental results, several authors conducted experiments in reactive distillation columns to synthesize butyl propionate in the presence of liquid and solid catalysts.

Andres F. martnizr [18] presented the kinetic modeling of the liquid-phase esterification of isobutyl acetate. First, the effects of internal and exterior mass transfer phenomena were assessed in preliminary experiments, and they were ruled out using the Weisz–Prater criterion. Then they considered specific development studies for the esterification of isobutyl alcohol and acetic acid.

Yachun Chen et al [19] investigated a three-stage catalytic reactive distillation (RD) column with an integrated chemical reaction and distillation process for the continuous production of caprolactam. They developed a mathematical model for the esterification reaction. Thermodynamic characteristics and reaction kinetics of this process, a steady-state simulation of RD column was carried out with the process simulator Aspen Plus.

The steady state optimization and dynamic control of the RDWC process for the synthesis of AmAc. The steady state economics are evaluated by comparing the optimal TACs of these processes, and three control schemes have been put forward to implement the robust control was published by Qingrui Zhang et al.[20] . The vapors split ratio control structure is designed, and a novel comprehensive analysis including the vapors flow rate and conversion were applied to the analysis of the dynamic response results.

Kreul et al. [21] suggested a rate-based model based on the Maxwell-Stefan technique for simulating the mass transfer component of RDC. The total model takes into account hydrodynamic factors, diffusion effects, reaction kinetics, and thermodynamic non-idealities in column performance. The ODEs are represented step by stage in the model and solved. In a semi-continuous operation, a series of studies were carried out in a pilot plant size reactive distillation column of three meters height. When the experimental findings were compared to the model results, it was discovered that the model could predict experimental data.

In the presence of a cation-exchange resin, 1,3-dioxolane was made from ethylene glycol and formaldehyde. Shubham H et al. [22] investigated the reaction in batch mode, semi-batch reactive distillation mode, and a continuous reactive distillation column. In a semi-batch reactive distillation mode, ethylene glycol was extracted from aqueous solutions using a reaction kit with solid paraformaldehyde.

The esterification of an aqueous solution of acetic acid with n-butanol/iso-amyl alcohol is a reversible reaction, according to B Saha et al. [23]. Because there is an excess of water in the reaction mixture, the conversion is severely limited by equilibrium constraints.

Popken et al. [24] used a structured catalytic packing in a packed bed reactive distillation to explore the generation and hydrolysis of methyl acetate. Katapak was used to fill the structural packaging. -S. Amberlyst 15 acid catalyst ion exchange resin. They used single-feed and double-feed column topologies for methyl acetate synthesis and double-feed configurations for methyl acetate hydrolysis in their research. The RADFRAC model from the commercial Aspen Plus programme was used for all simulations. The effect of numerous factors such as residence time distribution, heat loss, and packing separation efficiency was investigated. They discovered that when reaction kinetics based on an adsorption model, heat loss, and separation efficiency were included, the equilibrium stage model provided a good forecast near the experimental data.

Schneider et al. (2001) have developed a two-film theory-based mathematical model for a semi-batch reactive distillation column. The experimental data under varied situations were used to validate the model.

Horstmann et al. [25] investigated the vapors liquid equilibrium and excess enthalpy data for binary systems needed to design reactive distillation for methyl acetate production. The temperatures of mixing were determined using a commercial isothermal calorimeter. The temperature-dependent UNIQUAC model was fitted to the experimental data by the authors.

Gorak and Hoffmann [26] investigated the catalytic distillation of methyl acetate utilizing structured packing's. They conducted tests in the reactive distillation column to investigate the properties of the Multipak structured packing, such as pressure drop, loading, and separation efficiency. The Aspen custom modular environment has been used to build the non-equilibrium stage model. The simulated findings were compared to the experimental data for the methyl acetate synthesis. They discovered several discrepancies between the experimental data and the modeling results.

Noeres et al. [27] used Multipak structured packing in reactive distillation to undertake dynamic studies for methyl acetate production in a pilot plant scale column. A dynamic mass transfer rate model was created. The model accounted for hydrodynamic phenomena such as liquid back mixing, liquid holdup, pressure loss, and response kinetics. A rigorous control structure selection procedure was followed. They discovered that linear control performs better over various operational situations.

Singh et al. [28] used the stochastic continuation approach to investigate the potential of numerous stable states in a reactive distillation process model. The industrial products MTBE and methyl acetate were subjected to the continuation approach. They detected three stable states overall in kinetically regulated and equilibrium controlled regimes of methyl acetate synthesis at a fixed reflux ratio and reboiler duty.

Singh et al. [29] investigated acetic acid recovery using an ion-exchange resin catalyst to esterify dilute acetic acid with methanol in a reactive distillation column. The experiments were carried out in a batch reactor, and a kinetic expression was developed as a result. Under some conditions, the insensitivity of reaction rate to catalyst loading was considered. Experimentally, the influence of several factors such as feed flow rate, reboiler duty, and feed composition was investigated. The equilibrium stage model accurately predicted the reactive distillation well's performance. The model predictions accord well with the experimental data. The authors also proposed several plausible alternative setups for full dilute acetic acid recovery.

Singh et al. [30] presented the construction of a reactive distillation column for recovering acetic acid from dilute acetic acid esterification with methanol. The one-parameter continuation approach was used to vary the parameters such as feed molar ratio, feed position, reflux ratio, and Reboil ratio, and the best feasible configuration was given. They discovered that the system is very nonlinear and that several stable states are attainable.

Kumar and Kaistha [31] investigated the effect of stable sate multiplicities on the reactive distillation column's management of a simulated industrial-scale methyl acetate process. In addition, the authors examined the significance of input-output relationships in control system design and the dynamic nature of the RD process.

Rahul et al. [32] created a fast approach for solving the set of differential and algebraic equations that describe the dynamics of a reactive distillation column. They analyzed the rate of change of specific enthalpy on each equilibrium stage/tray to the methyl acetate process. They discovered that the devised technique outperformed previous algorithms in computing speed for solving RD column differential and algebraic models.

Sandesh et al. [33] used an ion-exchange resin catalyst in a packed bed reactive distillation column to make methyl acetate from acetic acid and methanol's liquid phase esterification process. The ion exchange resin catalyst was Indion190. Based on the concentration of methyl acetate in the

top product, the performance of the reactive distillation column was studied. The process's steady-state and unstable behaviour are modelled, and the results are confirmed with experimental data. The effect of process parameters such as reboiler temperature, feed location, catalyst loading, feed molar ratio, feed flow rates, enriching section temperature, and reactor temperature was also investigated, and optimal values were discovered.

Using a reactive distillation column, Saha et al. [34] explored the esterification of dilute acetic acid with n-butanol/isoamyl alcohol. The catalyst was Indion 130, which was housed in stainless steel wire cages. The studies were carried out to determine the best column configurations for synthesizing isoamyl acetate and n-butyl acetate. In addition, the influence of several operational parameters on reactive distillation column was explored, including feed flow rate, reflux ratio, feed position, reactant mole ratio, and reactive zone length.

Hiwale et al. [35] investigated reactive distillation's industrial uses. They explained the many sorts of reactions that are feasible with the reactive distillation process.Almeida-Rivera et al. [36] evaluated the design of the reactive distillation process and proposed optimal design requirements and existing and future reactive distillation directions.Schmitt et al. [37] conducted experiments in a reactive distillation column to produce n-hexyl acetate in the presence of a heterogeneous catalyst. Experiments were carried out in the laboratory and on a pilot plant scale using various catalytic packing. The effect of different essential factors on column performance was investigated. We measured phase equilibrium, chemical equilibrium, and reaction kinetics. They described the reactive distillation method based on the reaction kinetics and thermodynamic parameters.

Kumar et al. [38] report a unique reactive distillation technique that combines esterification, distillation, and hydrolysis into a single unit. The pseudo homogeneous model was used to determine kinetic parameters such as activation energy and rate constants. An equilibrium stage model was created for the batch reactive distillation column. The simulation's conclusions are compared to the results of the experiments. The influence of different factors on lactic acid conversion was addressed, including feed mole ratio, boil-up ratio, catalyst loading, and feed concentration.

Calvar et al. [39] studied the kinetics of acetic acid esterification with ethanol to create ethyl acetate, which was catalyzed both homogeneously by acetic acid and heterogeneously by Amberlyst15. The experimental data were correlated using the pseudo homogeneous model. They

also performed reactive distillation studies under various operating circumstances, such as varied feed rates and reflux ratios, to extract ethyl acetate in a heterogeneous catalyst.

Tavan and Hosseini [40] used the reactive distillation column model in HYSYS simulation software to investigate the manufacture of high purity ethyl acetate. A unique arrangement for a single reactive distillation column was presented, with reactive distillation and rectifier components separated. In order to find the ideal process conditions in terms of energy demand, the effect of reactant flow rate, reaction stages, and feed position were investigated in the column. Avami [41] investigated the feasibility of operating parameters for a double feed RD using pinch point map analysis for the middle section and the feed angle method as a shortcut design. The process was used to make methyl acetate and ethyl acetate.

The following aspects have been suggested as future study areas in reactive distillation based on the literature review. The effect of catalyst loading on the reaction rate constant was studied using a phenomenological model rather than a correlation, and simultaneous reactive distillation could be investigated in a simple distillation apparatus for the production of butyl propionate in the presence of a solid catalyst. Under varied parametric settings, the start-up procedure of the continuous reactive distillation column and its approach to steady-state may be studied, and the model for the synthesis of butyl propionate could be developed.

2.1.3 Reactive divided wall column

Huss et al. [42] discussed the computer-aided tools for conceptualizing a reactive distillation column to produce methyl acetate from methanol and acetic acid. The authors carried out a survey of available techniques and emphasized the geometric methods for the design. They pointed out the opportunities for further research. In the geometric method, they used a simple equilibrium model, which acts as a starting point for designing the kinetically controlled reactive distillation process.

Patil et al. [43] found that the RDWDC has been a prominent example of process intensification. RDWDC is the result of integrating the reactive distillation process with a dividing wall column. Their paper used a novel approach for the design of RDWDC, and the methodology of design is based on the graphic-based boundary value method (BVM). The reaction system is analyzed with four components in one reaction. Chemical equilibrium is assumed at14 each stage. In addition, they developed the cost function for ranking the design from several other designs proposed in the design procedures.

Mueller and Kenig [44] expressed the need for rate-based modeling and simulation. They discovered that assuming the vapor-liquid streams leaving the tray are in equilibrium does not give an accurate result because separation depends on the rate of mass transfer from the vapour to the liquid phase, and these rates are further dependent on how far the vapour and liquid streams deviated from equilibrium. To overcome this problem, generally, efficiencies are used in the case of tray columns and height equivalent to a theoretical plate (HETP) in the case of a packed column. Since the efficiency varies from tray to tray in a tray column and HETP varies with the height in a packed column, the calculated results deviate from the actual results in both cases. Therefore the rate-based approach is needed to model the RDWDC by earlier investigators. This model was applied to a non-reactive ternary alcohol mixture in an RDWDC, and the results were successfully validated. Besides high conversion, the selectivity was found to be low. It was proved that this selectivity can be increased by integrating the dividing wall column with reactive distillation yielding the RDWDC.

Mueller and Kenig [45] considered the transesterification of carbonates, modeled this system with a rate-based approach, and carried out the ASPEN Custom Modeler simulation environment. They divided each packing section into smaller segments (stages), and each stage was described with a film model. Their work gave special attention to both 15 the heat transfer through the dividing wall, and the vapor flow rate split below the wall. As a result, the results obtained are more accurate and clearly validated by the experiment result.

Rodrigo et al. [46] used the Aspen plus and Aspen dynamics process simulators to design and implement an RDWDC. They employed a reflux valve to adjust the distillate composition and temperature in the packed portion in this setup. They also use a reboiler in the lower section of the column to manage the composition of the bottom product as well as the temperature of the reboiler, which is heated with heat duty. This design is simulated by using steady-state and dynamic simulation. They found that the steady-state simulation predicted minimum energy consumption more efficiently.

Gabriel et al. [47] used a multi-objective genetic algorithm for the optimized design of the RDWDC for producing biodiesel. Biodiesel production is carried out by esterifying laurie acid and methanol using sulfuric acid as a catalyst. This catalyst is processed in thermally coupled distillation sequences with the side stripper. The result showed that the biodiesel obtained from the above-explained unit operation is high purity diesel oil, resulting in a drastic decrease in the energy consumption for the column.

Delgado et al. [48] reviewed the previous research on the RDWDC has been presented. They concluded that although much research was carried out in the early 1949's on thermally coupled distillation columns, the actual application of this column was significantly reported in the 1980's when the reactive dividing wall column came into existence. Therefore, in the present work, they carried out experiments to produce ethyl acetate using RDWDC. The results obtained were compared with ASPEN ONE ASPEN plus simulator simulation results.

Gabriel et al. [49] developed a novel biodiesel manufacturing process using fatty acid methyl esters (FAMEs) in a reactive dividing-wall distillation column (RDWDC) that requires just 15% more methanol to completely convert the fatty acid feedstock. The design is a tough global optimization problem with discrete and continuous choice factors. The optimal arrangement was created using MATLAB, which was then paired with rigorous simulations in ASPEN Plus and the FAME manufacturing system. They demonstrated that this design approach consumes 25% less energy and requires 25% less equipment than traditional processes.

Tavan and Hosseini [50] studied dimethyl ether production from the dehydration of methanol in the RDWDC. With the help of ASPEN HYSYS software, they analyzed the process's cost and compared it with the other processes available in the literature. They have shown that using a reactive dividing wall distillation column, the operating cost is reduced by 44.53 % as compared to the conventional distillation column, while both schemes predict almost the same output specifications.

Ignat and Kiss [51] produced the optimal design and worked on the dynamics and control of the RDWDC. Based on RDWDC technology, they proposed an efficient control structure for a biodiesel process. Computer-aided process engineering (CAPE) tools ASPEN Tech, ASPEN Plus, and ASPEN Dynamics were utilised to run rigorous steady-state and dynamic simulations and optimise the RDWDC for the biodiesel process. They also discovered that using an alcohol vapour feed was necessary to meet the product criteria. The sensitive trays for inferential temperature control were found using singular value decomposition (SVD).

2.4. Objectives of the study

Based on the literature survey and the gaps identified it is proposed to study the performance of commercial cation exchange resins and synthesized catalyst for esterification of propionic acid with butanol in in a batch reactive distillation and to simulate the performance using Aspen Plus simulation for divided wall reactive distillation process with the following objectives:

1. To study the activity of selected commercial ion exchange resins for esterification kinetics of propionic acid with n-butanol in a batch reactor.
2. To synthesize mesoporous catalyst and to evaluate the performance for esterification process
3. To develop kinetic models for the best suitable catalyst using experimental data from a batch reactor.
4. Experimental and simulation studies of catalytic batch reactive distillation for esterification of propionic acid with n-butanol.
5. Modelling and simulation of reactive divided wall column for esterification of propionic acid with n-butanol over mesoporous catalyst.

References:

[1] J. Lilja, J. Wärnå, T. Salmi, L.J. Pettersson, J. Ahlkvist, H. Grénman, M. Rönnholm, D.Y. Murzin, Esterification of propanoic acid with ethanol, 1-propanol and butanol over a heterogeneous fiber catalyst, Chem. Eng. J. 115 (2005) 1–12. https://doi.org/10.1016/j.cej.2005.08.012.

[2] S.H. Ali, A. Tarakmah, S.Q. Merchant, T. Al-Sahhaf, Synthesis of esters: Development of the rate expression for the Dowex 50 Wx8-400 catalyzed esterification of propionic acid with 1-propanol, Chem. Eng. Sci. 62 (2007) 3197–3217. https://doi.org/10.1016/j.ces.2007.03.017.

[3] H.L. HOŞGÜN, A. ÇITAK, PROPİYONİAsitiİzobutil Alkolİle Amberlyst 36 Ve Amberlyst 7Katalizörleri Varliğinda EsterleşKinetiği, Uludağ Univ. J. Fac. Eng. 23 (2018) 237–248. https://doi.org/10.17482/uumfd.382516.

[4] Â. Silva, K. Wilson, A.F. Lee, V.C. dos Santos, A.C. Cons Bacilla, K.M. Mantovani, S. Nakagaki, Nb2O5/SBA-15 catalyzed propanoic acid esterification, Appl. Catal. B Environ. 205 (2017) 498–504. https://doi.org/10.1016/j.apcatb.2016.12.066.

[5] F. Leyva, A. Orjuela, D.J. Miller, I. Gil, J. Vargas, G. Rodríguez, Kinetics of propionic acid and isoamyl alcohol liquid esterification with amberlyst 70 as catalyst, Ind. Eng. Chem.

Res. (2013). https://doi.org/10.1021/ie402349t.

[6] W.T. Liu, C.S. Tan, Liquid-phase esterification of propionic acid with n-butanol, Ind. Eng. Chem. Res. 40 (2001) 3281–3286. https://doi.org/10.1021/ie001059h.

[7] M.-J. Lee, J.-Y. Chiu, H. Lin, Kinetics of Catalytic Esterification of Propionic Acid and n -Butanol over Amberlyst 35 , Ind. Eng. Chem. Res. 41 (2002) 2882–2887. https://doi.org/10.1021/ie0105472.

[8] T. Ide, T. Nakayama, K. Takahashi, Y. Matsumi, Rate of N 2 O 5 Measured by Cavity Ring-Down Spectroscopy, Int. J. Chem. Kinet. 14 (2008) 1–6. https://doi.org/10.1002/kin.

[9] Y.T. Tsai, H.M. Lin, M.J. Lee, Kinetics of catalytic esterification of propionic acid with methanol over amberlyst 36, Ind. Eng. Chem. Res. 50 (2011) 1171–1176. https://doi.org/10.1021/ie1001179.

[10] A.P. Rathod, K.L. Wasewar, C.K. Yoo, Enhancement of Esterification of Propionic Acid with Isopropyl Alcohol by Pervaporation Reactor, J. Chem. (2014). https://doi.org/10.1155/2014/539341.

[11] W. Zhang, S. Na, W. Li, W. Xing, Kinetic Modeling of Pervaporation Aided Esterification of Propionic Acid and Ethanol Using T-Type Zeolite Membrane, Ind. Eng. Chem. Res. (2015). https://doi.org/10.1021/acs.iecr.5b00505.

[12] R.B. Bhandare, A. Katariya, Y.S. Mahajan, Production of isoamyl propionate: use of Amberlyst–15 in batch reactor and packed bed reactor, J. Chinese Inst. Eng. Trans. Chinese Inst. Eng. A. 44 (2021) 509–518. https://doi.org/10.1080/02533839.2021.1933597.

[13] A. Tiwari, A. Keshav, S. Bhowmick, Optimization of Esterification of Propionic Acid with Ethanol Catalyzed by Solid Acid Catalysts using Response Surface Methodology (RSM): A Kinetic Approach, Int. J. Chem. React. Eng. (2017). https://doi.org/10.1515/ijcre-2016-0101.

[14] A. Bhatia, S. Sharma, Solid acid catalyst for isobutyl propionate production from solid waste, Int. J. Pharm. Chem. Anal. 6 (2019) 63–68. https://doi.org/10.18231/j.ijpca.2019.013.

[15] J. Lilja, J. Aumo, T. Salmi, D.Y. Murzin, P. Mäki-Arvela, M. Sundell, K. Ekman, R. Peltonen, H. Vainio, Kinetics of esterification of propanoic acid with methanol over a fibrous polymer-supported sulphonic acid catalyst, Appl. Catal. A Gen. 228 (2002) 253–267. https://doi.org/10.1016/S0926-860X(01)00981-4.

[16] B. Erdem, M. Cebe, Kinetics of esterification of propionic acid with n-amyl alcohol in the presence of cation exchange resins, Korean J. Chem. Eng. (2006). https://doi.org/10.1007/s11814-006-0005-3.

[17] S.N. Kane, A. Mishra, A.K. Dutta, Preface: International Conference on Recent Trends in

Physics (ICRTP 2016), J. Phys. Conf. Ser. 755 (2016). https://doi.org/10.1088/1742-6596/755/1/011001.

[18] A.F. Martínez, C.A. Sánchez, A. Orjuela, I.D. Gil, G. Rodríguez, Isobutyl acetate by reactive distillation. Part II. Kinetic study, Chem. Eng. Res. Des. 160 (2020) 447–453. https://doi.org/10.1016/j.cherd.2020.06.023.

[19] T. Pöpken, S. Steinigeweg, J. Gmehling, Synthesis and hydrolysis of methyl acetate by reactive distillation using structured catalytic packings: Experiments and simulation, Ind. Eng. Chem. Res. 40 (2001) 1566–1574. https://doi.org/10.1021/ie0007419.

[20] H. Zhang, Q. Ye, J. Qin, H. Xu, N. Li, Design and control of extractive dividing-wall column for separating ethyl acetate-isopropyl alcohol mixture, Ind. Eng. Chem. Res. 53 (2014) 1189–1205. https://doi.org/10.1021/ie403618f.

[21] G. Fernholz, S. Engell, L.U. Kreul, A. Gorak, Optimal operation of a semi-batch reactive distillation column, Comput. Chem. Eng. 24 (2000) 1569–1575. https://doi.org/10.1016/S0098-1354(00)00553-6.

[22] S.P. Chopade, M.M. Sharma, Reaction of ethanol and formaldehyde: Use of versatile cation-exchange resins as catalyst in batch reactors and reactive distillation columns, React. Funct. Polym. 32 (1997) 53–65. https://doi.org/10.1016/S1381-5148(96)00069-7.

[23] B. Saha, H.T.R. Teo, A. Alqahtani, Iso-amyl acetate synthesis by catalytic distillation, Int. J. Chem. React. Eng. 3 (2005). https://doi.org/10.2202/1542-6580.1250.

[24] Schneider, R., Noeres, C., Kreul, L.U., Gorak, A., 2001. Dynamic modeling and simulation of reactive batch distillation. Computers and Chemical Engineering 1, 169-176.

[25] Horstmann, S., Popken, T., Gmehling, J., 2001. Phase equilibria and excess properties for binary systems in reactive distillation processes Part 1. Methyl acetate synthesis. Fluid phase Equilibria 180, 221-234.

[26] Gorak, A., Hoffmann, A., 2001. Catalytic distillation in structured packings: Methy acetate synthesis. American Institute of Chemical Engineers Journal 47, 1067-1076.

[27] Noeres, C., Dadhe, K., Gesthuisen, R., Engell, S., Gorak, A., 2004. Model based design, control and optimization of catalytic distillation processes. Chemical Engineering and Processing 43, 421-434.

[28] Singh, R.P., Singh, R., Kumar, M.V.P., Kaistha, N., 2005. Steady state analysis of reactive distillation using homotopy continuation. Chemical Engineering Research and Design 83,959- 968.

[29] Sing, A., Tiwari, A., Mahajani, S.M., Gudi, R.D., 2006. Recovery of acetic acid from aqueous solutions by reactive distillation. Industrial and Engineering Chemistry Research 45, 2017- 2025.

[30] Sing, A., Tiwari, A., Bansal, V., Gudi, R.D., Mahajani, S.M., 2007. Recovery of acetic acid by reactive distillation: Parametric study and non linear dynamic effects. Industrial and Engineering Chemistry Research 46, 9196-9204.

[31] Kumar, M.V.P., Kaistha, N., 2008. Role of multiplicity in reactive distillation control system design. Journal of Process Control 18, 692-706.

[32] Rahul, M., Kumar, M.V.P., Dwivedi, D., Kaistha, N., 2009. An efficient algorithm for rigorous dynamic simulation of reactive distillation columns. Computers and Chemical Engineering 33, 1336-1343.

[33] Sandesh, K., Jagadeeshbabu, P.E., Math, S., Saidutta, M.B., 2013. Reactive distillation using an ion exchange catalyst: Experimental and simulation studies for the production of methyl acetate. Industrial and Engineering Chemistry Research 52, 6984-6990.

[34] Saha, B., Chopade, S.P., Mahajani, S.M., 2000. Recovery of dilute acetic acid through esterification in a reactive distillation column. Catalysis Today 60, 147-157.

[35] Hiwale, R.S., Bhate, N.V., Mahajan, Y.S., Mahajani, S.M., 2004. Industrial applications of reactive distillation: Recent trends. International Journal of Chemical Reactor Engineering 2,1-54.

[36] Almeida-Rivera, C.P., Swinkels, P.L., Grievink, J., 2004. Designing reactive distillation processes: present and future. Computers and Chemical Engineering 28, 1997-2020.

[37] Schmitt, M., Hase, H., Althaus, K., Schoemakers, H., Gotze, L., Moritz, P., 2004. Synthesis of n-hexyl acetate by reactive distillation. Chemical Engineering and Processing 43, 397-409.

[38] Kumar, R., Mahajani, S.M., 2007. Esterification of lactic acid with n-butanol by reactive distillation. Industrial and Engineering Chemistry Research 46, 6873-6882.

[39] Calvar, N., Gonzalez, B., Dominguez, A., 2007. Esterification of acetic acid with ethanol: Reaction kinetics and operation in a packed bed reactive distillation column. Chemical Engineering and Processing 46, 1317-1323.

[40] Tavan, Y., Hossein, S., 2013. Design and simulation of reactive distillation process to produce high purity ethyl acetate. Journal of Taiwan Institute of Chemical Engineers 44, 577- 585.

[41] Avami, A., 2013. Conceptual design of double feed reactive distillation columns. Chemical Engineering Technology 36, 186-191.

[42] Huss, R.S., Chen, F., Malone, M.F., Doherty, M.F. 1999. Computer aided tools for the design of reactive distillation systems. PII: S0098-1354/99/00074-5

[43] Patil, P., Daniel, G., Dragomir, R., Jobson, M. 2006. Conceptual design of reactive dividing wall columns. I. Chem E. Symposium Series No. 152, 364-372.

[44] Mueller, I. C., Bhatia, D., Kenig, E. Y. 2007. Rate-based analysis of reactive distillation sequences with different degrees of integration, Chemical Engineering Science, 62,7327-7335.

[45] Mueller I., Kenig, E. Y. 2007. Reactive Distillation in a Dividing Wall Column - Rate Based Modeling and Simulation, Industrial & Engineering Chemistry Research, 46,3709-3719.

[46] Rodrigo, S. V., Fabricio, O., Hecter, M. 2008. Implementation of a reactive dividing wall Distillation column in a pilot plant. European symposium on computer aided process Engineering, 18,229-234.

[47] Gabriel, J., Kiss, A. A., 2011. Reactive DWC leading the way to FAME and fortune. Fuel. 95, 352-359.

[48] Delgado, R., Hernandeez, S., Gabriel, J. 2011. From simulation studies to experimental tests in a reactive dividing wall distillation column. Chemical Engineering Research and Design, 41,902-910.

[49] Delgado, R., Hernandeez, S., Gabriel, J. 2011. From simulation studies to experimental tests in a reactive dividing wall distillation column. Chemical Engineering Research and Design, 41,902-910.

[50] Tawan, Y., Hosseni, S. H. 2013. From laboratory experiment to simulation studies of methanol dehydration to produce DMC reaction part-2 , Simulation and cost estimation. Chemical Engineering and Processing: Process Integration, 73, 151-157.

[51] Ignata, M., Kiss, A. A., 2013. Optimal design, dynamics and control of a reactive DWC for biodiesel production. The Institution of Chemical Engineers. Elsevier, 41,1160-1172.

Chapter 3

Materials and Methods

3.1 Materials and methods

Butyl propionate is obtained by the esterification of propionic acid with n-butanol. The reaction scheme is shown below

$C_3H_6O_2$ + C_4H_9OH ←------→ $C_7H_{14}O_2$ + H_2O

Propionic Acid N-Butanol Butyl Propionate water

To find out what happens when Amberlite IR-120, Indion-190, and Indion-180 are present. The esterification reaction was carried out in an isothermal batch reactor with the catalyst. The effects of varying variables such catalyst loading, acid-alcohol molar ratio, reaction temperature, and stirring speed on propionic acid conversion were investigated.

Table 3.1. Physical and chemical properties of the reactants and products.

The physical and chemical properties of the components of propionic acid, n-butanol, n-butyl propionate, and water are given in Table 3.1. Among the four components, butyl propionate is the high boiling component. Butyl propionate is miscible in butanol, propionic acid and water [1].

S.No.	Property	propionic acid	n-butanol	n-butyl propionate	Water
1	Chemical formulae	$C_3H_6O_2$	$C_4H_{10}O$	$C_7H_{14}O_2$	H_2O
2	Physical state and appearance at room temperature	Liquid	Liquid	Liquid	Liquid
3	Molecular weight (g/g-mole)	74.08	74.121	130.2	18
4	Melting Point (^{0}C)	-21	-89.8	-75	0
5	Boiling Point (^{0}C)	141.2	117.7	146	100
6	Specific gravity	0.993g/ml	0.81g/ml	0.875g/ml	1g/ml
7	Odour	Pungent, vinegar- like	Alcohol like, Pungent when crude	Fragrance like, RUM	Odourless
8	Colour	Colour less clear liquid	Colour less clear liquid	Colour less clear liquid	Colour less clear liquid
9	Water solubility	Yes	Yes	Yes	---
10	Taste	Sour (strong)	Burning taste	Slight bitter Taste	Taste less

Therefore, the mixture of the above four components is completely miscible for all possible compositions. Butanol of purity=99% w/w, propionic acid of purity 99.95% w/w, and Sulphuric acid of purity=98% w/w was purchased from SD Fine Chemicals Ltd. (Mumbai, India) and used as supplied without any further purification.

3.2 Selection of the catalyst for the esterification reaction

The catalyst used in the esterification process considerably impacts the chemical reaction rate and the entire process. In organic synthesis, many liquids and solid chemical catalysts are utilized. Every chemical catalyst has advantages and drawbacks. In the esterification process, a liquid catalyst such as Sulphuric acid has a higher reaction rate than a solid catalyst such as ion-exchange resins [2]. However, the reaction in the solid catalytic process may be slowed because of mass transfer resistances. Advantages of heterogeneous catalysts include simpler separation of the catalyst from the product mixture, greater selectivity toward the intended product, high purity due to reduced side reactions, and removal of the corrosive environment [3].

In the commercial industry, a wide variety of solid catalysts are accessible. There are market zeolites, ion exchange resins, acid catalysts, and novel solid acids and bases. The catalysts may be used in acid-catalyzed processes such as esterification, etherification, trans-esterification, etc. When solid catalysts are used in the reactive distillation process, they must have specific qualities [4].

1. Catalytic activity must be high.
2. Catalyst deactivation is either absent or extremely slow.
3. The effective temperature of the catalyst across the entire range of the reactants' and products' boiling points
4. Stability of the structure.

In reactive distillation, most of the reactions occur in the liquid phase. Because catalyst activity impacts reaction rate, it determines the liquid hold-up required in reactive distillation to obtain the desired conversion.

Table 3.2 Physical and chemical Properties of catalysts used in this study

	Amberlite IR-120	Indion-90	Indion-180
Manufacturer	Merck	Indion resins	Indion resins
Physical structure	Brown colored sphere-shaped beads	Opaque grey to dark grey beads	Misty grey to colored grey beads
Matrix Type	Styrene-divinyl benzene (gel)	Styrene-divinyl benzene copolymer	Styrene-divinyl benzene copolymer
Polymer type	Microporous	Microporous	Microporous
Ionic form	hydrogen form	Hydrogen form	Microporous
Functional group	Sulfonic Acid	Sulfonic acid	Sulfonic acid
Ion-exchange capacity(eq L^{-1})	1.8 meq/mL by wet bed volume	4.7 meq/dry g minimum	5.0 meq/dry g minimum
Particle size(mm)	620-830 μm	0.42-1.22	0.42-1.2
Thermal stability	121°C max. temp	130°C	130°C
Moisture Holding Capacity	53-58%	3% maximum	1 %

Most chemical industries currently use ion-exchangers such as Sulfonated macromolecular resins as catalysts for reacting alcohols with acids. These catalysts are stable at temperatures ranging from 368 K to 398 K and provide the high H+ ion concentration necessary for catalyzing the esterification process. The resin catalysts are similar in structure to activated carbon or silica gel, which are used in adsorption. Because of the large surface area of the inside and exterior pores, liquid molecules may easily access the sulfonic group hydrogen ions in the inner catalyst particle. As a result, these solid catalysts are appropriate for a wide range of Bronsted acid-catalyzed processes [5].

Ion-exchange resin catalysts Indion190, Indion180, and Amberlite IR-120 were used in this work. The physical and chemical parameters of the catalyst are listed in Table 3.2. The solid catalysts Indion 180 and Indion 190 were supplied by Ion-Exchange India Limited in Mumbai, while Amberlite IR-120 was supplied by Rohm & Hass in Mumbai. In these catalysts, sulfonation of a polystyrene-divinilbenzene (DVB) copolymer yields cross-linked three-dimensional polymeric structures[6].

The equilibrium criteria determine the maximal conversion of reactants. In the absence of a catalyst, the esterification process is extremely sluggish; however, the inclusion of a catalyst speeds up the reaction rate, and the system quickly reaches equilibrium. The major goal of this research is to construct a kinetic model for the batch reactor that can be used to design a reactive distillation column and to manufacture an effective catalyst. The developed kinetic equation was used to design and optimize conventional reactive distillation, divided wall columns, and the vapor compression heat integrated reactive distillation process.

In this study, a Ti-based SBA 15 Sulfonated catalyst was synthesised and kinetic tests for the esterification of propionic acid with n-butanol were carried out. In the presence of Ti-based SBA 15 Sulfonated catalyst, the ER kinetic model is created. The experiments in reactive batch distillation were conducted and proposed a mathematical model. The simulations have been performed with reactive distillation, reactive distillation divide wall columns, and heat integration of reactive distillation and divided wall columns.

3.3 Determination of ion exchange capacity of resins

The ion exchangeability of each resin was experimentally verified. 1 g catalyst was spread in 100 ml of sodium chloride (1M) solution in a typical experiment and ultrasonicated for 2 hr. The resin was filtered, and the filtrate used phenolphthalein as an indicator to titrate against 0.1 N NaOH. Acid site concentration obtained by difference (average of results) was 1.8 ± 0.05 eq L-1 for Amberlite IR-120, 4.7 ± 0.05 eq L-1 for Indion-190, 5.0 ± 0.05 eq L-1 for Indion-180, according to manufacturer's reported values.

3.4 Catalyst preparation

Pluronic P123 is a unique, linearly substituted triblock copolymer composed of polyethylene oxide (PEO) and polypropylene oxide (PPO) (PPO). In one experiment, 5 g of triblock copolymer (i.e., P123) with structured mesoporous components such as SBA-15 is dispersed in 116.25 g of distilled water, and 29.13 g of hydrochloric acid is added to the solution. During this steady 24-hour mixing, a final 11 grams of tetra-ethyl-ortho-silicate was added to tetra-iso-propoxide titanium (Si/Ti=100) as a medication addition of silica. The resulting slurry was then rinsed with distilled water before being combined with N-Butanol. The material was dried at 110°C for 12 hours before being

calcined at 500°C for 8 hours [7].

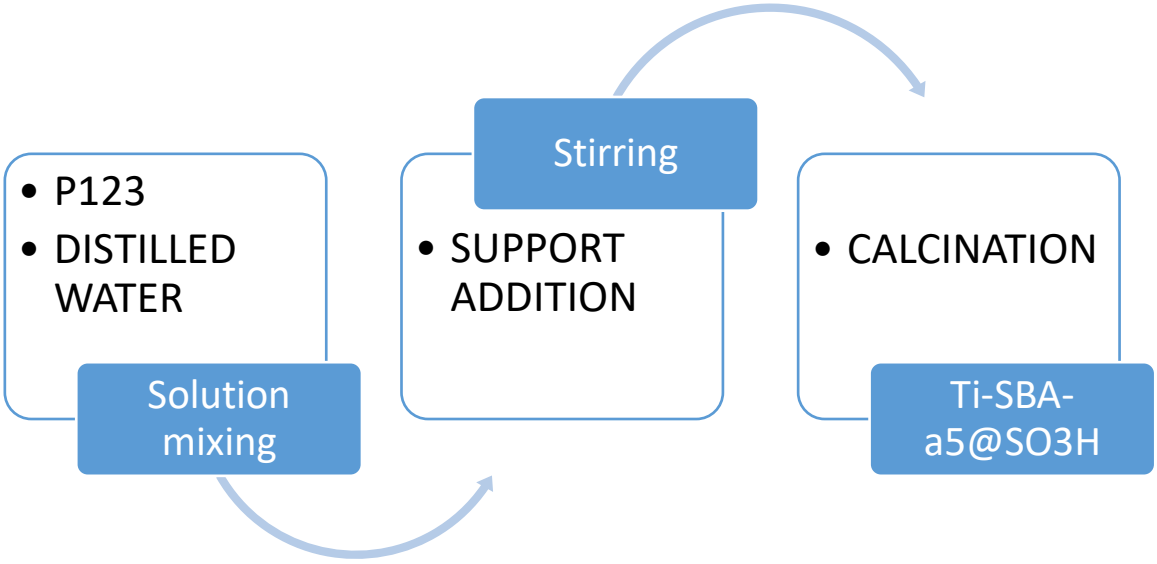

Fig 3.1: Flow Diagram of Sol-Gel Method (Redraw)

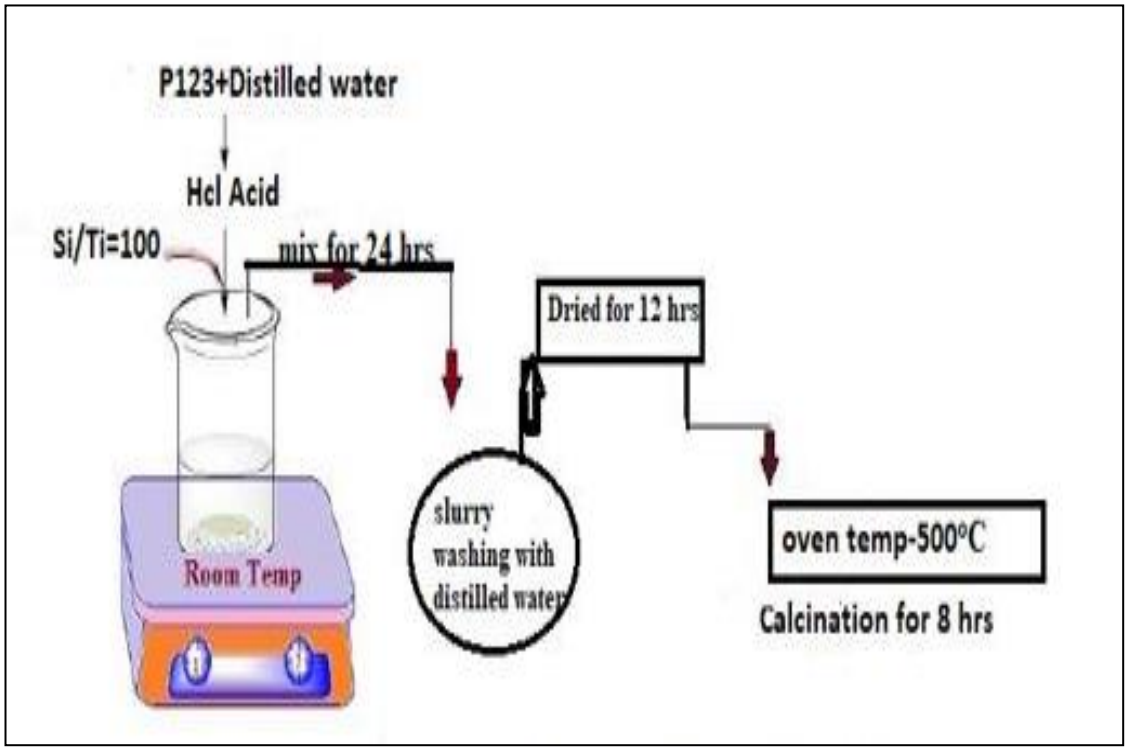

Fig.3.2 Experimental Procedure for Sol-Gel Method

3.4.1 Characterization

The Ultima IV diffractometer (XRD) displays the powdered X-ray diffraction pattern. The following statistical results are acquired within the range of 0.1-5 with a phase of 0.008 ° and a scanning speed of 0.5° per minute, using a non-filtered Cu K radiation source with 30 mA and 40 kV. A scanning electron microscope was utilized for surface morphology research at TESCAN and VEGA 3 LMU in Australia (SEM)[8]. The pictures of the samples were analyzed using a JEOL Australia instrument with a 200 kV acceleration voltage. The STA 2500 Regales NETZSCH, Japan, was utilized for thermogravimetry/differential thermal analysis (TG-DTA). Liquid nitrogen (77K) and the Chinese surface inspection equipment, Quanta Chrome Nova-1000, and the de Boer t map, BET, and pore size, are used to specify sample pores and surface area. Samples were collected at 1:10 KBr room temperature using 10 FT-IR scans using a PerkinElmer Spectrum 100 in the United States. The samples were registered using a Fourier transform spectra. The sample spectrum was recorded on the Evolution 300 Thermo Science using a UV-Visible Spectrometer from the United States and BaSO4 as a reference [9].

3.5. Experimental setup

3.5.1 Batch reactor for esterification reaction

Figure 3.3 depicts a schematic representation of the experimental setup. In a 500 mL three-neck round-bottom flask placed in a heated Rota mantle, the esterification reaction was carried out. A heating control knob and a magnetic stirrer speed control knob are located on the Rota mantle. The heating control knob [10] regulates the amount of heat added to the reaction mixture. The magnetic stirrer is

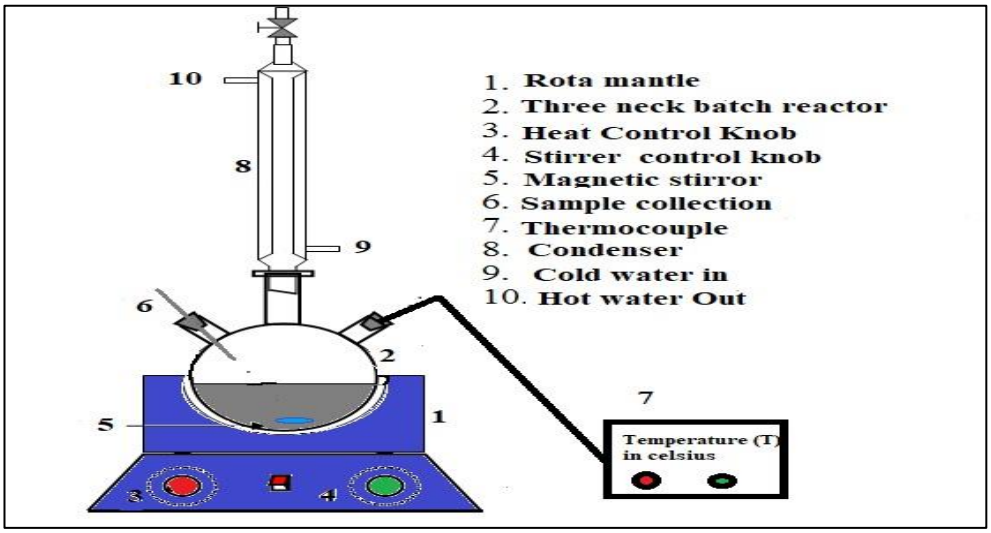

Fig.3.3 Experimental setup for kinetic studies

used to uniformly mix the catalyst particles with the reaction mixture. A mercury thermometer is employed in the reactor to measure the temperature of the reaction mixture. A vertical spiral condenser is connected to the reaction flask to reduce vapour loss in the reactor. The image of the laboratory experimental setup used for the kinetic study is shown in Fig.3.4.

Fig.3.4 The laboratory batch reactor setup for the kinetic study.

3.5.2 Batch reactive distillation

At various reboiler heat input rates, experiments were carried out on the reaction combination of propionic acid and n-butanol. Fig. 3.5 depicts the experimental setup in schematic form. It comprises of a one-liter round bottom flask with an electric heater surrounding it. In the reboiler, a PT-100 temperature probe with a digital display is provided for manually recording the temperature. The applied voltage can be changed to change the heater power. The current flowing through the heater is displayed on an ammeter. The product of applied voltage and current is used to compute the power input [11]. On the top of the round bottom flask, a packed column of 0.5m height is supplied. Raschig rings, approximately 1 cm in diameter, were used to pack the items. Glass is used for both the packing and the column wall. A vertical condenser with a three-way valve and recycle tubing is connected to the top of the column. The coolant water is available at 300°C and circulates at a moderate flow rate in the vertical condenser, resulting in minimal vapour losses. Laboratory experimental setup is shown in Fig 3.6

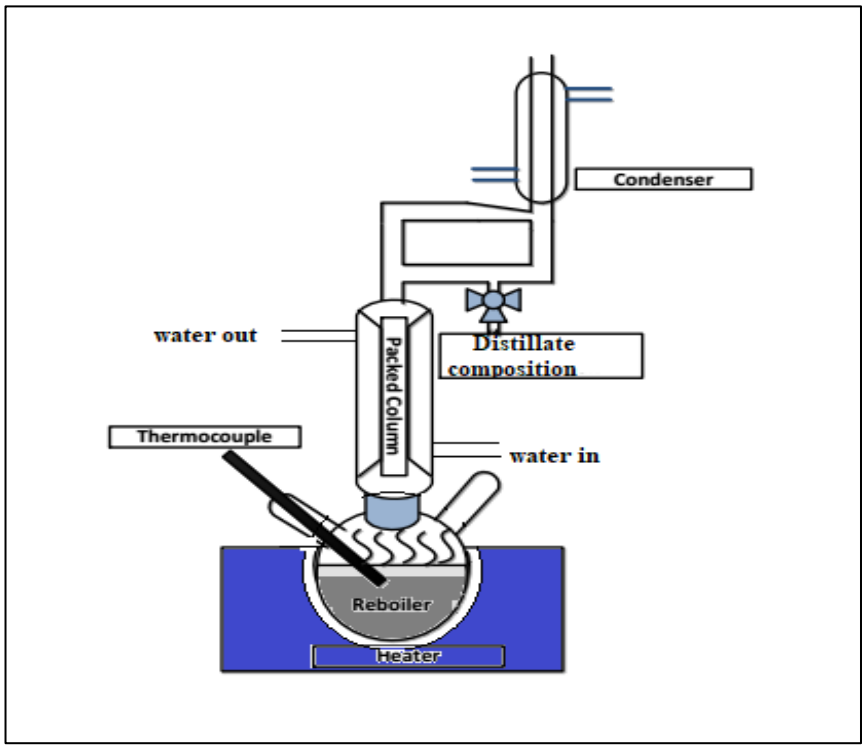

Fig.3.5 Schematic diagram of batch reactive distillation

Fig.3.6 Experimental setup for batch reactive distillation

3.6 Experimental procedure

Two types of experiments were conducted in this work.

(i) The studies were carried out in a batch reactor for the esterification of propionic acid and n-butanol in the presence of liquid and solid catalysts.

(ii) The experiments were conducted in the presence of the Ti SBA-15@SO3H, a novel catalyst in a batch reactive distillation apparatus. The detailed experimental procedure in batch kinetics, batch Reactive distillation apparatus of the reactive distillation column is described below.

3.6.1 Reaction kinetics in batch reactor

In this study, stoichiometric ratio of reactants are charged to the reactor and heated to a desired temperature in a short time and a known amount of the catalyst in grams of catalyst per cc of the reaction mixture is added. Propionic acid content is determined by taking samples at regular intervals and analysing them. Finally, the reaction is run long enough to attain equilibrium, at which point the concentration of propionic acid does not change.

Propionic acid and n-butanol were weighed correctly within an error of 0.0001g using a digital electronic balance in the instance of esterification with mesoporous catalyst. The batch reactor was charged with the weighted reactants. The total volume of the bulk solution is 170 ml. This gives the initial concentration of propionic acid as 12 mol/l. In the case of the mesoporous catalyst used in this study. The catalyst was added to the reactants in the calculated amount (as a weight % for propionic acid), and the reaction mixture was heated to the required temperature. When the catalyst was put to the reactor, t=0, the time was recorded. The catalyst was introduced to a heterogeneous reaction process when the reaction mixture reached the desired temperature. The time was recorded as the initial time, t=0, when the reaction mixture attained the desired temperature. Titration was used to determine the content of propionic acid in samples taken at regular intervals. Chemical equilibrium was achieved when the reaction had been carried out for a long enough time. The chemical equilibrium was established when the concentration of propionic acid did not decline any further. The content of propionic acid in the withdrawn samples was determined quickly and without delay. This data on propionic acid concentration vs. time could be used to calculate kinetic reaction parameters. A thermocouple with an accuracy of 0.5K was used to measure the temperature.

3.6.2 Batch reactive distillation apparatus

The reboiler at the bottom of the column is filled with n-butanol and propionic acid and a predetermined catalyst is added to the mixture. The heater is switched on, and it is noticed that after 15 to 20 minutes, the reaction mixture's vapors from the reboiler reach the condenser through a 0.5m column. The condensed distillate begins to accumulate. The column is initially run at full

reflux until it reaches a consistent temperature all the way down the column. The reflux from the top condenser is begun by adjusting the tap to the column at the correct pace once the temperatures along the column have reached a virtually constant value. Every 30 minutes, the bottoms (withdrawal from reboiler) and distillate flow rates were collected. The temperatures in the reboiler, column, and distillate were recorded with time. The samples were analyzed for their composition.

3.7 Sample analysis

The experiments were repeated to report the results. First, the level of propionic acid in the reaction mixture was evaluated using 0.5N NaOH and phenolphthalein as an indicator using the titration method.0.5 N oxalic acid standardized the NaOH. Microprocessor-based Karl Fischer titrator measured the water produced during the response. Product formation was discovered not to have happened after comparing measured water content to calculated values based on the stoichiometric equation.

3.7.1 Analysis by gas chromatography

Gas chromatography is separating and analyzing substances that can be evaporated without breakdown. Figure 3.7 shows a Gas Chromatography instrument. It comprises a long spiral column, an inert gas cylinder, a sample injection port, and an output detector linked to a computer for collecting data.

3.7.2 Working principle of GC

When you inject a liquid sample into the injection port, it vaporises and is transported to the detector by the carrier gas through the column. The detector sends signals to the recorder, which creates a chromatogram with the help of a computer. The thermal conductivity detector may detect any chemical other than the carrier gas. The application of power heats the metallic TCD filament. The thermal conductivity of sample compounds is lower than that of the carrier gas when they flow along the filament, causing the filament temperature to rise[12]. Temperature causes the filament resistance to change; the resistance is measured, and a chromatogram is created. The difference in thermal conductivities between the sample and the carrier gas determines TCD sensitivity.

Fig.3.7 The laboratory Gas Chromatography instrument for the Analysis of the chemical components.

Fig.3.7. Displays the Gas Chromatography device used in the laboratory to examine propionic acid, n-butanol, butyl propionate, and water. It had an injection port, packed/capillary columns, and a FID/TCD detector. The hydrogen supplied as the carrier gas. The control valves change the inlet and exit pressures of the hydrogen cylinder. The pressure controller valve allows the hydrogen carrier gas to enter the GC instrument at a consistent pressure.

References:

[1] Sami H. Ali, Alia Tarakmah 2007. Synthesis of esters: Development of the rate expression for the Dowex 50 Wx8-400 catalyzed esterification of propionic acid with 1-propanol. Chemical Engineering Science 62 (2007) 3197 – 3217

[2] Ho-mu Lin, and Ming-Jer Lee. Kinetics of Catalytic Esterification of Propionic Acid with Methanol over Amberlyst 36. *Ind. Eng. Chem. Res.* 2011, *50,* 1171–1176

[3] Peters, T.A., Benes, N.E., Holmen, A., Keurentjes, J.T.F., 2006. Comparison of commercial solid acid catalysts for the esterification of acetic acid with butanol. Applied catalysis A: General 297,182-188.

[4] Kenig, E.Y., Gorak, A., Bart, H.J., 2004. Reactive separations in fluid systems. Re-Engineering the chemical processing plant. Process Intensification, Stankiewicz, A., Mouzlin J.A., New York, 309-377.

[5] Van Hasselt, B.W., Calis, H.P.A., Sie, S.T., Van den Bleek, C.M., 1999. Liquid holdup in the three levels of porosity reactor. Chemical Engineering Science 54, 1405-1411.

[6] Mallaiah Mekala and Venkat Reddy Goli., 2015. Kinetics of esterification of methanol with acetic acid using mineral homogeneous acid catalyst. Chinese Journal of Chemical Engineering 23,100-105.

[7] Shaojun Miao, Brent H. Shanks. Mechanism of acetic acid esterification over sulfonic acid-functionalized mesoporous silica. Journal of Catalysis 279 (2011) 136–143

[8] P. R. Rajamohanan,and T. G. Ajithkumar. Immobilization of Phosphotungstic Acid (PTA) on Imidazole Functionalized Silica: Evidence for the Nature of PTA Binding by Solid State NMR and Reaction Studies.*J. Phys. Chem. C* 2009, *113,* 21114–21122.

[9] Katabathini Narasimha Rao, Adapa Sridhar. Zirconium phosphate supported tungsten oxide solid acid catalysts for the esterification of palmitic acid. Green Chem., 2006, 8, 790–797

[10] Ju-Yin Chiu, and Ho-mu Lin. Kinetics of Catalytic Esterification of Propionic Acid and *n*-Butanol over Amberlyst 35. *Ind. Eng. Chem. Res.* 2002, *41,* 2882-2887

[11]Ameer Khan Patan; Mekala, Mallaiah; Thamida, Sunil Kumar.2018. Dynamic Simulation of Heterogeneous Catalysis at Particle Scale to Estimate the Kinetic Parameters for the Pore Diffusion Model.Bulletin of Chemical Reaction Engineering & Catalysis; Semarang Vol. 13, Iss. 3, (2018): 420-428. DOI:10.9767/bcrec.13.3.2098.420-428

[12] Mallaiah Mekala and Venkat Reddy Goli., 2018. Data on acetic acid–methanol–methyl acetate–water mixture analysised by dual packed column Gas Chromatography. Data in Brief 2018.

Chapter 4
Results and Discussion

Results and Discussions

4.1. The activity of selected commercial ion exchange resins for esterification kinetics of propionic acid with n-butanol in a batch reactor

4.1.1 Esterification reaction by homogeneous catalyst

H_2SO_4 is the main catalyst for the industrial esterification reaction. It is highly successful, but strict regulation over the amount of H_2SO_4 is essential since a slight change in H2SO4 concentration and reaction temperature can condense alcohols to ethers. P-toluene sulfonic acid, on the other hand, has a higher catalytic activity and produces fewer side reactions than H2SO4. As a result, in the esterification process, P-toluene sulfonic acid is more effective than H2SO4 [1]. Because of the diffusion issue with the pores of the catalyst and their polymeric nature, ion-exchange resins could not be used in this investigation. The kinetics of Propionic acid esterification using a homogeneous catalyst are described in just a few papers in the literature. However, there are few research on the kinetics of the esterification process that have been published.

The main objective of this study is to improve process conditions for producing N-Butyl propionate by esterification of Propionic acid. In this StudyStudy, p-Toluene sulfonic acid, a monobasic organic acid, was used as a homogeneous catalyst. To investigate the effect of operational factors, i.e., catalyst quantity, the mole ratio of acid to alcohol, and reaction temperature, on determining the system's best operating conditions [2]. Additionally, applying second-order kinetics, the kinetics were examined, and kinetic parameters were determined at operating conditions. The reaction rate constants, equilibrium constants, activation energy, and pre-exponential factors were determined.

4.1.1.1 Esterification kinetics in a batch reactor with liquid catalyst: P-Toluene sulfonic acid

Fig 4.1 shows the study on esterification reaction with P-Toluene sulfonic acid catalyst is examined at 1:1 mole ratio of Propionic acid and n-butanol. Temperature varies from 85^{o}C to 115^{o}C. The catalyst concentration varies from 1wt% to 3wt%. The effect of various factors on reaction kinetics is discussed below.

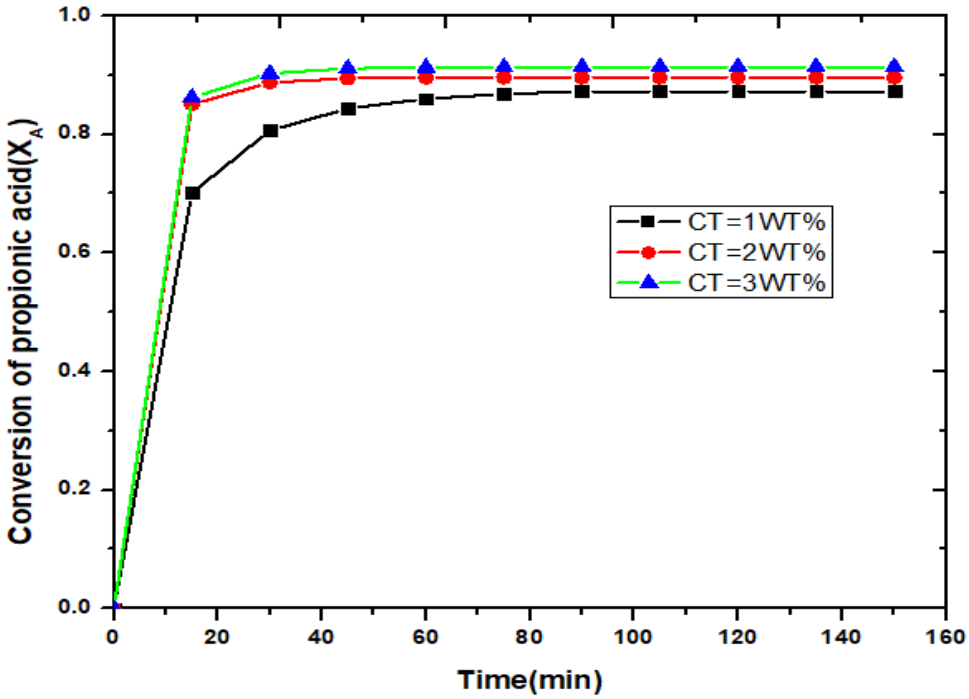

Fig.4.1 Effect of catalyst concentration on the conversion of Propionic Acid.

The extent of reaction's represented in the form of Propionic acid conversion

$$X_A = 1 - \frac{C_A}{C_{A0}} \quad (1)$$

Especially for the 1:1 mole ratio of reactants, it is sufficient to estimate Propionic acid conversion because the other ones would be increased by stoichiometry[3].

4.1.1.2 Effect of Temperature

The reaction was carried at a temperature ranging from 85 to 115oC, with an Acid-to-Alcohol mole ratio of 1:2, a catalyst loading of 2% and a stirrer speed 480 rpm. Figure 4.2 shows the influence of temperature on the conversion of propionic acid, which was found, that temperature increases propionic acid conversion [4]. As a result, the higher the temperature appears to favor the fastening of the reaction in forward direction. Furthermore, when the temperature increased time required for conversion to reach a steady-state decreased.

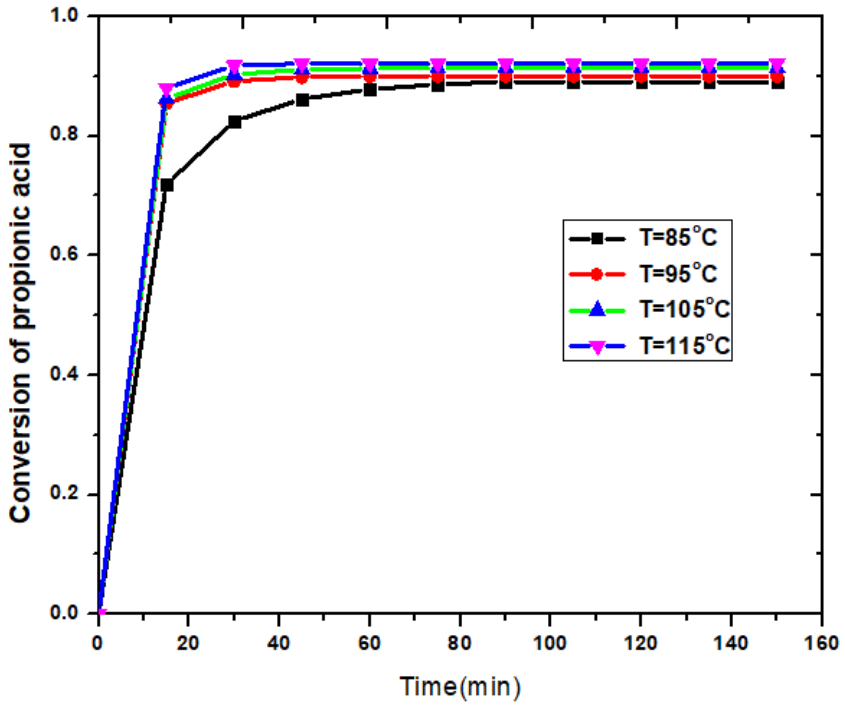

Fig.4.2 Effect of reaction temperature on the conversion of the Propionic Acid.

4.1.1.3 Effect of Mole Ratio

At Chemical equilibrium limits, the reaction between propionic acid and n-butanol, the equilibrium conversion, determines the amount of ester produced. Excessive alcohol changes equilibrium in the forward direction and increases propionic acid conversion. In this experiment, the mole ratio of acid to alcohol adjusted from 1:1 to 1:4 at 115oC, with a catalyst Concentration of 2% and stirrer speed of 480 rpm [5]. Figure 4.3 show that propionic acid conversion increases as the mole ratio increases.

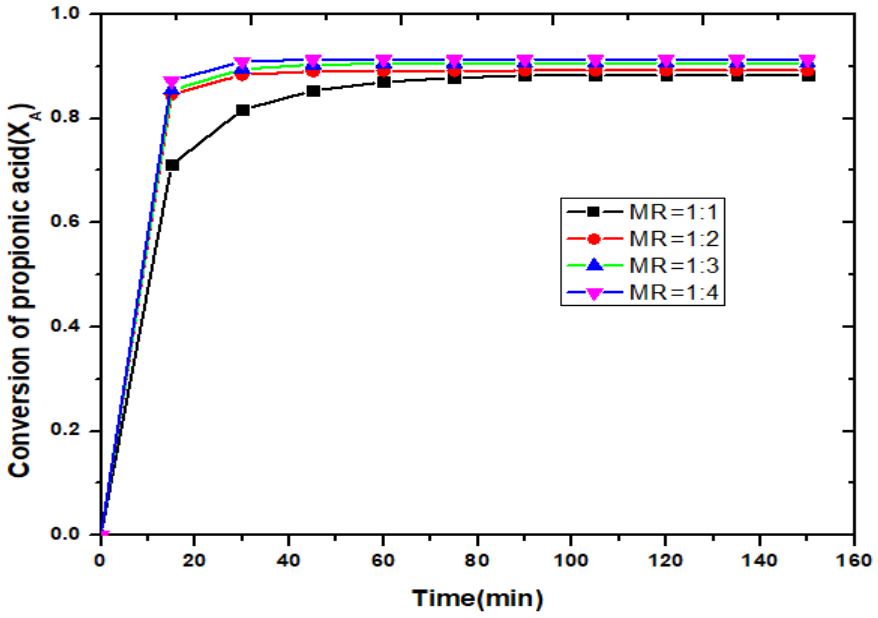

Fig.4.3 Effect of reactant mole ratio on the conversion of Propionic Acid.

4.1.2 Esterification reaction by heterogeneous Catalyst

The last chapter discussed the esterification reaction using a homogeneous catalyst. Although they have high catalytic activity, limitations include equipment corrosion, side reactions, and the need for an additional stage of product purification. Heterogeneous catalysts have received greater attention in recent years as a result of these limits. They have a number of benefits, including quick separation from the reaction mixture, high product purity, and the elimination of galvanic corrosion and side reactions. They are also non-corrosive and have high thermal stability. As a result, heterogeneous catalysts are now recommended for esterification processes [6]. Ion exchange resins holding sulfonic acid groups bonded to polymer carriers, such as polystyrene cross-linked with divinyl benzene, are the most widely employed catalysts. They are selective in reactant adsorption and have a swelling nature. As a result, they not only catalyze but also impact the esterification reaction's equilibrium conversion.

4.1.2.1 Determination of ion exchange capacity of resins

The ion exchangeability of each resin was experimentally verified. 1 g catalyst was spread in 50 ml of NaCl (1M) solution in a typical experiment and ultrasonicated for 2 hr. The resin was filtered, and the filtrate used phenolphthalein as an indicator to titrate against 0.1 N NaOH. Acid site concentration obtained by difference (average of results) was 1.8 ± 0.05 eq L-1 for Amberlite IR-120, 4.7 ± 0.05 eq L-1 for Indion-190, 5.0 ± 0.05 eq L-1 for Indion-180, according to manufacturer's reported values.

4.1.3 Esterification reaction by heterogeneous Catalyst (Amberlite IR-120)

4.1.3.1 Effect of catalyst loading

Catalysts play an essential role in improving total conversion by increasing reaction rates. In this work, catalyst concentration varies from 1% to 3% at 115^{o}C, with a mole ratio of acid to Alcohol of 1:2. Figure 4.4 illustrates propionic acid conversion at different catalyst concentrations, showing that the greater the catalyst concentration, the faster the reaction rate. This is because more active sites (H+) are available in ion exchange resins, improving conversion. It was also found, Propionic acid conversion increased from 1wt% to 3wt% catalyst Concentration. However, increasing the catalyst concentration above 3wt% did not substantially increase propionic acid conversion[7].

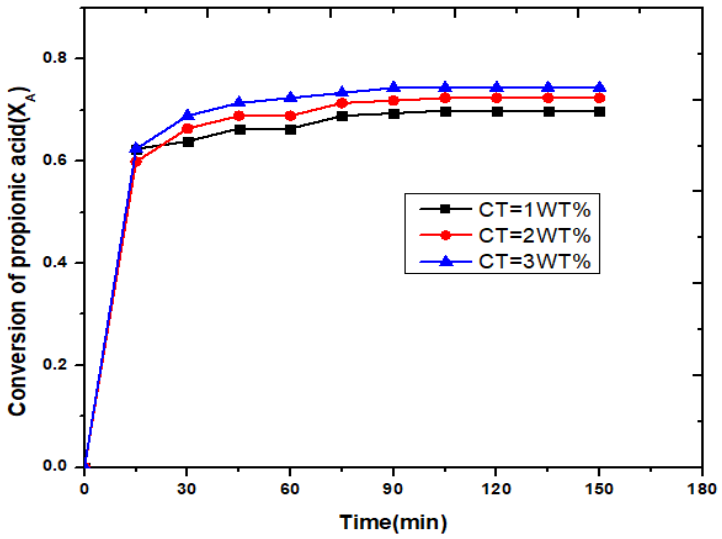

Fig.4.4 Effect of catalyst concentration on the conversion of Propionic Acid.

The finding was confirmed by estimated by rate of reaction for various Catalyst Concentrations. The rate of reaction was calculated as,

$$-r_{A0} = \frac{C_{A0}X_A}{t} \quad (2)$$

Where r_{A0} represents the initial reaction rate, C_{A0} represents the initial concentration of propionic acid, and X_A represents propionic acid conversion. Figure shows rate of reaction vs. catalyst loading, which shows that rate of reaction increases linearly with catalyst loading. The intercept of curve represented, rate of reaction for uncatalyzed reaction under given conditions. Figure revealed relationship between rate of reaction and catalyst Concentration.

$$-r_{A0}\left(\frac{mol}{L-min}\right) = 0.015X\left(\frac{gm}{L}\right) + 0.0106 \quad (3)$$

Where X indicates catalyst concentration. The expression valid at temperature of 115^{o}C and the mole ratio of Acid to alcohol of 1:2 used in this investigation.

4.1.3.2 Effect of mole ratio

At Chemical equilibrium limits, the reaction between propionic acid and n-butanol, the equilibrium conversion, determines the amount of ester produced. Excessive alcohol changes equilibrium in the forward direction and increases propionic acid conversion [8]. In this experiment, the mole ratio of acid to alcohol adjusted from 1:1 to 1:3 at 115^{o}C, with a catalyst Concentration of 2% and stirrer speed 480 rpm. Figure 4.5 show that propionic acid conversion increases as the mole ratio increases.

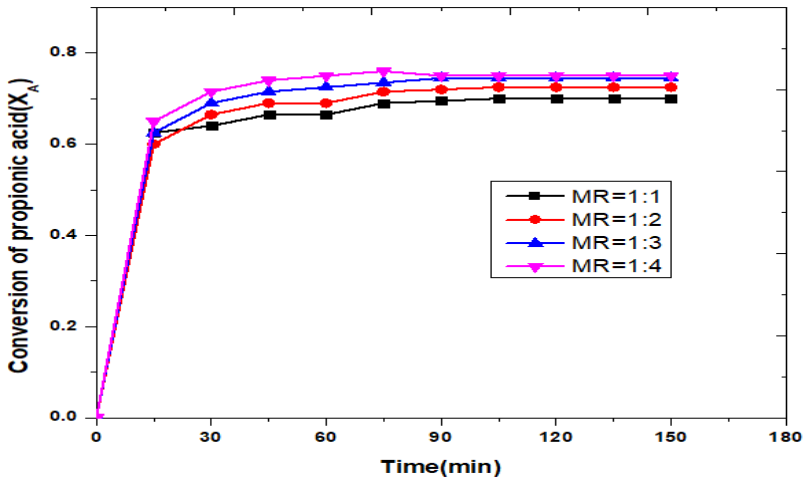

Fig.4.5 Effect of molar ratio on the conversion of Propionic Acid.

4.1.3.3 Effect of temperature

The reaction was carried out at temperatures ranging from 85 to 115oC with an acid-to-alcohol mole ratio of 1:2, a catalyst loading of 2%, and a stirrer speed of 480 rpm. The influence of temperature on propionic acid conversion is depicted in Figure 4.6, which shows that warmth accelerates propionic acid conversion. As a result, it appears that the higher the temperature, the more likely the reaction will quicken in a forward direction. Furthermore, when the temperature increased, the time required for conversion to reach a steady-state decreased.

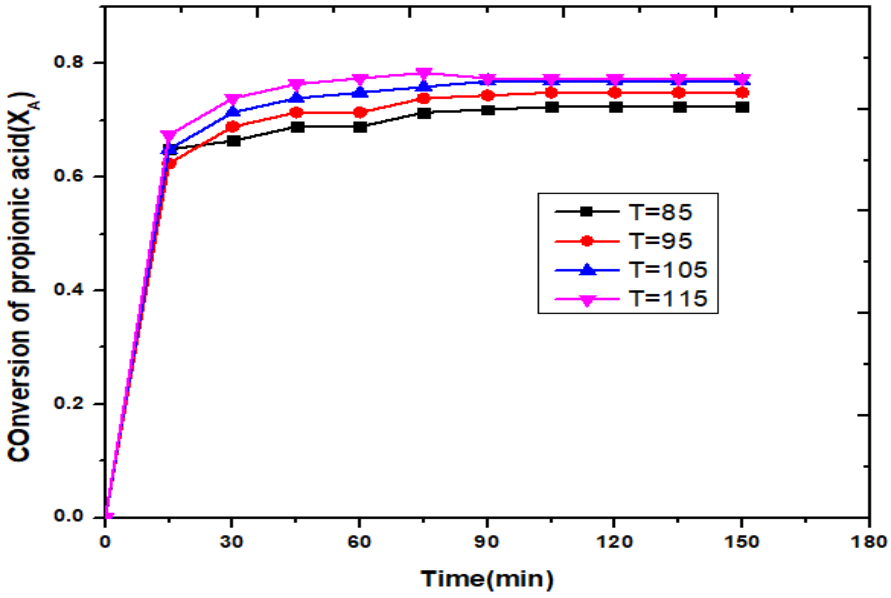

Fig.4.6 Effect of temperature on the conversion of propionic acid.

4.1.4 Esterification reaction by heterogeneous catalyst (Indion-190)

4.1.4.1 Effect of catalyst loading

Catalysts play an essential role in improving total conversion by increasing reaction rates. In this work, catalyst concentration varies from 1% to 3% at 115oC, with a mole ratio of acid to Alcohol of 1:2. Figure 4.7 illustrates propionic acid conversion at various catalyst concentrations, showing that the greater the catalyst concentration, the faster the reaction rate. This is because more active sites (H+) are available in ion exchange resins, improving conversion. It was also found, Propionic acid conversion increased from 1wt% to 3wt% catalyst Concentration. However, increasing the catalyst concentration above 3wt% did not substantially increase propionic acid conversion [1].

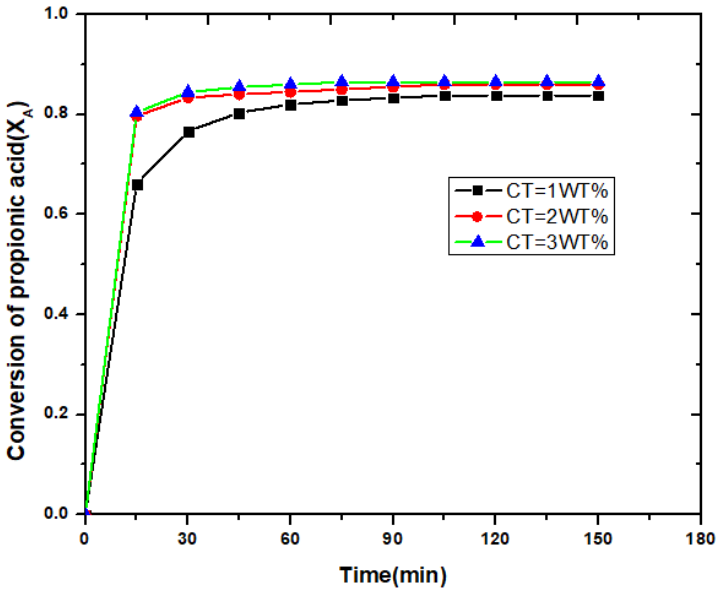

Fig.4.7 Effect of catalyst concentration on the conversion of Propionic Acid.

4.1.4.2 Effect of mole ratio

At Chemical equilibrium limits, the reaction between propionic acid and n-butanol, the equilibrium conversion, determines the amount of ester produced. Excessive alcohol changes equilibrium in the forward direction and increases propionic acid conversion[9]. In this experiment, the mole ratio of acid to alcohol was adjusted from 1:1 to 1:3 at 115oC with a catalyst concentration of 2% and stirrer speed of 480 rpm. Figure 4.8 show that propionic acid conversion increases as the mole ratio increases.

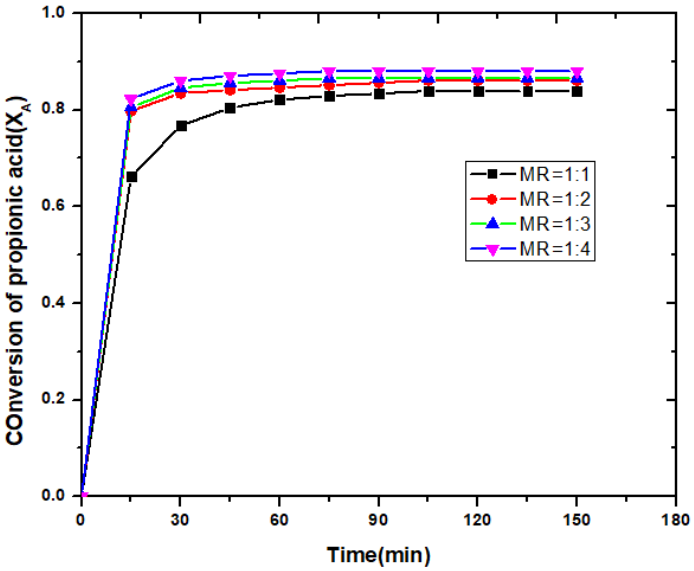

Fig.4.8 Effect of molar ratio on the conversion of Propionic Acid.

4.1.4.3Effect of temperature

The reaction was carried out at temperatures ranging from 85 to 115oC, with an Acid-to-Alcohol mole ratio of 1:2, a catalyst loading of 2%, and a stirrer speed of 480 rpm. Figure 4.9 shows the influence of temperature on the conversion of propionic acid, which was found, that temperature increases propionic acid conversion. As a result, the higher the temperature appears to favor the fastening of the reaction in the forward direction. Furthermore, when the temperature increased, the time required for conversion to reach a steady-state decreased.

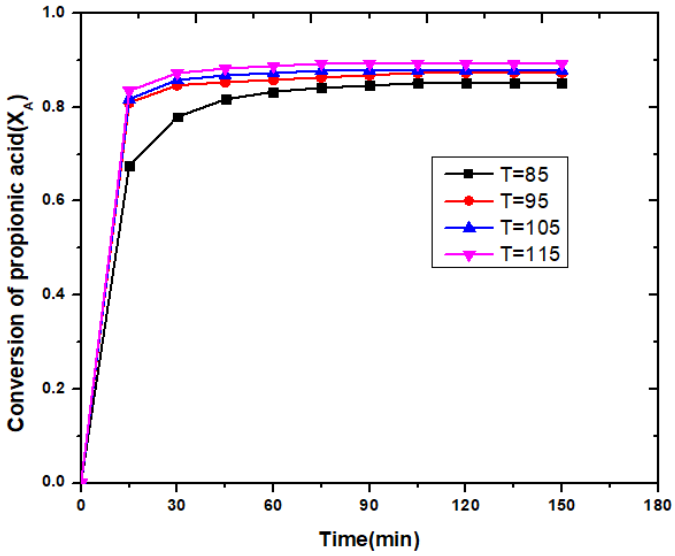

Fig.4.9 Effect of catalyst concentration on the conversion of Propionic Acid.

4.1.5 Esterification reaction by heterogeneous catalyst (Indion-180)

4.1.5.1 Influence of external mass transfer

Experiments were conducted by varying catalyst loading, molar ratio, and stirring speed from 240-720 rpm to explore the impact of internal heat and mass transfer. Conversion at 240 rpm was small, which further improved at 480 rpm. No significant rise of up to 720 rpm was noted after 480 rpm. These findings showed that stirring velocity had a negligible impact on response rate as follows by propionic acid conversion above 480 rpm. This shows a lack of internal resistance to the transfer of mass; thus, all tests were conducted at a stirring velocity 420 rpm.

4.1.5.2 Influence of internal mass transfer

Estimating observable modulus (2) and using the Weisz-Prater criterion as Equation was used to investigate the influence of internal mass transfer resistance (4) [10].

$$\phi = \frac{r^2 k_e}{9 D_e} \tag{4}$$

Where r and k_e are particle catalyst radius and response mechanism rate respectively, D_e is an efficient coefficient of diffusion and can be assessed as Thiele modules.

$$D = \frac{\varepsilon D_e}{\tau} \tag{5}$$

Where catalyst particle porosity and tortuosity are ε and ζ, respectively. In general, resin catalysts for ion exchange range from 0.12 to 0.50. It was 0.12 for Indion-180. D is the coefficient of liquid phase diffusion extracted from the equation Wilke-Chang. The efficacy factor (τ) was assessed from observable modulus by assuming that the original rate was maximum [1].

$$\eta = \frac{tanh\phi}{\phi} \tag{6}$$

D_e, D, Φ and η values are shown in Table ?. The rate is less than 1, and the efficiency factor result is less than 0.999. This describes the lack of resistance to inner mass transfer.

4.1.5.3 Effect of catalyst loading

Catalysts play an important role in improving total conversion by increasing reaction rates. In this work, catalyst concentration varies from 1% to 3% at 115oC, with a mole ratio of acid to Alcohol of 1:2. Figure 4.10 illustrates propionic acid conversion at different catalyst concentrations, showing that the greater the catalyst concentration, the faster the reaction rate. This is because more active sites (H+) are available in ion exchange resins, improving conversion. It was also

found, Propionic acid conversion increased from 1wt% to 3wt% catalyst Concentration. However, increasing the catalyst concentration above 3wt% did not substantially increase propionic acid conversion [10].

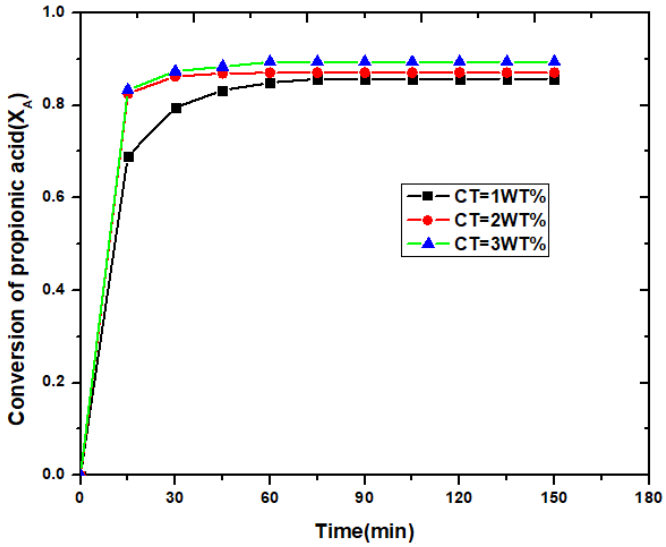

Fig.4.10 Effect of catalyst concentration on the conversion of Propionic Acid.

4.1.5.4 Effect of mole ratio

At Chemical equilibrium limits, reaction between propionic acid and n-butanol, the equilibrium conversion determines the amount of ester produced. Excessive alcohol changes equilibrium in forward direction, increases in propionic acid conversion. [2].In this experiment, mole ratio of acid to alcohol adjusted from 1:1 to 1:3 at 115°C, with a catalyst Concentration of 2% and stirrer speed 480 rpm. Figure 4.11 show that propionic acid conversion is increased as the mole ratio increased.

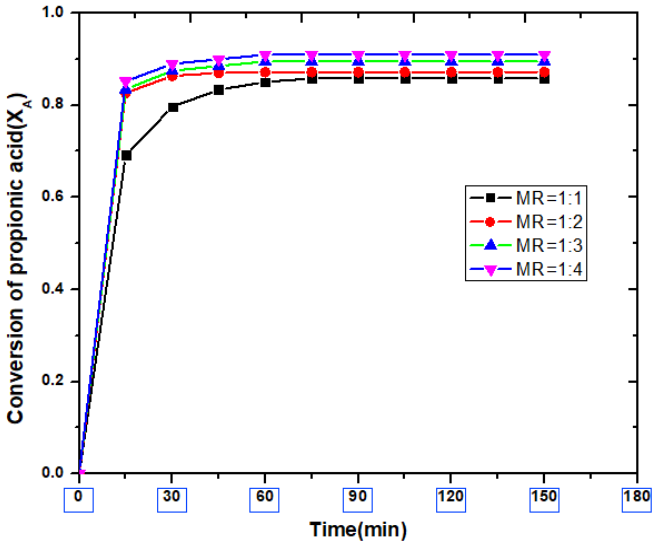

Fig.4.11 Effect of reactant mole ratio on the conversion of propionic Acid.

4.1.5.5 Effect of temperature

The reaction was carried out at a temperature of 85 to 115oC, with a mole ratio of 1:2 acid to alcohol, a catalyst loading of 2%, and a stirrer speed of 480 rpm. Figure 4.12 depicts the effect of temperature on propionic acid conversion, revealing that warmth promotes propionic acid conversion. As a result, it appears that the higher the temperature, the more likely the reaction will fasten in the forward direction. Furthermore, when the temperature increased, the time required for conversion to reach a steady-state decreased.

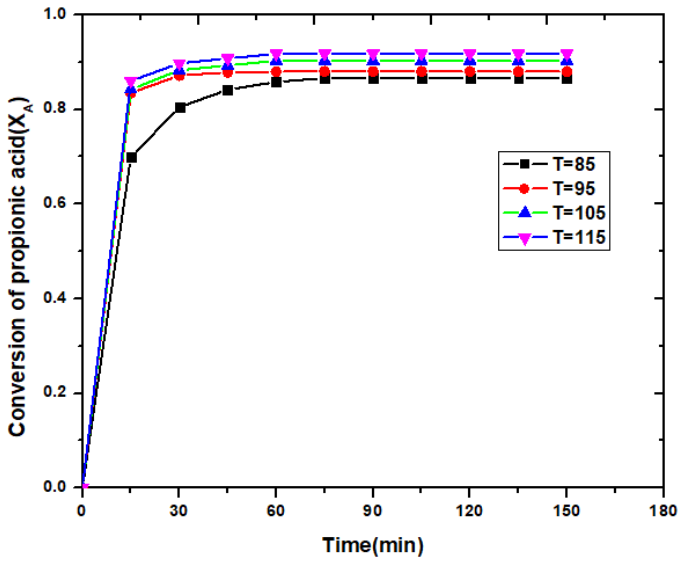

Fig.4.12 Effect of reaction temperature on the conversion of the Propionic Acid

.

4.1.5.6. Comparison of efficiency in solid catalyst for conversion of propionic acid

Amberlite IR-120, Indion-180, and Indion-190 ion exchange resins were utilized in the studies. Experiments were conducted at 115°C with a mole ratio of acid to alcohol of 1:2 and a catalyst concentration of 2wt%. Figure 4.13 depicts the results. Indion-180 sped up the reaction rate and attained the highest conversion, followed by Indion-190 and Amberlite IR-120, with Amberlite IR-120 having the lowest conversion. Differences in H+ ion concentration on the catalyst's surface, as well as the distribution of their pore size, can explain the observed pattern. As a result, Indion-180 was chosen to be studied further as an ion exchange catalyst.

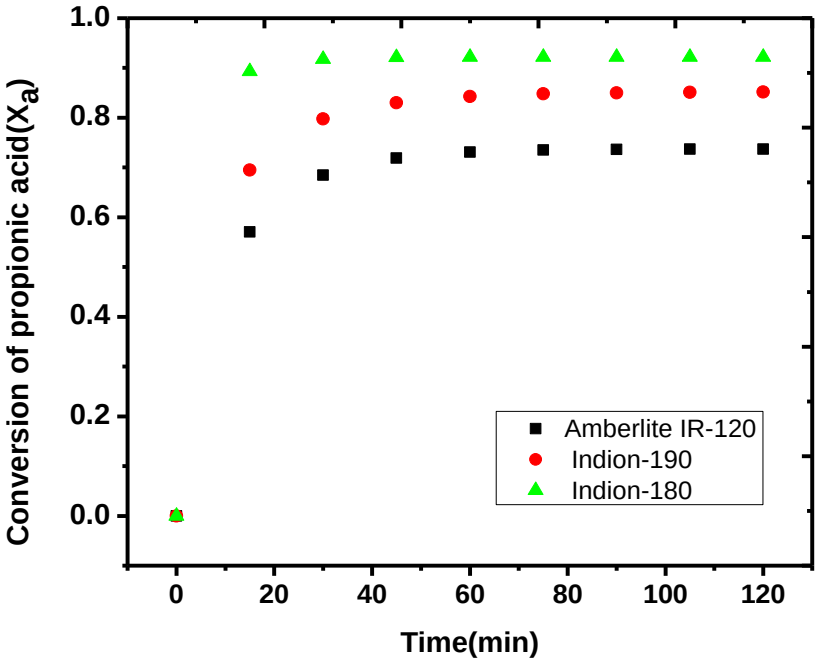

Fig.4.13 Comparing the conversion of the Propionic Acid with different catalyst.

4.2. To synthesize mesoporous catalyst and to evaluate the performance for esterification process

4.2.1 Esterification reaction by the prepared catalyst (Ti SBA-15@SO_3H)

We reviewed the esterification process over commercial ion exchange resins in the previous work. However, commercial resins are typically costly. As a result, an effort was made to create a low-cost, effective solid acid catalyst for the esterification reaction. As a result, the esterification process in this chapter was catalyzed by the Mesoporous catalyst developed in the laboratory. It mainly comprises silica and alumina, with traces of Ca, Mg, Na, Mn, Fe, and Ti oxides [13]. The development of many mesoporous catalysts provided a problem for refuse disposal and environmental management.

4.2.2 Synthesis of mesoporous acid (Ti SBA-15@SO_3H) catalyst

Pluronic P123 is a unique, linearly substituted triblock copolymer composed of polyethylene oxide (PEO) and polypropylene oxide (PPO). In one experiment, 5 g of triblock copolymer (i.e., P123) with structured mesoporous components such as SBA-15 is dispersed in 116.25 g of distilled water and 29.13 g of hydrochloric acid is added to the solution [40-47]. During this steady 24-hour mixing, a final 11 grams of tetra-ethyl-ortho-silicate was added to tetra-iso-propoxide titanium (Si/Ti=100) as an addition of silica. The resultant slurry was mixed with sulphuric acid and washed

with distilled water. The material was dried for 12 hours at 110^{o}C before being calcined for 8 hours at 500^{o}C.

4.2.3 Characterization

The Ultima IV diffractometer (XRD) displays the powdered X-ray diffraction pattern. The following statistical results are acquired within the range of 0.1-5 with a phase of 0.008 ° and a scanning speed of 0.5° per minute, using a non-filtered Cu K radiation source with 30 mA and 40 kV. A scanning electron microscope was utilized for surface morphology research at TESCAN and VEGA 3 LMU in Australia (SEM). The pictures of the samples were analyzed using a JEOL Australia instrument with a 200 kV acceleration voltage. The thermogravimetry/differential thermal analysis was performed using the STA 2500 Regulus NETZSCH, Japan equipment (TG-DTA). Pore size and surface area were measured using the Quanta Chrome Nova-1000 [24-79]. Samples were collected at 1:10 KBr room temperature using 10 FT-IR scans using a PerkinElmer Spectrum 100. The samples were registered using Fourier transform spectra. The sample spectrum was recorded on the Evolution 300 Thermo Science using a UV-Visible Spectrometer and BaSO4 as a reference.

4.2.4 Synthesis of catalyst Ti SBA-15@SO_3H: Mechanism

An ionized particle of propionic acid reacts between a sorbed and un-sorbed molecule of n-butanol. This outcome differed from earlier studies where a single-site method for heterogeneous catalysts was discovered. A pre-adsorbed molecule of n-butanol reacts with an adsorbed particle of propionic acid in the single-site system, whereas both reactant molecules must be solubilized in the dual-site system. The literature reported the adsorption of n-butanol molecules over acidic catalysts for the esterification response. Adsorption of n-butanol molecules over active catalysts for esterification response and other acid-catalyzed responses was recorded in the literature. The response mechanism seems to rely on the nature of the mesoporous catalyst as a technique used in research comparable with distinct catalysts. Active sites on catalyst's comparable distinct supports that can alter n-butanol sorption.

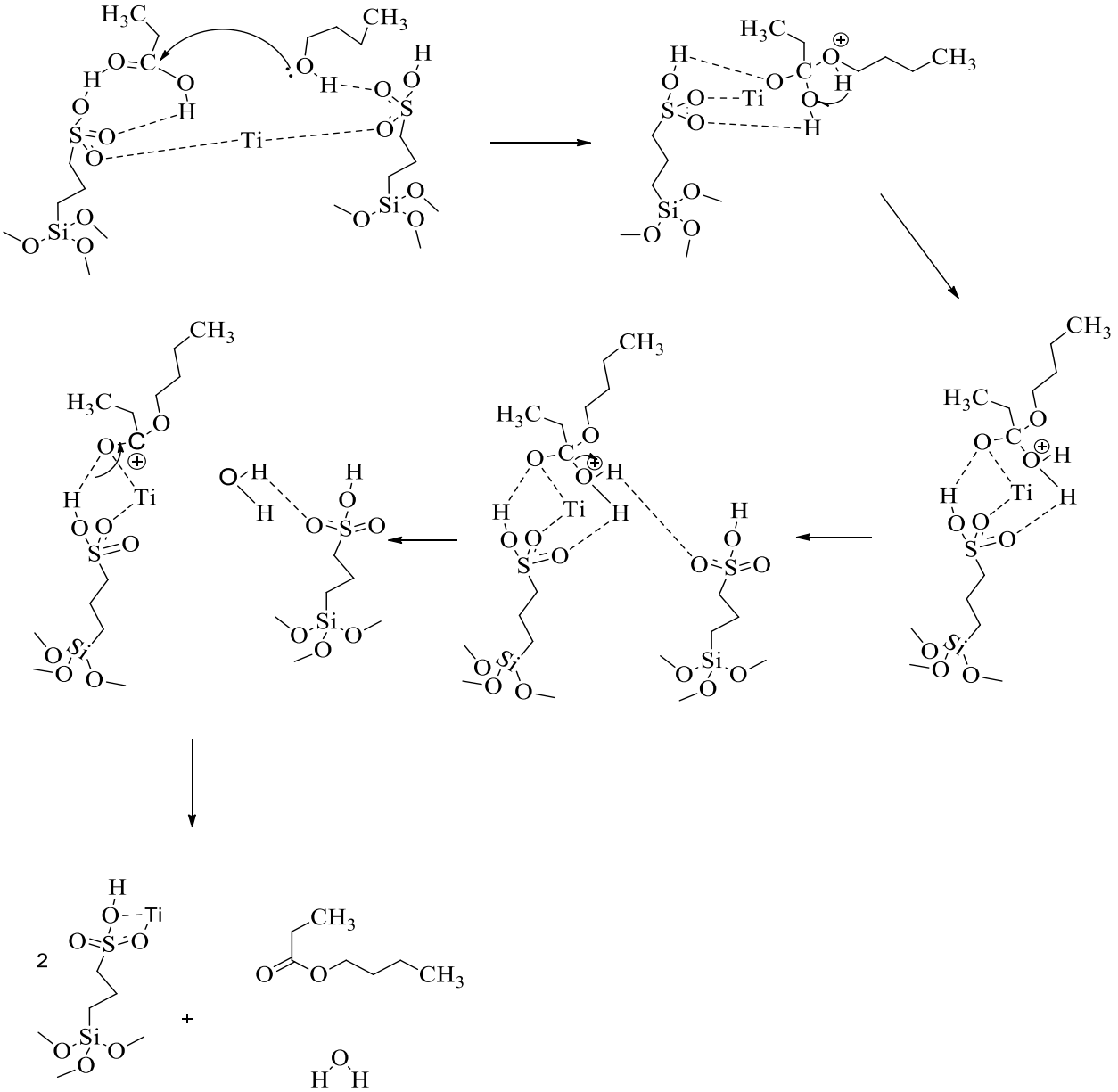

Fig. 4.14 Reaction mechanism for the propionic acid esterification with n-butanol over silica-supported Sulfonated Ti SBA-15

4.2.5.1 Powder X-ray diffraction (XRD)

Figure 4.15 shows the Powder X-ray diffraction (XRD) pattern of Ti-SBA-15-SO3H. Two weak peaks and one strong peak are observed. The two weak peaks are observed at 1.4 and 1.7o, while the sharp peak is observed at 0.8, indicating the periodicity of the high mesoporous structures due to more significant condensation between the silanol and titanium groups observed [122]..

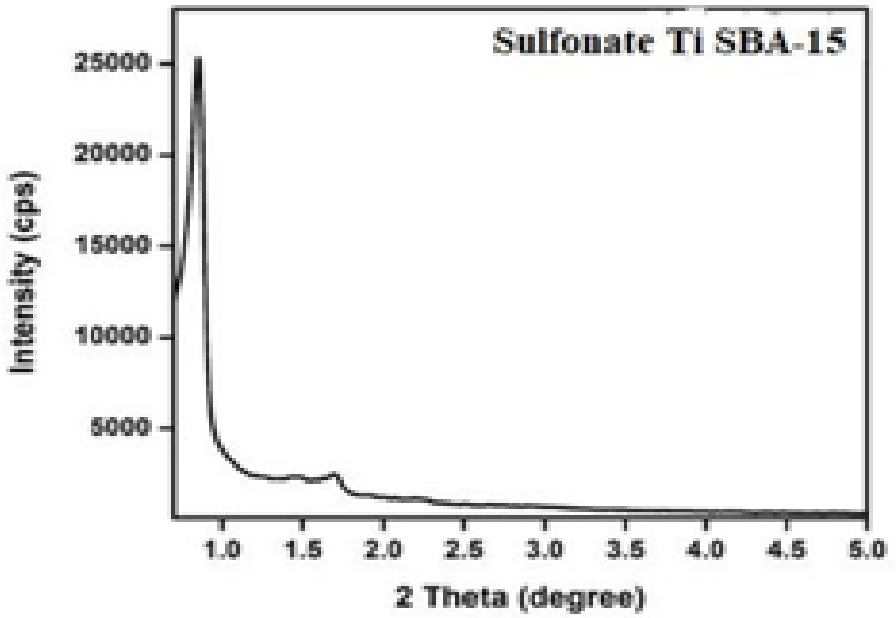

Fig. 4.15 Small-angle XRD pattern of Ti Supported SBA-15 functionalized with sulfonic acid

4.2.5.2 Transmission electron micrograph analysis (TEM)

The Figure 4.16 (Ti-SBA-15-SO3H) shows that a hexagonally well-organized mesoporous catalyst which has a porous structure with a parallel channel[44]. Furthermore, the uniform particle size and shape of the sulfonated silica materials and long-range mesoporous order are identified in Ti-SBA-15-SO_3H.

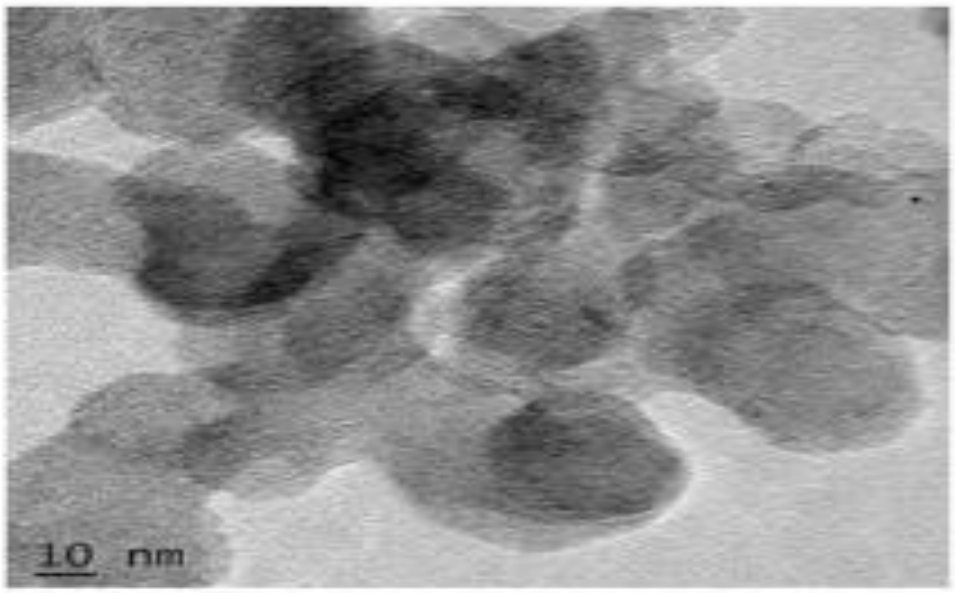

Fig. 4.16 TEM images of Ti Supported SBA-15 functionalized with sulfonic acid

4.2.5.3 Thermogravimetry/Differential thermal analysis

The TG-DTA of Ti-SBA-15-SO_3H is shown in Figs 4.17 and 4.18. It explains the early weight loss (4.31 %) from 0 to 300°C is due to the loss of Physisorbed water and ethanol molecules. The rapid weight loss between 350 and 600 °C (58.75 %) due to the loss of decomposed SO_2. A significant exothermic peak with a temperature of 308.7°C has been observed. There is no significant weight loss seen in the Ti-SBA-15-SO_3H at 500-700°C. The Ti-SBA-15-SO_3H composites are also thermally stable up to 700°C.

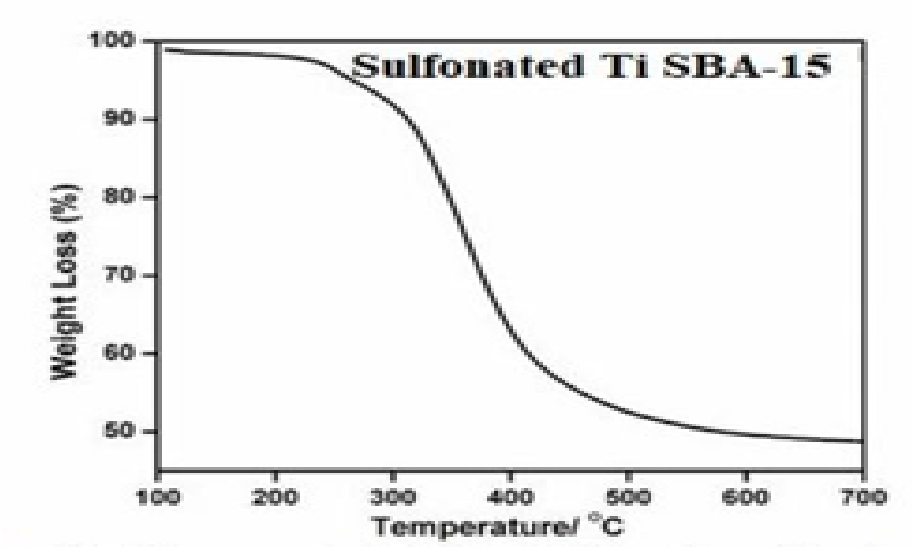

Fig. 4.17 TGA analysis of Ti Supported SBA-15 functionalized with sulfonic acid

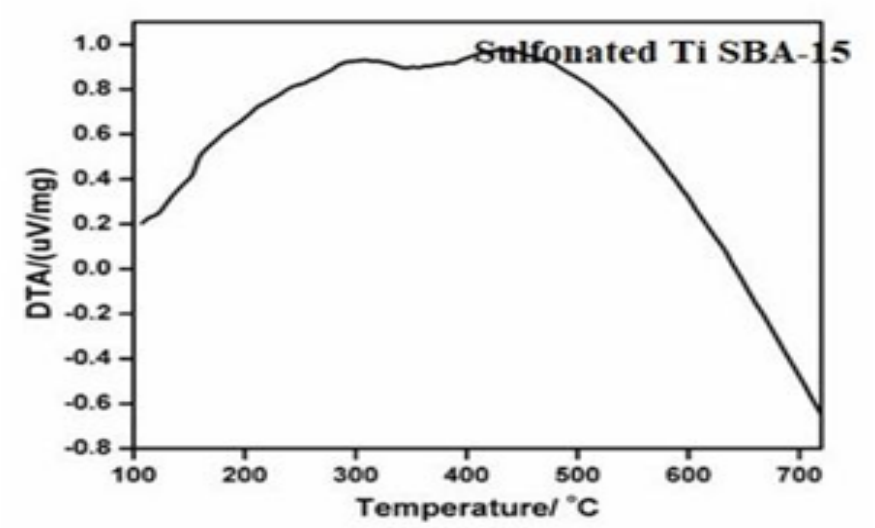

Fig. 4.18 DTA analysis of Ti Supported SBA-15 functionalized with sulfonic acid

4.2.5.4 *N_2 adsorption-desorption studies*

N_2 Adsorption isotherms of Ti-SBA-15-SO_3H are shown in Fig. 4,19. This is demonstrated by mesoporosity as type IV nitrogen isotherms with the H1 hysteresis loop. When Ti is introduced into the SBA-15 framework, the distribution of mesoporous diameters expands. The pore size

distribution curve was used to confirm these findings. The results show that when Ti was included in the SBA-15 with a Sulfonic acid framework, the uniformity of the mesoporous size distribution reduced. It was also revealed that increasing the incorporation of Ti into the SBA-15 with Sulfonic acid samples resulted in a significant decrease in pore volume, surface area, pore diameter, and peak intensities. This might be due to titanium-based mesoporous channels blocking the flow observed. Table 4.1 shows the BJH pore size distribution method and the BET surface analysis.

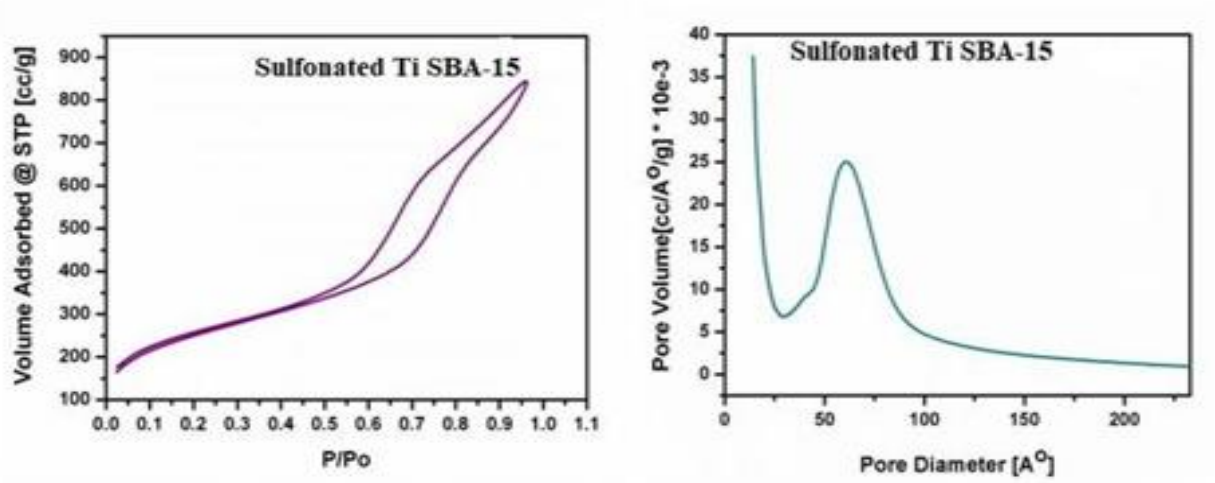

Fig.4.19 Ti Supported SBA-15 functionalized with sulfonic acid with adsorption/desorption isotherms, pore diameter and pore volume distribution

Table 4.1: BET – isothermic adsorption and porosity data

Mesoporous Material	**Pore Volume (cc/g)**	**Average Pore Diameter (nm)**	**Surface Area (m^2/g)**
Ti-Supported SBA-15 functionalized with Sulfonic acid	1.02	3.178	0.457

4.2.5.5 Fourier transforms infrared spectroscopic Analysis (FT-IR)

Fig. 4.20 shows the FT-IR spectrum of Ti-SBA-15-SO_3H. The 1088 cm^{-1} signal indicates the presence of a Si-O-Si bond in a Ti SBA-15 fused sulfonated binding. The symmetrically stretching vibrations of Si–O–Si was 802 cm^{-1} and 466 $cm^{-1,}$ respectively. Peaks at 910 and 960 cm^{-1} came from the vibration of Ti-O-infrastructure Si, indicating that Ti is clearly indicated in the SBA-15 matrix. The precise location of the images was discovered to contribute to the chemical composition and the calibration and resolution of the equipment utilized in the research. The highest band strength in the Ti-Supported SBA-15 catalyst is 960 $cm^{-1.}$ Breaks between the silanol groups and the water molecules adsorbed were seen at 1630 and 3400 cm^{-1} due to hydrogen interaction (SI-OH). Peaks at 1052 and 1140 cm^{-1} demonstrate that the functional groups -SO_3H

similar to the observations made by ridhawati & Tahir[122]exhibit symmetrical and asymmetrical vibrations, respectively.

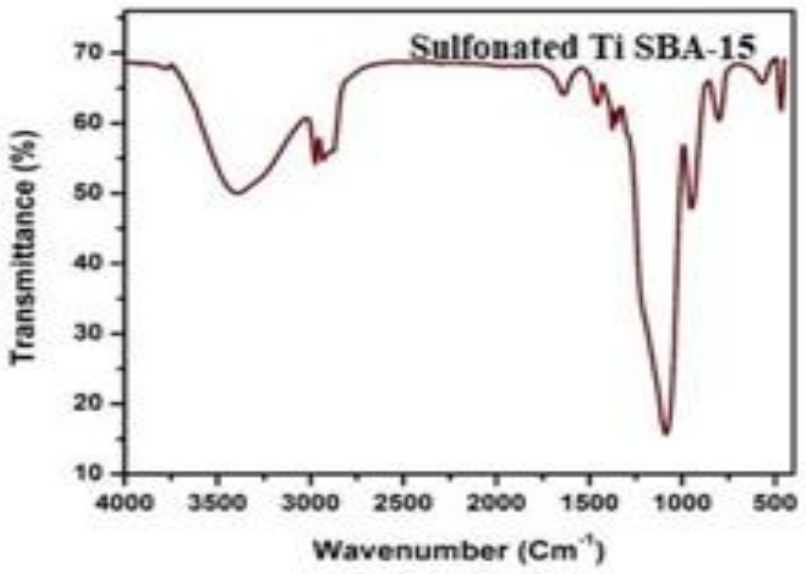

Fig.4.20 FTIR analysis of Ti Supported SBA-15 functionalized with sulfonic acid

4.2.5.6 Diffuse reflectance Ultraviolet-Visible spectroscopic analysis

Fig. 4.21 shows the UV-Vis-DRS spectrum of Ti-SBA-15- SO_3H. Two significant peaks of 210-230 nm and 330-350 nm were detected and restricted to the presence and integration of the tetrahedral environment and the homogenous distribution of Ti ions.

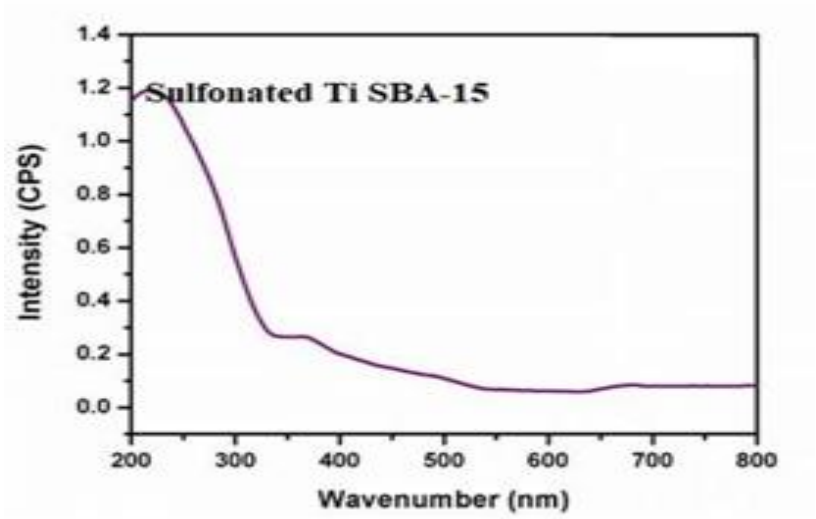

Fig.4.21 Ti Supported SBA-15 functionalized with sulfonic acid UV-Vis-DRS study

4.2.6 Reaction study

To study the activity of the prepared catalyst, equal moles, i.e., one mole of propionic acid and one mole of n-butanol, were fed with 0.5g of catalyst in a round bottom glass reactor. The reactor was rapidly heated to the test temperature, with a turn rate of 480 rpm spread over four hours. Additional information on the reaction may be obtained elsewhere to separate the catalytic characteristics of the Ti and the group from those of the SBA-15. Because esterification is an endothermic process, they are assessed to 115°C for varied reaction durations. As a result, propionic acid and n-butanol are miscible at this temperature in the absence of mass transport constraints. The three most active materials were chosen for deactivation studies at 115 °C. These materials have been thoroughly researched and have exhibited the best catalytic activity and resistance. The equilibrium constants have been established as well. The Propionic Acid percentage titration with NaOH was employed in the experimental conversion (0.1 N).

4.2.6.1 Effect of catalyst loading

Catalysts play an important role in improving total conversion by increasing reaction rates. In this work, catalyst concentration varies from 1% to 3% at 115oC, with a mole ratio of acid to Alcohol of 1:2. Figure 4.22 illustrates propionic acid conversion at various catalyst concentrations, showing that the greater the catalyst concentration, the faster rate of reaction. This is because more active sites (H+) are available in ion exchange resins, improving conversion. It was also found, Propionic acid conversion increased from 1wt% to 3wt% catalyst Concentration. However, increasing the catalyst concentration above 3wt% did not substantially increase propionic acid conversion [2].

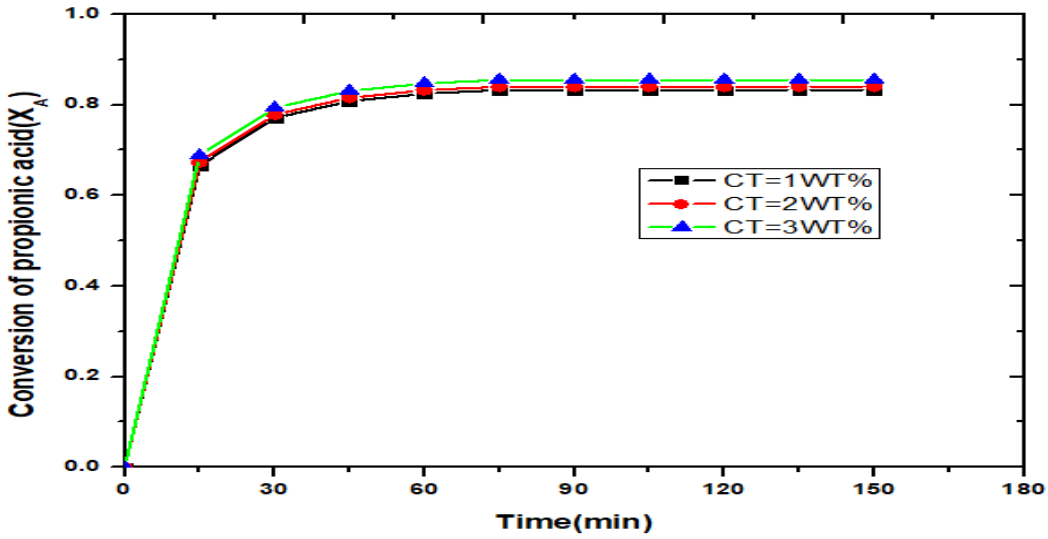

Fig.4.22 Catalyst effect on propionic acid conversion

4.2.6.2.1 Effect of mole ratio

At Chemical equilibrium limits, the reaction between propionic acid and n-butanol, the equilibrium conversion, determines the amount of ester produced. Excessive alcohol changes equilibrium in the forward direction and increases propionic acid conversion[2]. In this experiment, the mole ratio of acid to alcohol was adjusted from 1:1 to 1:3 at 115oC, with a catalyst concentration of 2% and stirrer speed 480 rpm. Figure 4.23 show that propionic acid conversion increases as the mole ratio increases.

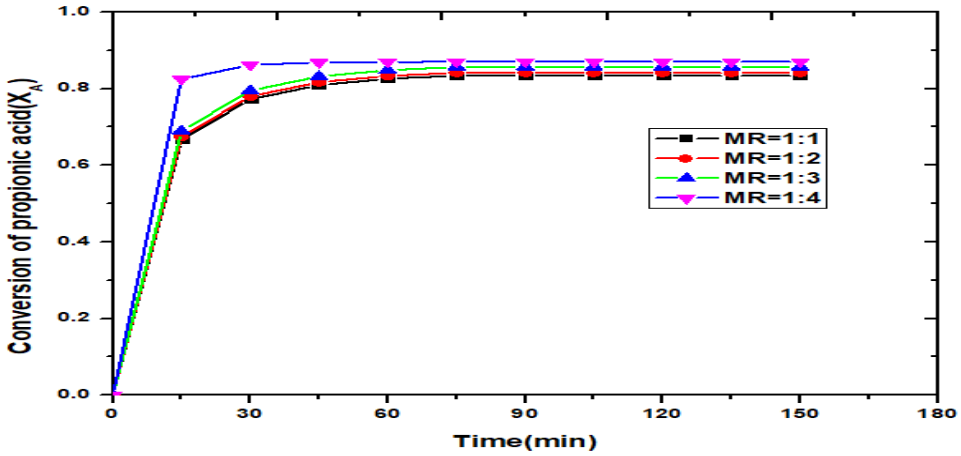

Fig.4.23 Molar ratio effect on propionic acid conversion

4.2.6.3 Effect of temperature

The reaction was carried out at a temperature of 85 to 115oC, with a mole ratio of 1:2 acid to alcohol, a catalyst loading of 2%, and a stirrer speed of 480 rpm. Figure 4.24 depicts the effect of temperature on propionic acid conversion, revealing that warmth promotes propionic acid conversion. As a result, it appears that the higher the temperature, the more likely the reaction will fasten in the forward direction. Furthermore, when the temperature increased, the time required for conversion to reach a steady-state decreased.

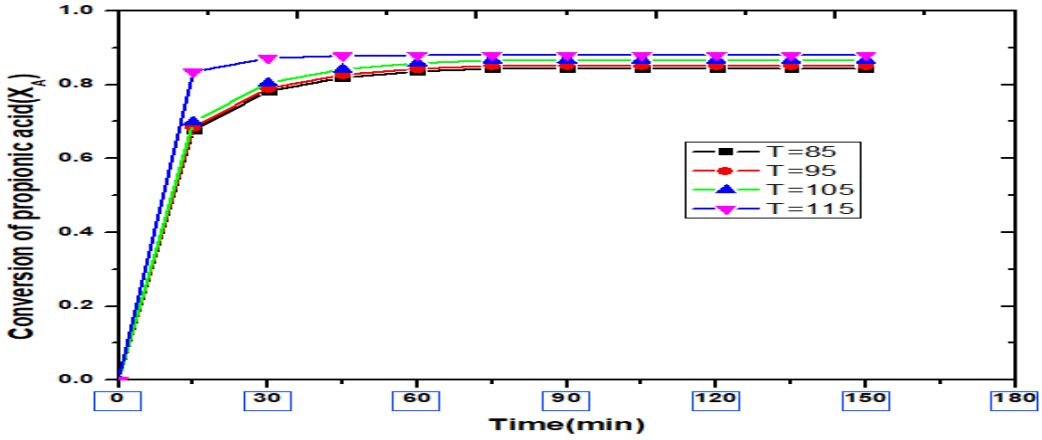

Fig.4.24 Temperature effect on propionic acid conversion

4.3 Modelling and simulation

A rate expression for catalytic esterification is required to design a reactive distillation column. Such a rate expression should account for various operating conditions. The kinetic models are developed based on existing literature, starting with a simple elementary reaction to adsorption-based model.

The next sections explain the various modelling methodologies for reaction kinetics in a batch reactor for the esterification of Propionic acid with n-Butanol in the presence of liquid and solid catalysts. First, for liquid catalysts homogeneous concentration-based model is developed based on the literature approach. For solid catalysts, pseudo homogeneous and adsorption-based models are fitted using the literature approach.

4.3.1 Concentration based model

The reaction mechanism of propionic acid and n-butanol to produce n-butyl propionate and water was modeled as a first-order reversible process. The chemical mechanism for propionic acid esterification reaction [20]. For the proposed esterification process, a similar mechanism was explored. The proton donor in the esterification process was considered P-Toluene sulfonic acid. Based on this approach, the reaction rate equation is as follows [20]:

The representation of the esterification of reaction for the catalyzed process is shown below.

$$A + B \underset{k_2}{\overset{k_1}{\rightleftarrows}} C + D \tag{7}$$

$$-r_A = k_1\left[C_A C_B - \frac{C_C C_D}{K_e}\right] \tag{8}$$

The Eq. (5) is rearranged in terms of reactant conversion, the rate equation is modified as

$$-r_A = C_{A0}\frac{dX_A}{dt} = k_1 C_{A0}^2\left[(1-X_A)(M-X_A) - \frac{X_A^2}{K_e}\right] \tag{9}$$

Where M= C_{B0}/C_{A0}.

The Eq. (6) arranged to linear form, the equation is

$$\ln\left[\frac{(1+M+\eta_2-2\eta_1 X_A)(1+M-\eta_2)}{(1+M-\eta_2-2\eta_1 X_A)(1+M+\eta_2)}\right] = \eta_2 k_1 C_{A0} t \tag{10}$$

$$\eta_1 = 1 - \frac{1}{K_e} \tag{11}$$

$$\eta_2 = \left[(M+1)^2 - 4\eta_1 M\right]^{0.5} \tag{12}$$

The Ke values at different temperatures are determined from steady sate data using Eq. (11) as below.

$$K_e = \frac{X_{Ae}^2}{(1 - X_{Ae})^2} \tag{13}$$

Where X_{Ae} is equilibrium conversion of propionic acid. The reaction rate constant k_1 value obtained at different temperatures by plotting the LHS of Eq.(8) on y-axis is represented as Y. The straight line measurement is a confirmation of the kinetic model's fitness. It shows that the model is well-suited to the system's conditions.

The forward reaction rate constants, k1 are found from slope of straight lines in Fig.4.25at 2% and at different temperatures.

$$k_1 = k_{01} \exp\left(\frac{-E_1}{RT}\right) \tag{14}$$

$$k_2 = k_{02} \exp\left(\frac{-E_2}{RT}\right) \tag{15}$$

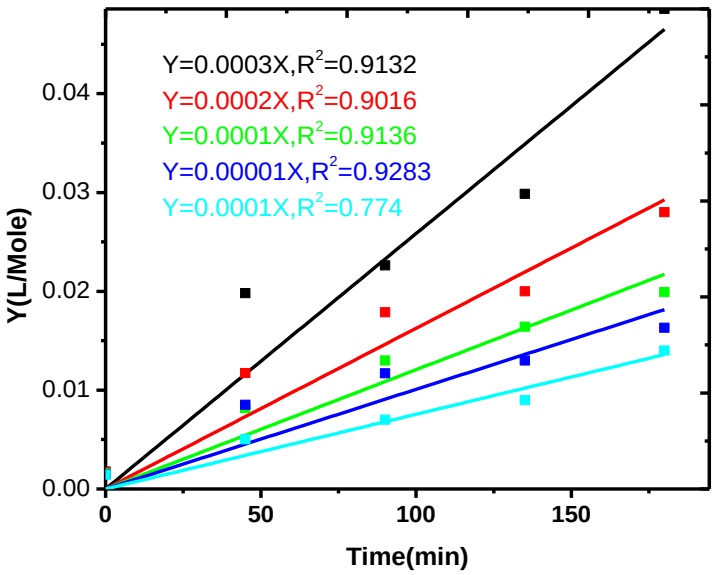

Fig.4.25 Linear regression to fit Eq. (5.6) as s straight line for finding forward reaction rate constant(kf) from the slopes at various temperatures**.**

The temperature dependent reaction rate and forward activation energy are found to be as

$$k_1 = \exp\left[2.612 - \frac{3729.0}{T}\right] \tag{16}$$

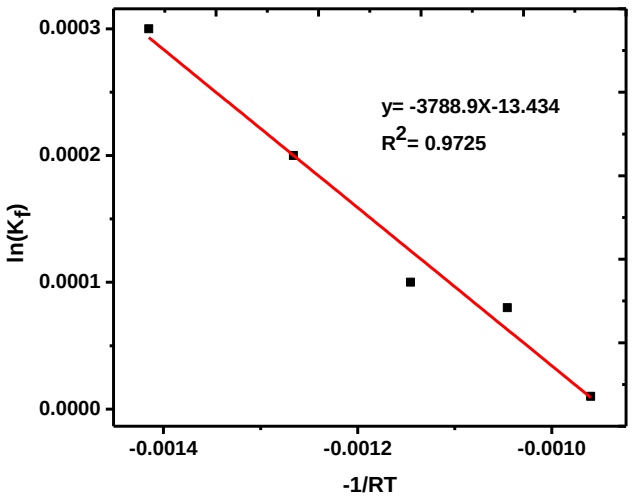

Fig.4.26 Plot of Arrhenius equation for determination of activation energy and pre-exponential constant.

The equilibrium constant is calculated as the temperature dependence of the ln(K_f). The slope of the line is also calculated and the activation energies is 3.788kJ/mol evaluated using this figure 4.26. The pre-exponential constant is 13.4 kJ/mol.

The heat of a reaction is calculated from Van't Hoff equation as given below.

$$\ln K_e = \frac{-\Delta H_R}{RT} - \frac{\Delta S_R}{R} \tag{17}$$

The Van't Hoff equation shows the equilibrium constant temperature effect. It is used for analyzing the heat of reaction.

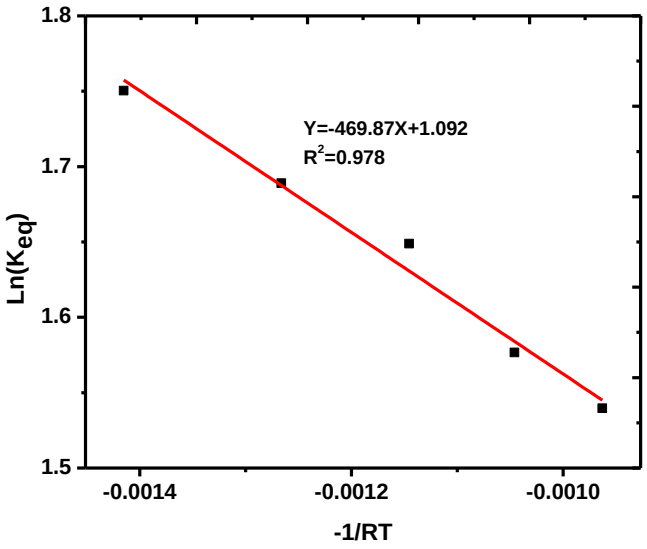

Fig.4.27 Plot of Ventoff's equation for determination of heat of reaction and enthalpy.

The equilibrium constant is calculated as the ln(Ke) temperature dependence. The slope of the line is also calculated, and the heat of the reaction is evaluated using this figure 4.27. The present reaction's heat is 28.414 kJ/mol, indicating an endothermic reaction.

Table 4.2: Reaction rate constants

Temperature	K	k_f (L/mol-min)	k_b(L/mol-min)
358	5.6574	0.0003	$6.432*10^{-5}$
368	5.614	0.0002	$4.132*10^{-5}$
378	5.2012	0.0001	$1.922*10^{-5}$
388	4.839	0.00008	$1.42*10^{-5}$
398	4.663	0.0001	$1.76*10^{-5}$

4.3.2 Kinetic Model:

4.3.2.1 Pseudo homogeneous model

In the presence of Ti SBA-15@SO3H catalyst, the propionic acid (PA) esterification response with N-butanol (NB) for the synthesis of butyl propionate (BP) and water (W).

PA + NB ←-------→ BE + W (18)

An independent kinetic analysis was carried out under optimal operating circumstances, with the findings displayed in Figures 4.29 and 4.30. Internal and external limitations on mass transport were absent. Butyl propionate (BP) formation may be split into three separate steps

PA + C ←-------→ PA.C; $-r_1 = k_1 C_{PA} C_C - k_{-1} C_{PA} C_C$ (19)

PA.C + NB ←--------→ BE.C + W; $-r_2 = k_2 C_{PA.C} C_{NB} - k_{-2} C_{BE.C} C_W$ (20)

BE.C ←-----→ BE + W; $-r_3 = k_2 C_{BE.C} C_{NB} - k_{-3} C_{BE} C_C$ (21)

$$-r_a = -r_2 = \frac{k_2 K_1 C_t \left(C_{PA.C} C_{NB} - \frac{k_{-2} C_{BE.C} C_W}{K_{eq}} \right)}{(1 + k_1 C_{PA} + k_{-3} C_{BE})} \quad (22)$$

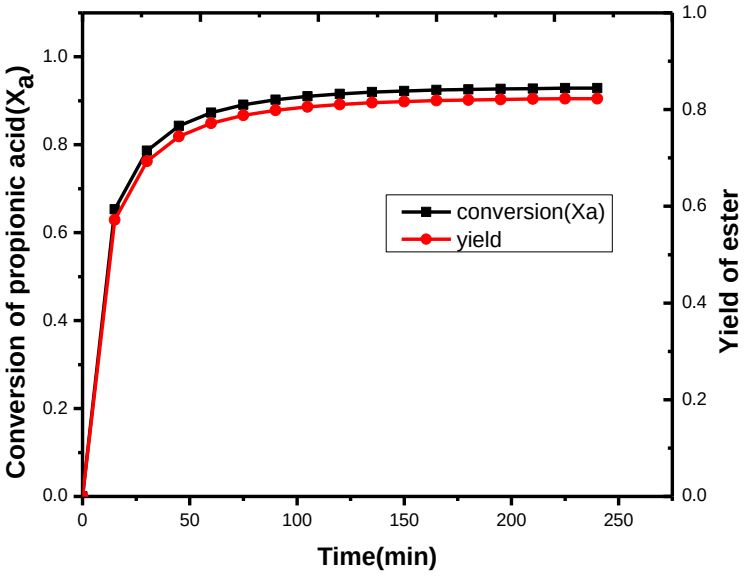

Fig.4.28 Conversion and yield of ester Vs Time

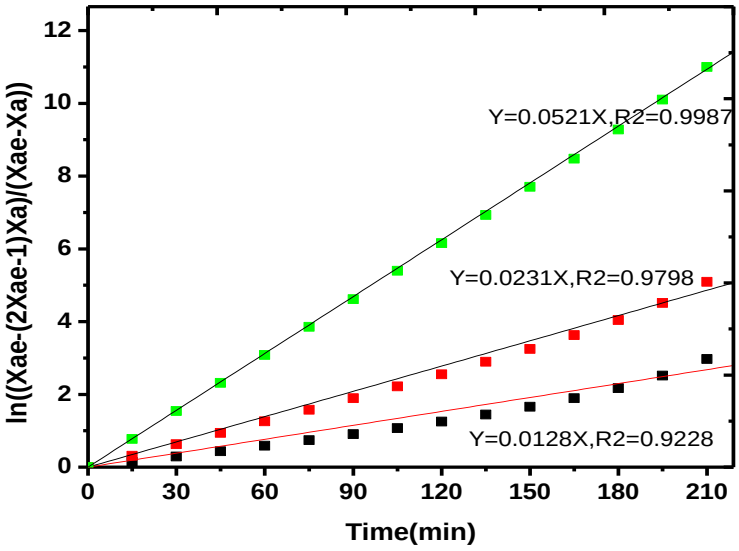

Fig.4.29 Linear regression to fit Eq. (5.6) as s straight line for finding forward reactionRate constant (kf) from the slopes at various temperatures.

$$K_{eq} = \frac{C_{BE}C_W}{C_{PA}C_{NB}} = \frac{X_{eq}^2}{(1-X_{eq})(M-X_{eq})} \quad (23)$$

$$-r_a = -r_2 = k_a\left(C_{PA.C}C_{NB} - \frac{k_{-2}C_{BE.c}C_W}{K_{eq}}\right) \quad (24)$$

$$k_a = k_2K_1C_t \quad (25)$$

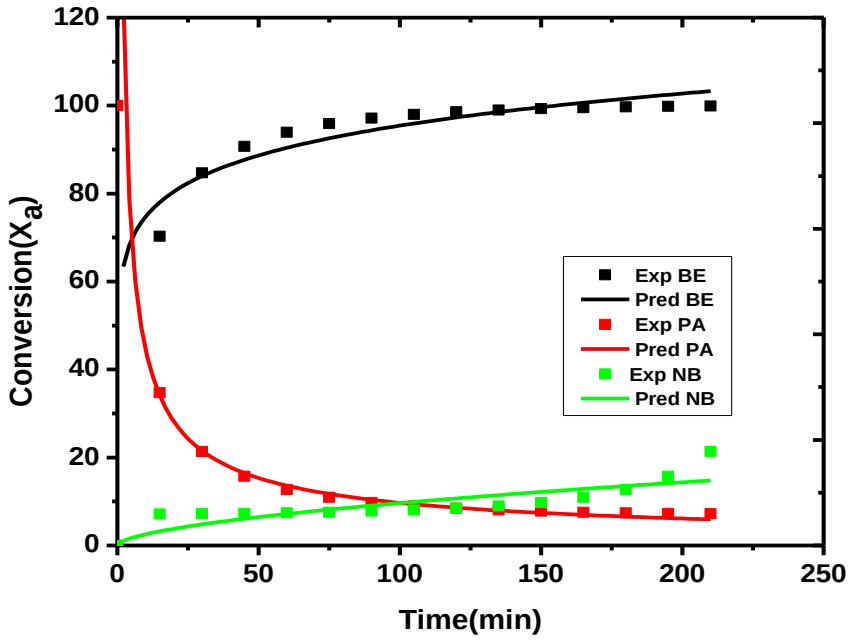

Fig.4.30 Conversion Vs Time

Using the regression technique, the constant reaction rate, K1, may be calculated for the information received under ideal process conditions using Equation. The equation was also used to calculate the response rate using the resultant equation. A plot of experimental and anticipated data is shown in Figure 4.30.

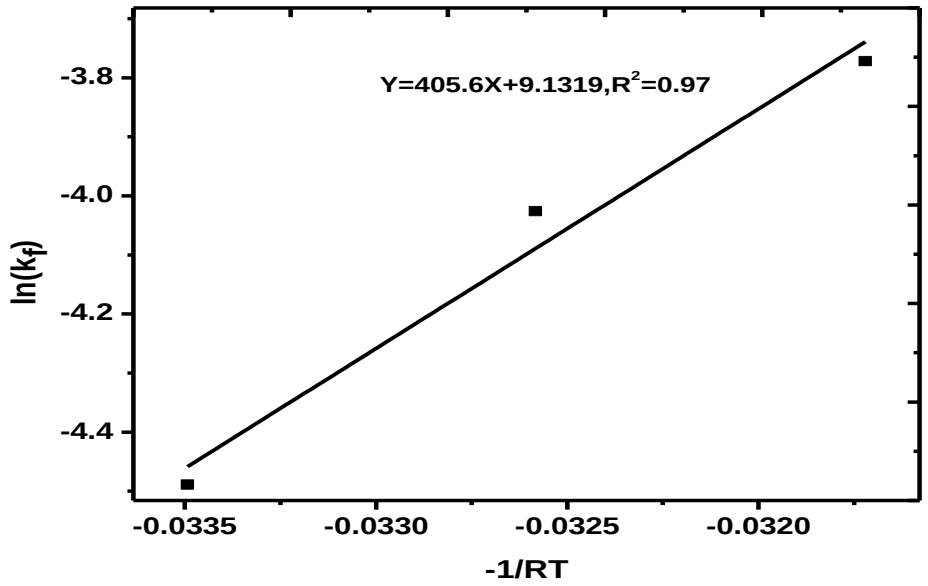

Fig.4.31 Linear regression to fit Eq. (5.6) as s straight line for finding forward reaction rate constant (kf) from the slopes at various temperatures.

4.3.3 Eley-Rideal model: The Ti-supported sba-15 functionalized with sulfonic acid for the kinetic analysis and the thermodynamic parameters

4.3.3.1 Mathematical Model

The interfacial area between the catalyst particles and the liquid is not considered in the previous pseudo-homogeneous model. If the reaction is assumed to occur just on the catalyst surface, as proposed by (Song et al., 1998; Popken et al., 2000), then two surface adsorption models, Eley-Rideal (E-R) and Langmuir-Hinshelwood-Hougen-Watson (LHHW) might be used. The LHHW model suggests that the reaction occurs primarily between the two adsorbed reactant molecules on the catalyst surface. On the other hand, the ER model proposes that the reaction occurs between one adsorbed reactant molecule and another non-adsorbed reactant molecule.

$$H_6O_2 + S \leftrightarrow C_3H_6O_2.s \quad (26)$$

$$C_3H_6O_2.s + C_4H_{10}O \leftrightarrow E.s \quad (27)$$

$$E.s + B \rightarrow D.s + W \quad (28)$$

Desorption of products

$$D.s \leftrightarrow D + s \quad (29)$$

The following kinetic model equations are based on adsorption:

$$r_D = \frac{C_T k_5 K_1'' K_{C_3H_6O_2} C_{C_3H_6O_2} C_B}{1+K_{C_3H_6O_2} C_{C_3H_6O_2} + K_W C_W + K_D C_D} \quad (30)$$

$$\frac{dX_{C_3H_6O_2}}{dt} = C_T k_5 K_1'' K_{C_3H_6O_2} C_{C_3H_6O_2,o}^2 (1 - X_{C_3H_6O_2})(\gamma - 2X_{C_3H_6O_2}) \quad (31)$$

$$\frac{1}{(\gamma-2)} ln \frac{\gamma-2X_{C_3H_6O_2}}{\gamma(1-X_{C_3H_6O_2})} = k_1'' t \quad (32)$$

$$f_2(X_A) = k_1'' t \quad (33)$$

Mechanism 2:

$$B + s \leftrightarrow B.s \quad (34)$$

$$C_3H_6O_2 + B.s \leftrightarrow E.s \quad (35)$$

$$E.s + B.s \rightarrow D.s + W.s \quad (36)$$

Desorption of products

$$D.s \leftrightarrow D + s \tag{37}$$

$$W.s \leftrightarrow W + s \tag{38}$$

$$r_D = \frac{C_T^2 k_6 K_1''' K_B^2 C_{C_3H_6O_2} C_B^2}{\left(1+K_{C_3H_6O_2} C_{C_3H_6O_2} + K_W C_W + K_D C_D\right)^2} \tag{39}$$

$$\frac{1}{(\gamma-2)^2}\left[\frac{(2-\gamma)}{(\gamma-2X_{C_3H_6O_2})\gamma} + ln\frac{(\gamma-2X_{C_3H_6O_2})}{\gamma(1-X_{C_3H_6O_2})}\right] = k'''t \tag{40}$$

Different levels of propionic acid and n-Butanol has shown in figure 4.32 were observed at the initial reaction rate($r_{Ao} = \frac{\Delta C_{Ao}}{\Delta_t}$) specific for conversion by 2%. The concentrations have been modified to account for the reaction mixtures' non-ideal behaviour [40]. The general kinetic expression for the catalyzed heterogeneous esterification reaction can be written as Eq.(40):

$$-r_A = \frac{k_f w_{cat}(a_A a_B - \frac{a_R a_w}{K_{eq}})}{(1 + K_A a_A + K_B a_B + K_E a_E + K_w a_w)^n} \tag{41}$$

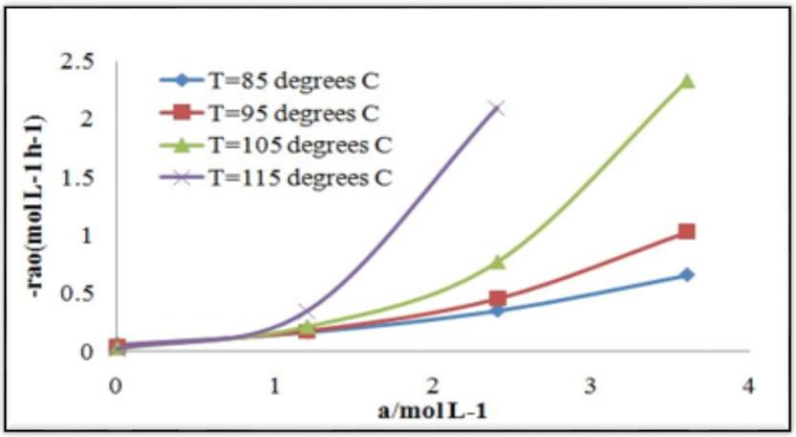

Fig.4.32 The effect on the initial reaction rate (-r_{A0}) at different temperature on the charging of catalyst.

For those of the rA reaction rate, the catalyst (wcat) weight for the dry catalyst number. Propionic acid, n-butanol, butyl propionate, and Water are represented as A, B, E, W.K is the adsorption constant, Ke is the constant equilibrium response rate, and kf is the constant rate, while n = 0 in the PH model, 1 in the ER model, and 2 in the LHHW. The starting reaction rate instead of the plated one is a linear feature, which means the adsorption of propionic acid on the Ti-Supported SBA-15 functionalized with Sulfonic acid catalyst surface is impossible at the same time. The initial rate of reaction increases in line with n-butanol concentrations. Therefore, we can infer that at low concentrations of n-butanol, it adsorbed n-butanol extremely low and almost continuously increases the concentration. This study concludes that the reaction mechanism is defined in the Eley-Rideal model, i.e., the reaction between adsorbed butanol molecules and propionic acid

molecules in the bulk solution. The literature found the solvent (dioxane) and ester adsorption insignificant. The rate-determining step is to take the stoichiometric and corresponding reaction rate as the Ely-Rideal (ER) model of a surface-reaction eq, after excluding the adsorption of acid and ester re-activities. The ER form can be written as Eq.(41)

$$-r_A = \frac{k_f w_{cat}(a_A a_B - \frac{a_R a_w}{K_{eq}})}{(1 + K_B a_B + K_w a_w)} \qquad (41)$$

A, B, E, W are propionic acid, n-butanol, butyl propionate and waters, respectively. In (L^2g^{-1} $mol^{-1}h^{-1}$) the kf is indicated as $k_i = k_i^o exp^{(\frac{-E_i}{RT})}$,$w_{cat}$ is catalyst weight in g L^{-1}, K is the constant adsorption, and Ke is the constant esterification reaction equilibrium, based on activity Ti-Supported SBA-15 functionalized with Sulfonic acid .

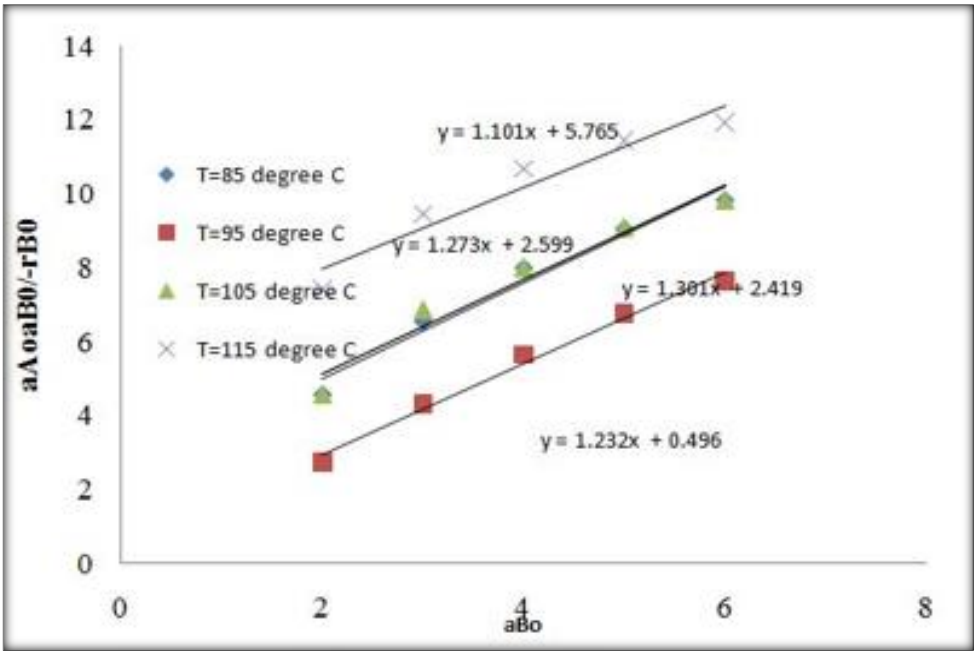

Fig.4.33 $\frac{a_{A0}a_{B0}}{-r_{A0}}$ versus $a_{B,0}$ at different temperature

Eq.(3) behavior is used for speed expression rather than concentration because the models' predictions adapted to the measured film data result in improved prediction[22]. Relocation of the eq. 41 can be described as eq for the initial reaction rate without a product present, shown in Eq.(42):

$$\frac{a_{Ao}a_{Bo}}{-r_{Ao}} = \frac{1}{(k_f w_{cat})} + \frac{K_B}{k_f w_{cat}} a_{Bo} \qquad (42)$$

Fig4.34 shows Plot of $\frac{a_{Ao}a_{Bo}}{-r_{Ao}}$ versus $a_{B,o}$ results in a direct slope line $\frac{K_B}{k_f w_{cat}}$ and intercept $\frac{1}{k_f w_{cat}}$ as shown in figure.

Slopes and intercepts in these figures indicates the constants in rates and adsorption constants k_F, K_B, K_W and their estimated values at three temperatures are shown in Table 2.

4.3.3.2 Activation energy and rate constants

The Arrhenius Law expresses the dependence of rate on temperature with the following:

$$k_i = k_i^o exp^{\left(\frac{-E_i}{RT}\right)} \qquad (43)$$

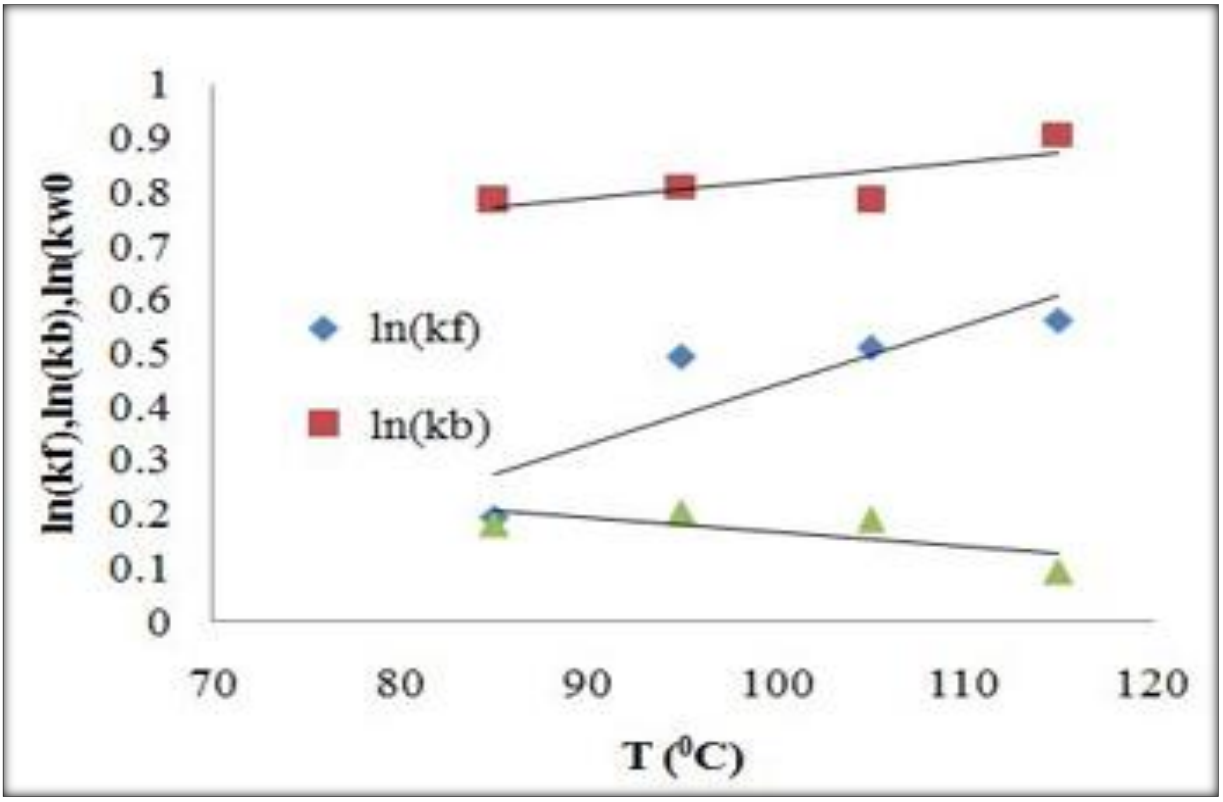

Fig.4.34 Arrhenius plot for $\ln K_B$, $\ln K_f$,$\ln K_W$ vs T

Where i=f,B,W,E_i is the energy of activation, and k_{io} is the factor of frequency[23]. The Eq. (5), a plot of ln K_F, ln K_B and ln K_W versus 1/T plot, lists a slope straight of (E/R) and, as shown in the fig.4.34 ln k_{io} intercept opposed to 1/T. In the presence of Sulfonic acid functionalized Ti SBA-15, the activation energy was found to be 39.5 kJ mol^{-1}.

The temperature of the adsorption and the rate dependence can be compared with the following equations:

$$K_F(L^2 g^{-1} mol^{-1} h^{-1}) = exp^{\left(232 - \frac{1109}{T}\right)} \quad (44)$$

$$K_B(L\ mol^{-1}) = exp^{\left(\frac{3125}{T} - 17.83\right)} \quad (45)$$

$$K_w(L\ mol^{-1}) = exp^{\left(\frac{4856}{T} - 54.9\right)} \quad (46)$$

4.3.3.3 Model prediction

Compared with the proposed ER model, the observation rate was determined using the rate constants defined for esterification of propionic acid with butanol over an entire range of expected parameters [24]. For example, the following equation 10 determined experimental data: CA is acid concentration, t is reaction time, and X is the acid conversion in figure 4.35

$$.-r_{A,experimental} = \frac{\Delta C_A}{\Delta t} = C_{Ao}\frac{\Delta X}{\Delta t} \quad (47)$$

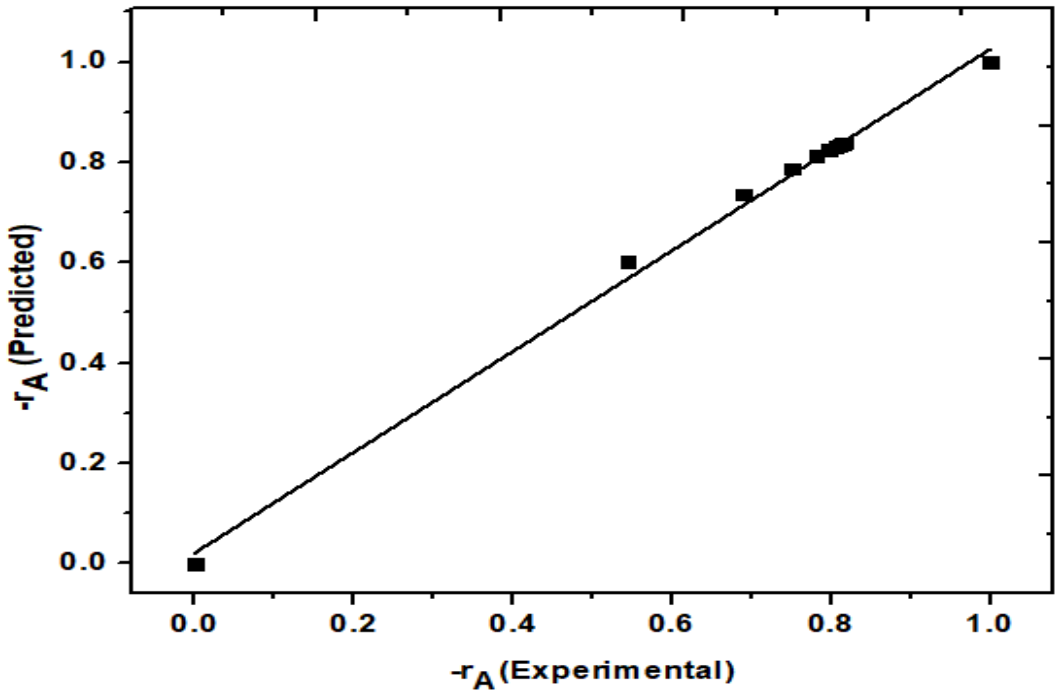

Fig.4.35 The parity between the experimental value and the calculated values and found that the findings are within ± 5 percent fairly well.

Figures 4.37 and 4.38 for the ER model compare experimental and simulation findings for propionic acid conversion and concentrations. As described in the section on experimental data, the rate of conversion of propionic acid rises with increasing temperature due to increased

collisions of reactants to create products. Similarly, when the catalyst loading increases, so does the conversion since more catalyst active sites are available for the esterification process. The modeling results and actual data are in good agreement, asshown in Figs. 4.36 and 4.37

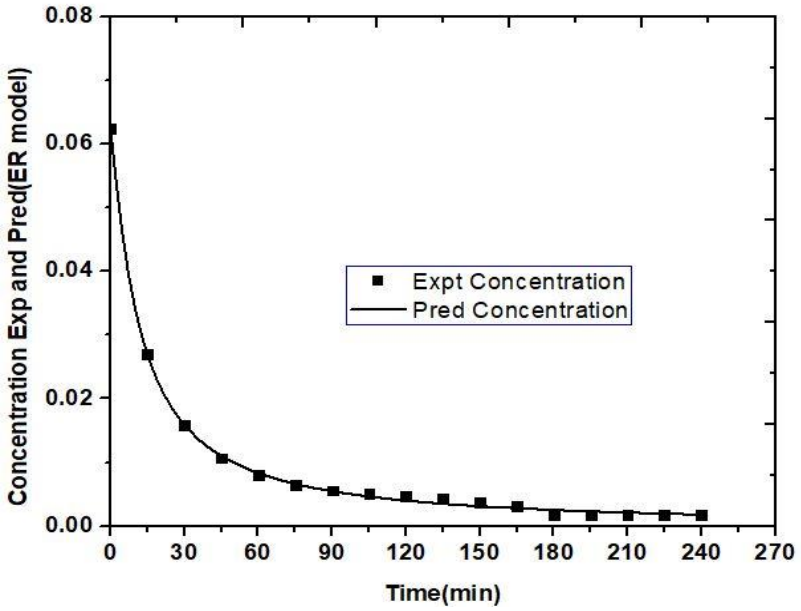

Fig.4.36 Comparison of experimental results with activity- based model results for the Conversion of Propionic acid at different catalyst concentrations at 388.15 K.

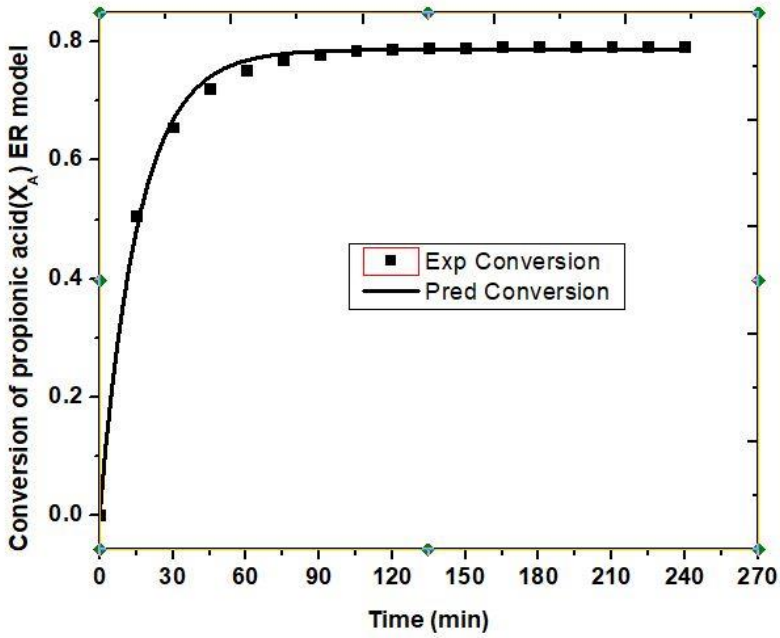

Fig.4.37 Comparison of experimental results with activity- based model results for the Conversion of Propionic acid at different catalyst concentrations at 388.15 K.

4.3.4 Langmuir-Hinshelwood model:

4.3.4.1 Mathematical Model

The pseudo-homogeneous model does not consider the interfacial area between the catalyst particles and the liquid. If the reaction is assumed to occur just on the catalyst surface, then two surface adsorption models, Eley-Rideal (E-R) and Langmuir-Hinshelwood-Hougen-Watson (LHHW) might be used. The LHHW model suggests that the reaction occurs primarily between the two adsorbed reactant molecules on the catalyst surface.

1.

$$C_3H_6O_2 + S \leftrightarrow C_3H_6O_2.S \tag{48}$$

$$B + S \leftrightarrow B.S \tag{49}$$

2.

$$C_3H_6O_2.S + B.S \leftrightarrow E.S + S \tag{50}$$

$$E.S + B.S \rightarrow D.S + W.S \tag{51}$$

3.

$$D.S \leftrightarrow D + S \tag{52}$$

$$W.S \leftrightarrow W + S \tag{53}$$

$$C_{i,s} = K_i C_i C_v \tag{54}$$

$$r_E = k_3 C_{A.s} C_{B.s} - k_3' C_{E.s} C_v \tag{55}$$

$$C_{E.s} = \frac{K_1' K_{C_3H_6O_2} K_B C_{C_3H_6O_2} C_B C_v^2}{C_v} = K_1' K_{C_3H_6O_2} K_B C_{C_3H_6O_2} C_B C_v \tag{56}$$

$$C_{E.s} = k_4 C_{E.s} C_{B.s} = k_4 K_1' K_{C_3H_6O_2} K_B^2 C_{C_3H_6O_2} C_B^2 C_v^2 \tag{57}$$

$$C_T = C_V + C_{C_3H_6O_2.s} + C_{B.s} + C_{D.s} + C_{W.s} \tag{58}$$

$$C_V = \frac{C_T}{1 + K_{C_3H_6O_2} C_{C_3H_6O_2} + K_B C_B + K_D C_D + K_W C_W} \tag{59}$$

The following kinetic model equations are based on adsorption:

$$r_D = \frac{C_T^2 k_4 K_1' K_{C_3H_6O_2} K_B^2 C_{C_3H_6O_2} C_B^2}{[1+K_{C_3H_6O_2} C_{C_3H_6O_2} + K_B C_B + K_D C_D + K_W C_W]^2} \quad (60)$$

$$r_D = \frac{dC_D}{dt} = -\frac{dC_A}{dt} = C_T^2 k_4 K_1^1 K_{C_3H_6O_2} K_B^2 C_{C_3H_6O_2} C_B^2 \quad (61)$$

$$\frac{dX_A}{dt} = C_T^2 k_4 K_1' K_A K_B^2 C_{Ao}^2 (1 - X_A)(\gamma - 2X_A)^2 \quad (62)$$

$$\frac{1}{(\gamma-2)^2}\left[\frac{(2-\gamma)}{(\gamma-2X_A)\gamma} + ln\frac{(\gamma-2X_A)}{\gamma(1-X_A)}\right] = k''t \quad (63)$$

4.3.4.2 Simulation Results

With the obtained constants of kfo and Ke, the Eq. (63) can be integrated numerically to predict the conversion of Propionic acid versus time, as shown in Fig.4.38 and 4.39. At 115°C, this figure 4.38 illustrates propionic acid conversion from experimental data to concentration-based model simulations for three distinct catalyst concentrations. At lower catalyst concentrations, the experimental findings closely match the model predictions. Initially, the experimental values are slightly higher than those estimated by the model, but as time passes, the actual data are in good agreement with the model predictions. Experiment findings with greater catalyst concentrations are larger in magnitude initially, but they come to approach the model estimated values closely over time. This may be because of the reversible nature of reaction kinetics. The conversion approaches equilibrium value accurately as Ke is specified based on experimental data. Whereas the initial kinetics predicted is dependent on the rate expression. Hence, a less deviation suggests that it is a good fit or vice-verse.

Figures 4.38 and 4.39 for the LHHW model compare experimental and simulation findings for propionic acid conversion and concentrations. As described in the section on experimental data, the rate of conversion of propionic acid rises with increasing temperature due to increased collisions of reactants to create products. Similarly, when the catalyst loading increases, so does the conversion since more catalyst active sites are available for the esterification process. The modeling results and actual data are in good agreement, as shown in Fig.

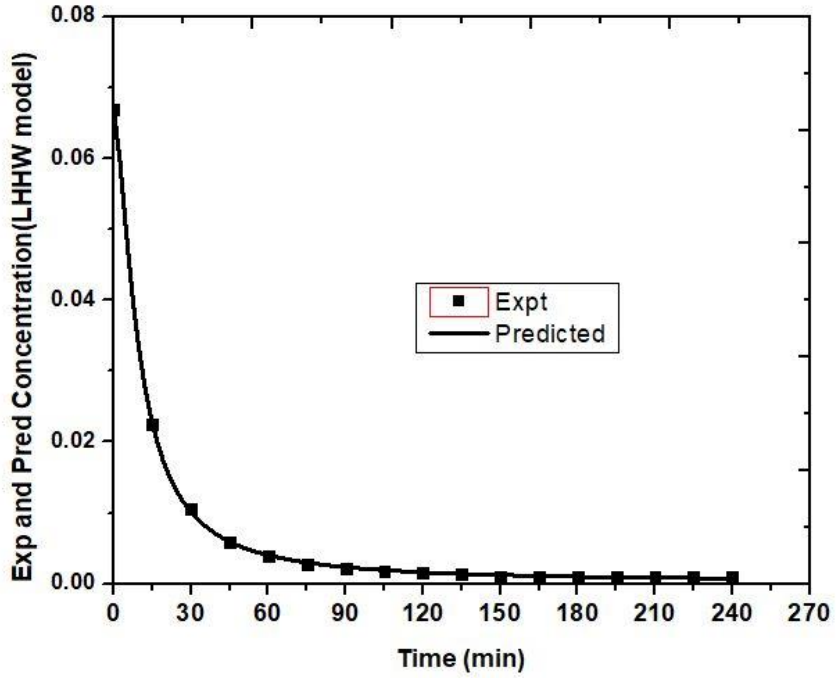

Fig.4.38 Comparison of experimental results with activity- based model results for the Conversion of Propionic acid at different catalyst concentrations at 115°C.

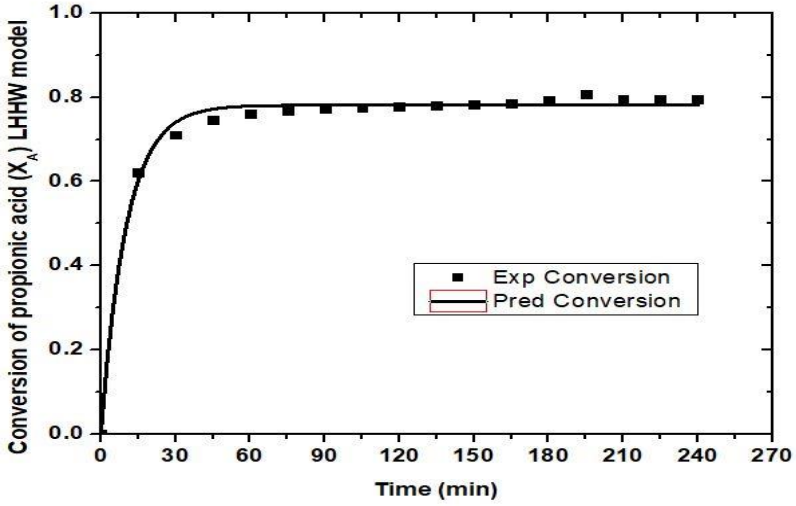

Fig.4.39 Comparison of experimental results with activity- based model results for the Conversion of Propionic acid at different catalyst concentrations at 115°C.

4.3.5. Comparisons with the literature:

The Ti SBA-15@SO3H solid catalyst is compared to other solid catalysts in terms of propionic acid conversion rate. The conversion kinetics of propionic acid in the presence of a solid catalyst at the same catalytic activity (2wt%) and temperature are shown in Fig.4.40. The conversion of Propionic acid in the presence of Ti SBA-15@SO3H is higher than the other solid catalysts available in the literature[11], as shown in Fig. 4.14. For the solid catalysed esterification reaction, a kinetic model is created, and it demonstrates good agreement with experimental results (Present work)

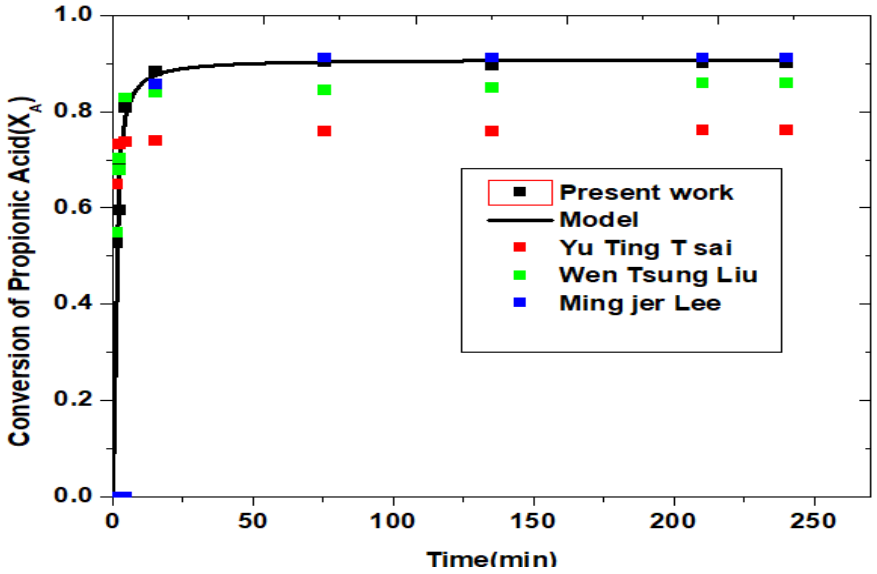

Fig.4.40 Comparing the conversion of the Propionic Acid with literature.

4.4. Batch Reactive Distillation

4.4.1 Batch reactive distillation using the synthesized catalyst.

Reactive distillation is carried out to produce butyl propionate from propionic acid and n-butanol using Ti SBA-15@SO3H as a mesoporous catalyst in a reactive distillation apparatus. The aim is to quantitatively measure the residue or product purity in terms of the butyl propionate mole fraction. In addition, the composition of instantaneous distillate, cumulative distillate, and reactant mixture in the reboiler is monitored. Such data provided a very interesting experimental kinetics of reactive distillation. Furthermore, the temperature in the reboiler and the electrical energy supplied to it were also measured as a time function.

4.4.1.1 Effect of Temperature:

The optimum temperature for butyl propionate synthesis was determined to rise to a temperature of 115°C. The effects of the reactor temp on RD output concerning the butyl propionate concentration in distillate are discussed and presented in Figure 4.41. The reactor temperatures ranged from 80°C to 150°C. The concentration of butyl propionate in the top product decreased at lower temperatures, i.e., around 115-125°C, due to a lower reaction rate. In addition, it was possible to raise the reactor's temperature to 145°C to achieve the maximum concentration and increase the reactor's temperature in the top product. While its frequency constant was high at 115° Butanol (boiling point 123° C) vaporized at a higher reactor temperature, it transferred to the enrichment section reducing the reactor section's butanol available, resulting in lower conversion rates. The increased levels of butanol in the top product as the concentration of butyl propionate also decreases in Figure 4.41. Higher reactor temperatures, particularly in RD phase, are therefore

not feasible for high volatile reactants.

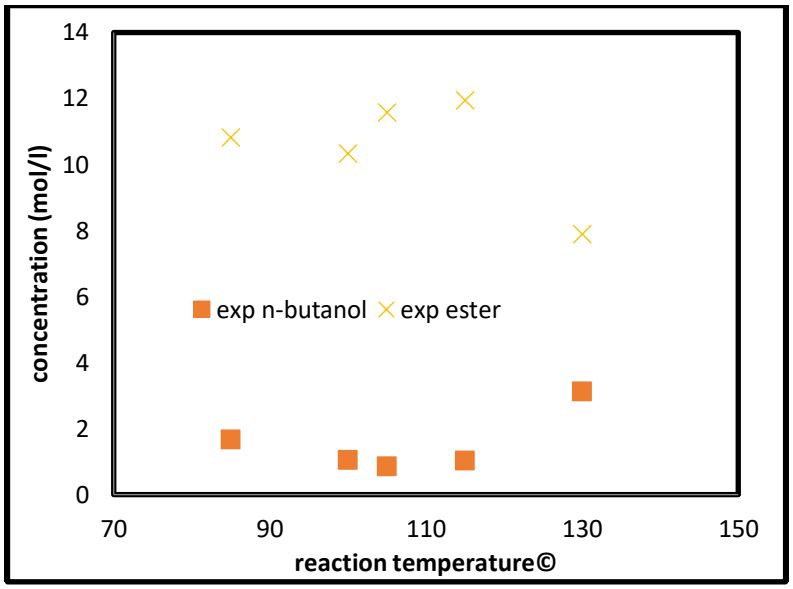

Fig.4.41 Reaction temperature effect on the output of butyl propionates

4.4.1.2 Effect of Catalyst loading:

Generally speeding up reaction rate is using a catalyst, which also affects selectivity. Figure 4.42 shows the catalyst loading effect on butyl propionate concentration in the top product. The figure shows that 2wt% of catalyst loading resulted in stronger conversion than 1 and 3wt%. The pressure drop across the column length grows as the catalyst volume of the reactor component increases. A rise in pressure drop increased the rate of floods that had entirely changed the hydrodynamic of .

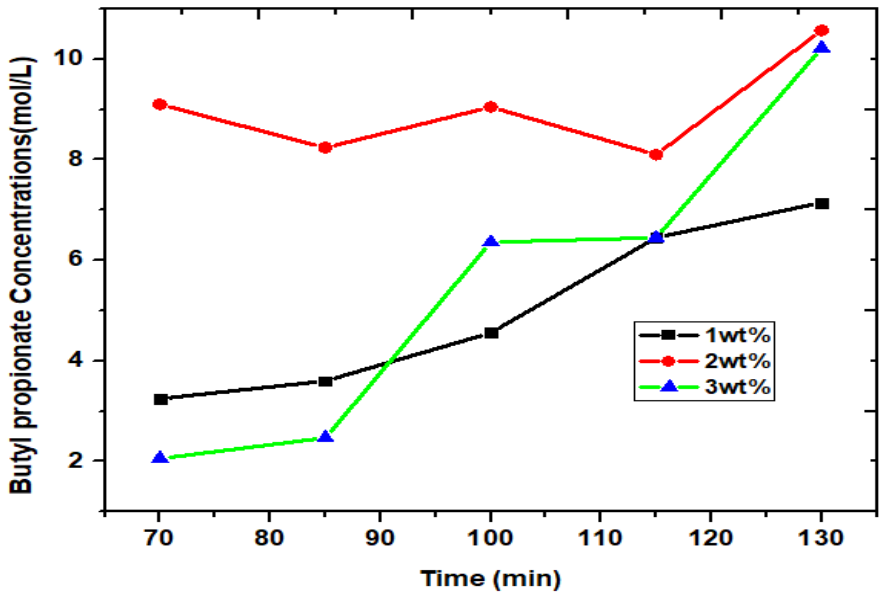

Fig.4.42 Catalyst load effect on butyl propionate

Upstream gases and downstream liquid in the reactor region. The decreased pressure shows simulated aspen results concerning catalyst loading of pressure drop and fraction floods in the reactor portion. As catalyst loading has been increased, pressure drop and section overflow have

increased, which have led, as observed in experimental results, to the reduction of the

4.4.1.3 Effect of Feed Molar Ratio:

To research its effect on butyl propionate production, the molar ratio of propionic acid to butanol was 1:1-1:4. Figure 4.43 shows the molar ratio effect on the concentration of butyl propionate. The optimum molar ratio is 1:2, with an increase in molar ratio found to increase the conversion to propionic acid. However, the butanol concentration in RD distillate increased beyond the decreased butyl propionate concentration. This may be attributed to an azeotrope formation from butyl propionate to butanol because butanol inside the reactor reached the azeotrope stage. The findings simulated with aspen, as shown in Figure 4.43, have been shown to show similar patterns.

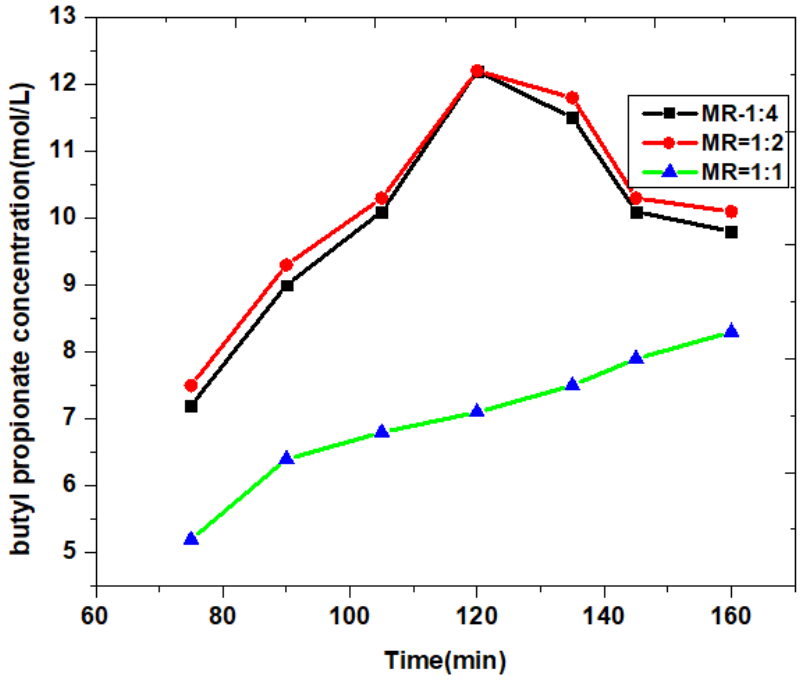

Fig.4.43 Effect of the molar feed ratio on butyl propionate production

4.4.2 Prediction of kinetics of a catalytic reactive distillation evaporation rate based model.

4.4.2.1 Mathematical modeling

The evaporation rate of every component is based on the Himus type of equation (Himus and Hinshley,1924) with an assumption that the concentrations of component vapors in the bulk vapor phase are zero as immediate condensation occurs

· It is assumed that the evaporation rate constant is the same whether the component evaporates from a pure liquid or from the reboiler mixture. Let n_i be the number of gram moles of the component i in the reboiler flask at any time. Since there are four components it is assigned that $i=1$ for the propionic acid, $i=2$ for n-butanol, $i=3$ for butyl propionate and $i=4$ for water. The rate of homogeneous reaction of each of the reactant component is given as

$$\left.\frac{dn_i}{dt}\right|_{rxn\_h} = -\frac{k_f}{V_t}\left[n_1 n_2 - \frac{n_3 n_4}{K_e}\right] \tag{64}$$

Here t is the time, V_t is the volume of reactant mixture in liters at time t, k_f is forward reaction rate constant, l/g min and K_e the equilibrium constant of the reaction which is a dimensionless value. The reaction rate constant $k_f$is given by Arrhenius equation as below (Mekala et al., 2013).

$$k_f = k_{f0}\exp\left(-\frac{E}{R(T+273)}\right) \tag{65}$$

Where T is in ^{o}C.Since the boiling point of n-butanol is less compared to that of propionic acid, it is assumed that n-butanol is limiting reactant in the perspective of the reaction occurring inside the porous catalyst at later stages of reactive distillation as more of n-butanol would evaporate than propionic acid.

The reaction rate of n-butanol or the consumption rate of the n-butanol in the reboiler solution due to pore diffusion effect (Mekala et al., 2013) is given by

$$\left.\frac{dn_2}{dt}\right|_{rxn\_p} = N_P 4\pi R_P^2 J_2 \tag{66}$$

where N_P is the number of catalyst particles, R_P is the average radius of the catalyst particle and J_2 is the inward surface molar flux into the catalyst particle. Here J_2 is given as

$$J_2 = D_{2m}\left.\frac{\partial C_2}{\partial r}\right|_{r=R_P} \tag{67}$$

Where D_{2m} is the effective diffusivity of n-butanol in the pores which takes into account the porosity of catalyst particle, $C_2(r)$ is concentration profile of n-butanol in the catalyst particle and r is the radial position measured from the center of the catalyst particle.

The molar reaction rates of other three components due to heterogeneous reaction are calculated in stoichiometric ratio to that of n-butanol. Hence we have

$$\left.\frac{dn_1}{dt}\right|_{rxn\_p} = \left.\frac{dn_2}{dt}\right|_{rxn\_p} = -\left.\frac{dn_3}{dt}\right|_{rxn\_p} = -\left.\frac{dn_4}{dt}\right|_{rxn\_p} \tag{68}$$

The number of particles N_P is related to the catalyst loading W_C as described in reference (Mekala et al., 2013). Since the volume of the reactant solution decreases with time the effective catalyst loading increases with time according to

$$W_C = W_{C0}\frac{V_0}{V_t} \tag{69}$$

Where $W_{C0}$is the initial catalyst loading, V_0 is the initial volume of the reactant mixture and V_t is the instantaneous volume of the reactant mixture remaining in the reboiler. The volume of the solution in the reboiler is calculated as

$$V_t = \sum_{i}^{4} \frac{n_i MW_i}{\rho_i} \tag{70}$$

Where MW_i is the molecular weight of the component i, ρ_i is the liquid density of the respective component i.

The evaporation rate of each of the component is calculated as

$$\left.\frac{dn_i}{dt}\right|_{evap} = A_c k_i x_i p_i^{sat} \tag{71}$$

Generally the total vapor pressure of the reboiler solution is equal to 1 atmosphere as in a column distillation where only the liquid components are present in the vapor. In the present simple distillation, the vapors are condensed as soon as they enter the horizontal condenser. Since there is condensation of the vapor, the gas phase in the condenser and the gas phase in reboiler contain air in addition to the vapors of the four components. Therefore, it is assumed that condensation of vapors occurs only when the total vapor pressure P_t exceeds certain threshold value of P_0. This P_0 could be anywhere between 0 to1 atmospheres. P_t is calculated as below according to Raoult's law.

$$P_t = \sum_{i=1}^{4} x_i p_i^{sat} \tag{72}$$

The mole fractions x_i are calculated as $n_i/\Sigma n_i$. The saturation vapor pressure of each component is calculated using Antoine equation as given below (Green and Perry, 2007).

$$\ln(p_i^{sat}) = A + \frac{B}{C+T} \tag{73}$$

The constants A, B, and C are given in Table 4.2. Here, T is the instantaneous temperature of the reboiler solution. The condensation will occur based on the temperature of the coolant fluid. In the present experiment, the coolant fluid is water at a temperature of 25 ^{o}C. Hence condensation may occur when the total vapor pressure of the reboiler solution exceeds a certain threshold value. This particular threshold value, *P0* would be obtained by optimizing the error between the experimental temperature profile and the theoretical prediction, as well as that of cumulative distillate volume and the time for onset of distillation.

Another parameter that needs to be optimized is the efficiency factor of the heating mantles electrical to thermal energy conversion. Generally, its value could be anywhere between 0 to 1.

Table 4.3 Antoine constants

Component	A	B	C
Propionic acid	16.8	3295.5	-55.34
N-butanol	18.5	3988	-53.5
Butyl propionate	16.1	2569	-54.1
water	18.3	3798	-43.1

The composition in the reboiler is updated as below provided the total vapor pressure P_t is greater than the threshold value of P_0.

$$\left.\frac{dn_i}{dt}\right|_{total} = \left.\frac{dn_i}{dt}\right|_{rxn\_h} + \left.\frac{dn_i}{dt}\right|_{rxn\_p} + \left.\frac{dn_i}{dt}\right|_{evap} \tag{74}$$

If P_t is less thanP_0 than the reaction terms are only considered for updating the composition in the reboiler solution.

If $P_t > P_0$ then the composition of the instantaneous reboiler is determined as

$$x_{ID,i} = \frac{\left.\frac{dn_i}{dt}\right|_{evap}}{\sum_i^n \left.\frac{dn_i}{dt}\right|_{evap}} \tag{75}$$

The composition or the mole fraction in the cumulative reboiler is estimated as

$$x_{CD,i} = \frac{\left.\int_0^t \frac{dn_i}{dt}\right|_{evaporation}}{\sum_i^n \left.\int_0^t \frac{dn_i}{dt}\right|_{evaporation}} \tag{76}$$

The cumulative reboiler volume is calculated as

$$V_{CD} = V_0 - V_t \tag{77}$$

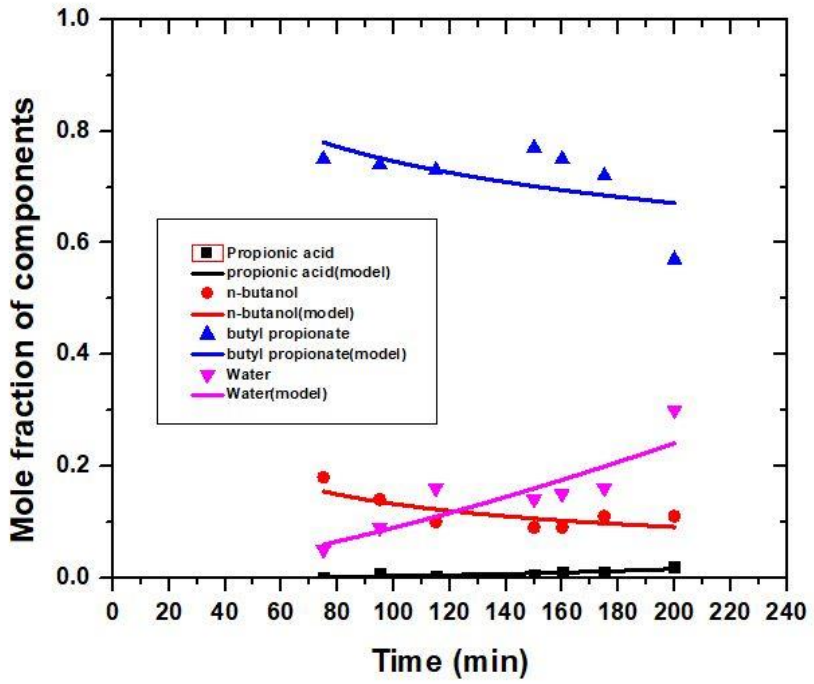

Fig.4.44 Composition of instantaneous reboiler versus time: comparison of experimental data and predicted dynamics.

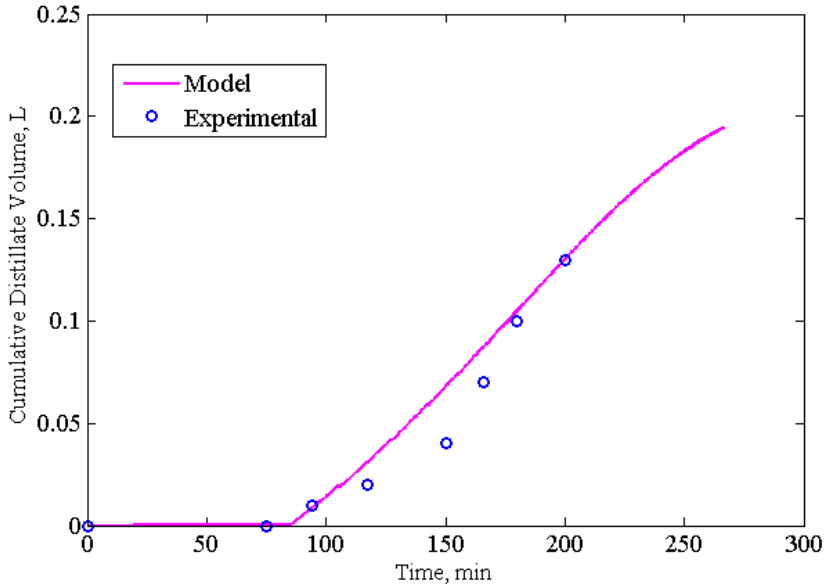

Fig.4.45 Volume of cumulative distillate collected versus time: comparison of experimental and predicted dynamics

Where V_t is calculated from the Eq. (77). Here, it is assumed that there are no vapor loses from the condenser.

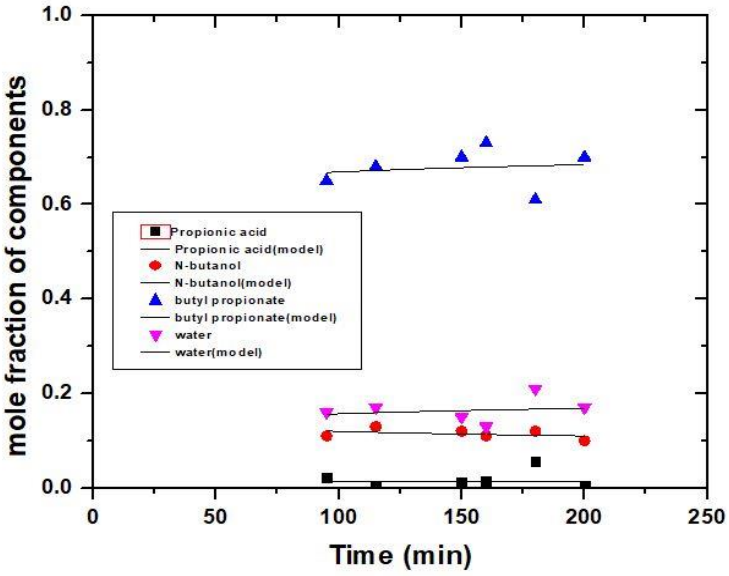

Fig.4.46 Composition of cumulative reboiler versus time: comparison of experimental and predicted dynamics.

Composition of cumulative reboiler versus time for experimental and predicted dynamics in terms of the mole fractions are shown in fig 4.44 and 4.46 which observed the purity of the butyl propionate. And the simulated results are good fit for experimental data.

After the above calculations the temperature of the solution in the reboiler flask is updated as

$$\frac{dT}{dt} = \frac{1}{\sum_{i=1}^{4} n_i C_{Pi}} \left[\dot{Q} - \sum_{i=1}^{4} \lambda_i \frac{dn_i}{dt}\bigg|_{evap} \right] \tag{78}$$

The heat supply $\dot{Q}$ is applied only when the total vapor pressure is less than P_0. This ensures that only drop wise condensation occurs. Fig. 4.45 could be referred to notice the rate of energy supplied to the reboiler solution increases gradually. Although the rate of heat supply is increased manually it is obtained from the time derivative as

$$\dot{Q}^{*} = \eta_e (400 + 11.05t) \quad \text{Watts} \tag{79}$$

Whereη_e is the thermal efficiency of the electrical heating mantle. All other properties such as C_{Pi} and λ_i are taken from the literature (Green and Perry, 2007) as dependent on temperature as shown below

$$C_{p,i}(T) = \alpha_1 + \alpha_2 (T + 273) + \alpha_3 (T + 273)^2 + \alpha_4 (T + 273)^3 \tag{80}$$

$$\lambda_i(T) = \beta_1\left(1-\frac{T+273}{T_c}\right)^{(\beta_2+\beta_3((T+273)/T_c)+\beta_4((T+273)/T_c)^2)} \quad (81)$$

Here T_c is the critical temperature of the pure components.

4.4.2.2 Simulation results

Initially, the amounts of reactants are taken as n_1=1 moles, n_2 =1 moles, and that of products are n_3=0 and n_4=0. The initial temperature of the reactant solution is taken as 115°C. When the above algorithm is implemented, it is found by trial and error method that the optimum values of parameters are *P0*=0.7 atm, ηe=0.3 and *k3* = 18.18 mol/min m2 atm to minimize the overall standard deviation between model prediction and experimental data of temperature versus time, cumulative reboiler volume versus time and mole fraction of butyl propionate in instantaneous reboiler versus time. An Euler explicit method with an adaptive time step is utilized for updating the temperature and composition of the reboiler solution and that of the distillate composition and volume using the kinetic equation of Eqs. (13-17). The adaptive time step is such that there is only a 1 ºC change in the temperature of the reboiler solution for each iteration. The numerical code is implemented using MATLAB. The obtained model predictions are compared with the experimental data for temperature of the reboiler solution, instantaneous reboiler composition, cumulative reboiler composition, composition of the reboiler solution, and cumulative reboiler volume, as shown in Fig. 4.47. A good fit is found especially for predicting the butyl propionate composition in instantaneous reboiler and cumulative reboiler, as well as other variables.

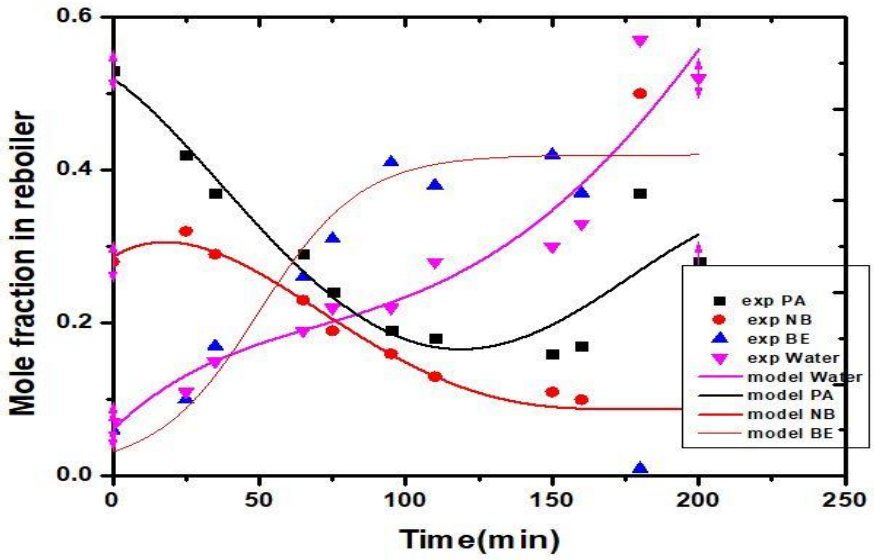

Fig.4.47 Composition of reboiler/heating flask versus time: comparison of experimental and predicted dynamics.

4.5.1 Simulation of continuous reactive distillation using the kinetics obtained by the synthesized catalyst.

The equilibrium model's equations are essentially mass and energy balances. Furthermore, the surface compositions are thought to be in balance with one another, implying that they are linked. As a result, we picked empirical HETPs for both reactive and non-reactive packing, and we employed the same number of theoretical stages in our simulations. The equilibrium stage is shown schematically in Fig.4.48.

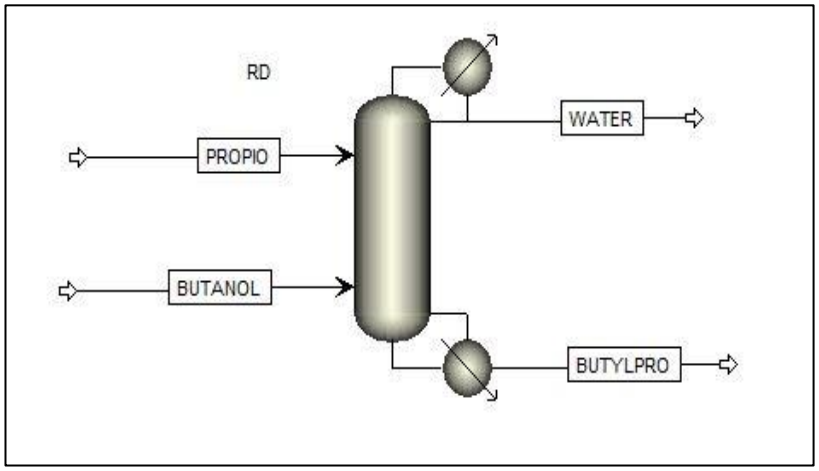

Fig.4.48 Continuous reactive distillation

The activation energies E_f and E_b for both forward and backward processes in the presence of Sulphonic acid supported Ti SBA-15@SO_3H acid as a mesoporous catalyst for the esterification of propionic acid and n-butanol

Radfrac column was used to simulate the above-mentioned basic equilibrium model. The simulation's equipment specifications are for a reactive distillation column in our laboratory. Apart from the steady-state mass and energy balance equations reported in the model development, the kinetic equation obtained from our experimental data for esterification of propionic acid with n-butanol was employed in the simulation.

4.5.2.3.1 Continuous RD Process:

This work developed a conventional RD technique for propionic acid esterification with butanol, as shown in Figure 4.49. In this typical RD method, one distillation is used for both reaction and separation of products. Rectifying, reactive, and stripping parts of RDC were separated. The column is programmed to operate at 1.1 atm pressure, with a 0.1 atm pressure drop in the column. Two reactants, propionic acid & n-butanol, were provided into RDC from the top and bottom parts of the reactive section at flow rates of 25 kmol/h.

Butyl propionate was collected from the bottom of RD at a flow rate of 23 kmol/h after the

esterification reaction in the reactive section was catalyzed by Ti SBA-15@SO3H. Unreacted liquid mixture and water were extracted from the top of RD at a flow rate of 27 kmol/h. The product produced was 93 mol%[133] pure. RDC's overall stage count is still 25. Other parameters, including rectifying section (Nr), reactive section (Nrec), and stripping section (Ns) stage numbers, as well as RDC's reflux ratios, were also modified to guarantee that product purity criteria were achieved.

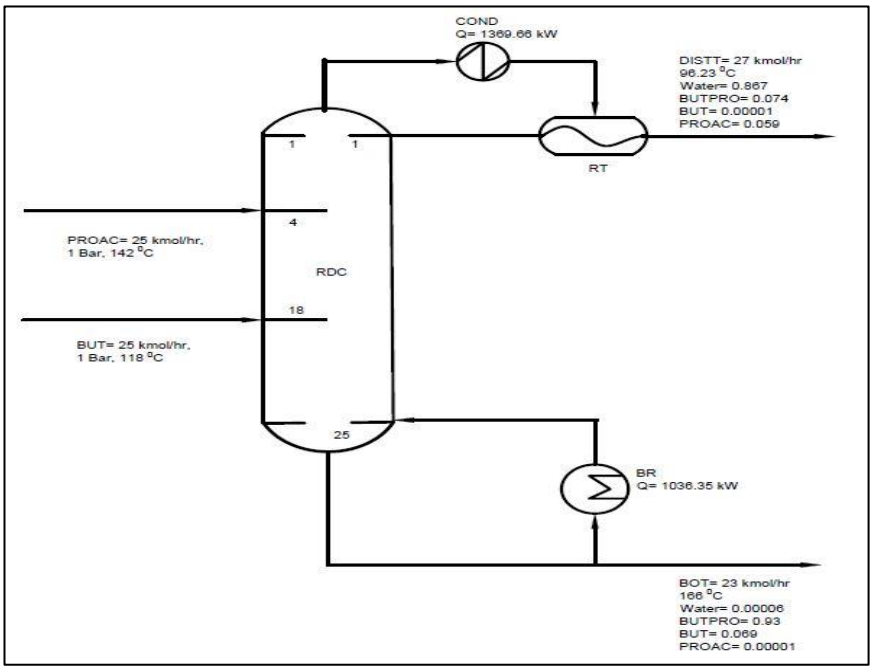

Fig 4.49 Schematic representation of Reactive distillation column for N-Butyl Propionate

4.5.2.3.2 Temperature variation along the height of the column

The figure 4.50, the temperature of the condenser is lowest at around 95°Celsius while the maximum temperature is at about 160 in Reboiler. Temperature goes on increasing randomly without any linear progress, which is similar in conventional distillation columns. However it can be seen a sudden jump in temperature at stage no 5 which is due to the reaction .

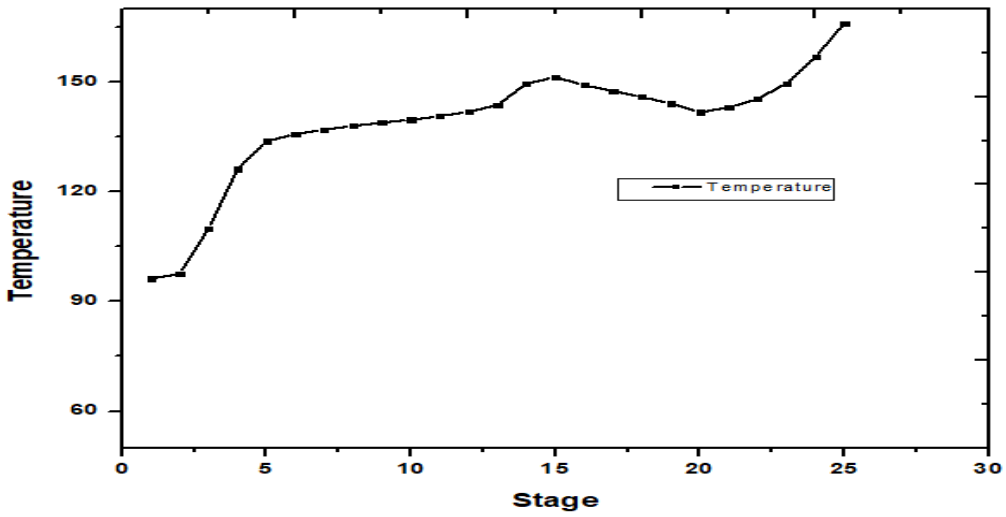

Fig.4.50 Temperature Profile in Reactive Distillation Column

4.5.2.3.3 Concentration profiles in the liquid phase

Figure 4.51 shows the composition profile of components inside the column. As seen from the graph, Propionic acid and butanol react between 5 to 20 stages. Due to the reaction formation of product i.e butyl propionate and conversion of reactant can be observed within these stages. Product butyl propionate is collected at the bottom at 93 mol%, while water is obtained from the top at 86 mol%.

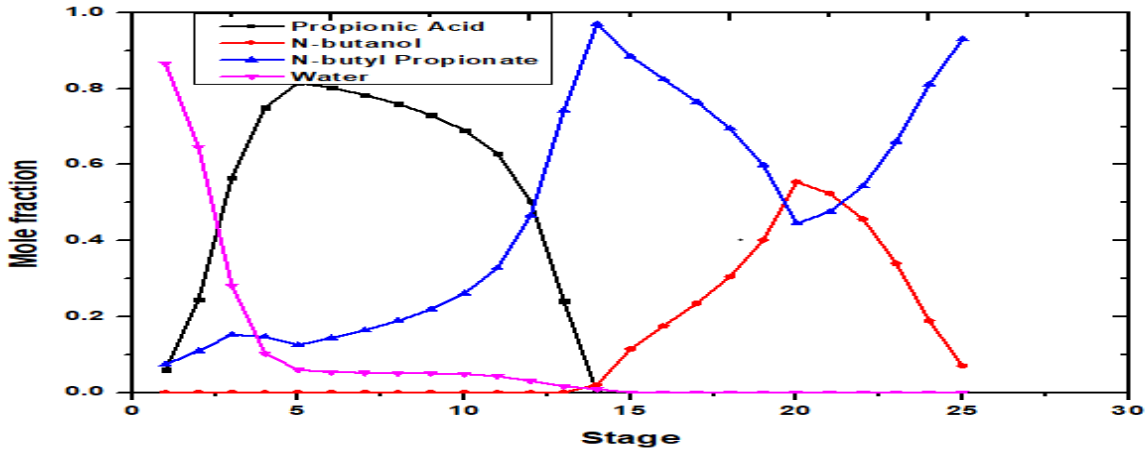

Fig. 4.51 Composition Profile in Reactive Distillation Column

4.5.2 Modelling and simulation of reactive divided wall column for esterification of propionic acid with n-butanol over mesoporous catalyst.

4.5.2.1 Reactive divided wall column

Reactive dividing wall columns (RDWCs) [130] are used to accomplish chemical reactions and multicomponent separations in the same unit. While reactive distillation columns (RDCs) and dividing wall columns (DWCs) are becoming more popular in chemical processes due to their ability to save money and energy, RDWCs have yet to garner general acceptance. In the recent decade, RDWC research has been active, with studies indicating that the technology is commercially viable.

When applying the reaction kinetics [131] to an RDWC, it is assumed that the solid catalyst occupies half of the tray holdup volume, and that a catalyst density of 770 kg/m3 is used to convert the volume into catalyst weight (mcat).

4.5.2.3 Phase Equilibria

The UNIQUAC model is used to account for non-ideal vapour liquid equilibrium (VLE) and vapor–liquid–liquid equilibrium (VLLE) in the quaternary system, with the model parameters stated in Table 4.3. Because the intended RDWC operates at atmospheric pressure, the Hayden-O'Conell second virus coefficient model [132] uses propionic acid dimerization to describe vapour phase non-ideality. To compute fugacity coefficients, Aspen Plus uses built-in parameters.

Table 4.4 Azoetrope data for butyl propionate esterification system

Azoetrope components	Butanol/butyl propionate	Water/butyl propionate
Mass bias	0.16/0.84	0.08/0.92
Temperature	117^{o}C	123^{o}C
Classification	Unstable node	Saddle
Type	Homogeneous	Homogeneous

Table 4.3 gives the azeotrope data for the propionic acid esterification system. The maximal relative errors between the predicted values and experimental data are less than 1.43% and 0.62% for azeotrope compositions and temperatures. Therefore, the selection of the UNIQUAC model was reliable.

4.5.2.4 Simulation of RDWC (Liquid Split) Process

The parameters were adjusted to minimize total energy usage of RD procedure. Figure 4.55 displays simulation results for most common RD process. The condenser's reflux drums is first stage, while the reboiler is final. Nr, Nrec, and Ns values were verified to be 4, 16, and 5, respectively.

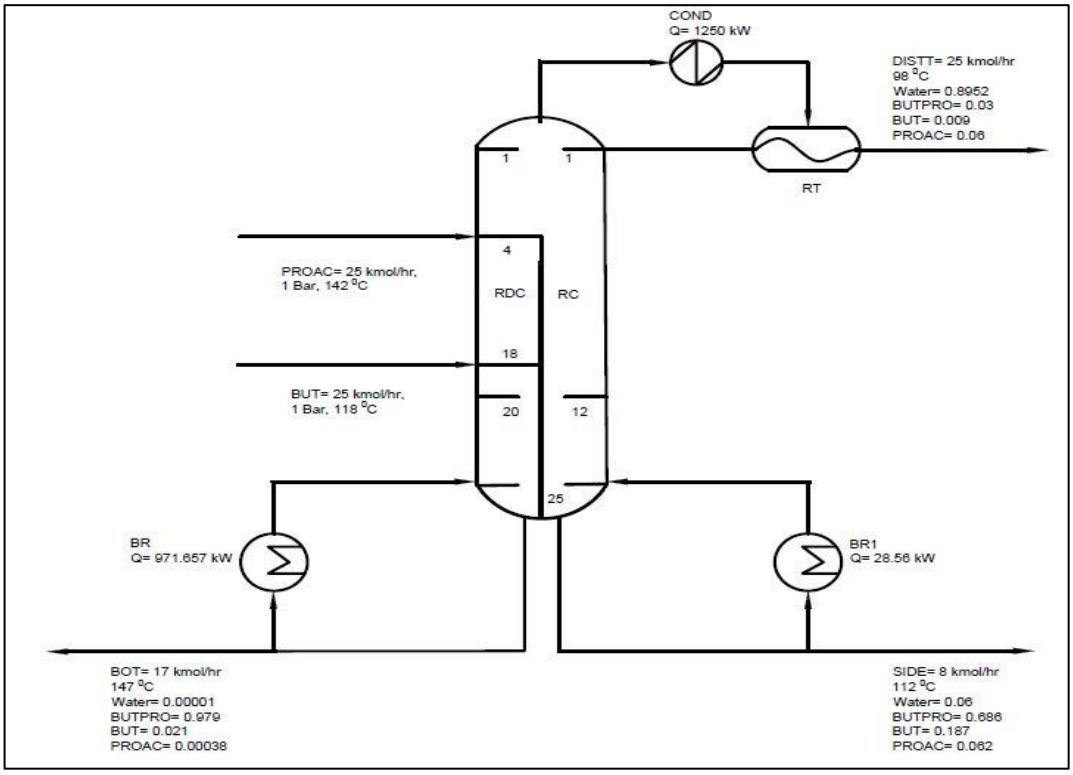

Fig.4.55 Schematic Representation of RDWC (LS) for N-Butyl Propionate

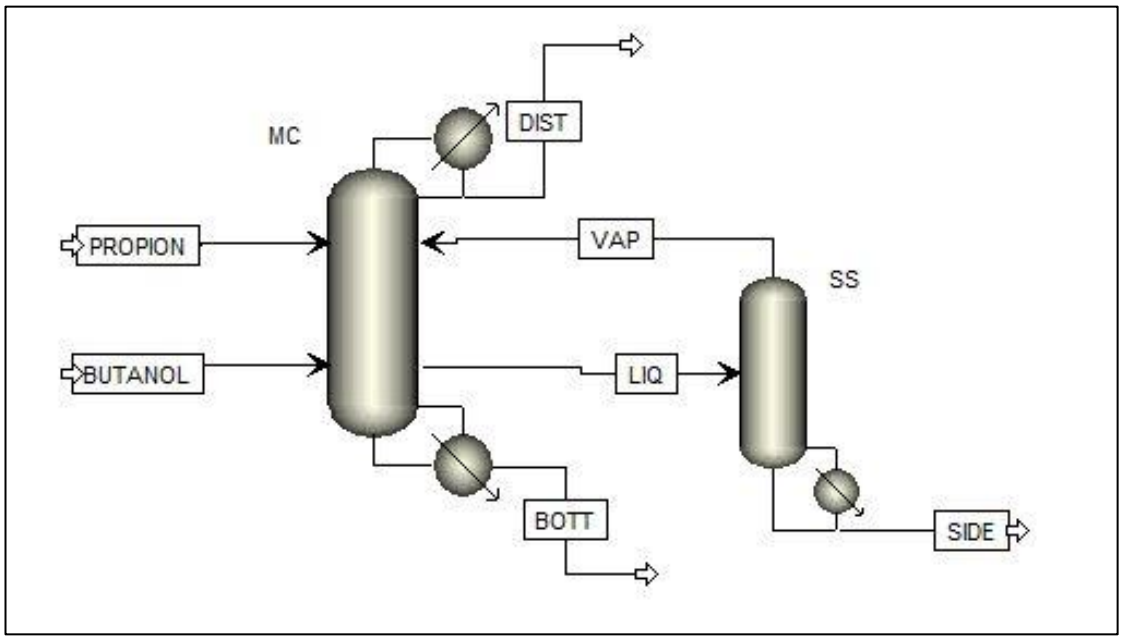

Fig.4.56 RDWC with Liquid Split

The standard RD process is integrated into a single RDWC, with the reactive component on the RDWC's left side. The percentage of Ls to L at the top of the separating wall is denoted as the internal liquid split ratio (L). Ls signifies the flow rate of liquid supplied to the right side of the separating wall in this equation, and L denotes the total flow rate of liquid coming down from rectifying section. Furthermore, L has generated automatically during simulation. There was no

vapor divide in RDWC. The bottoms of the left and right parts of RDWC (RDC and RC) give high-purity product Butyl propionate and unreacted reactants, respectively. The water is drawn from RDWC's top (RDC). Because just one column is needed in this situation, more space is conserved at the plant[133-140]. At the same time, two reboiler and condensers are required. RDWC cannot be directly reproduced in Aspen Plus using Radfrac units. As a result, with the premise that no heat transfer occurs across the dividing wall in RDWC, a similar design of two columns, as shown in Figure, is employed in Aspen Plus to replicate the RDWC process.

4.5.2.4.1 Temperature variation along the height of the column

Fig. 4.57 shows temperature profile throughout the column along the height of column per stage location. Temperature at the top of the column is around 370 K and bottom at is around 425 K. while temperature inside the column ranges between these two values as shown in Fig.4.57. After 13th stage temperature suddenly increased indicates that reaction start at that stage. As this profile is from Main column i.e Reactive column the profile is similar to standard RDC.

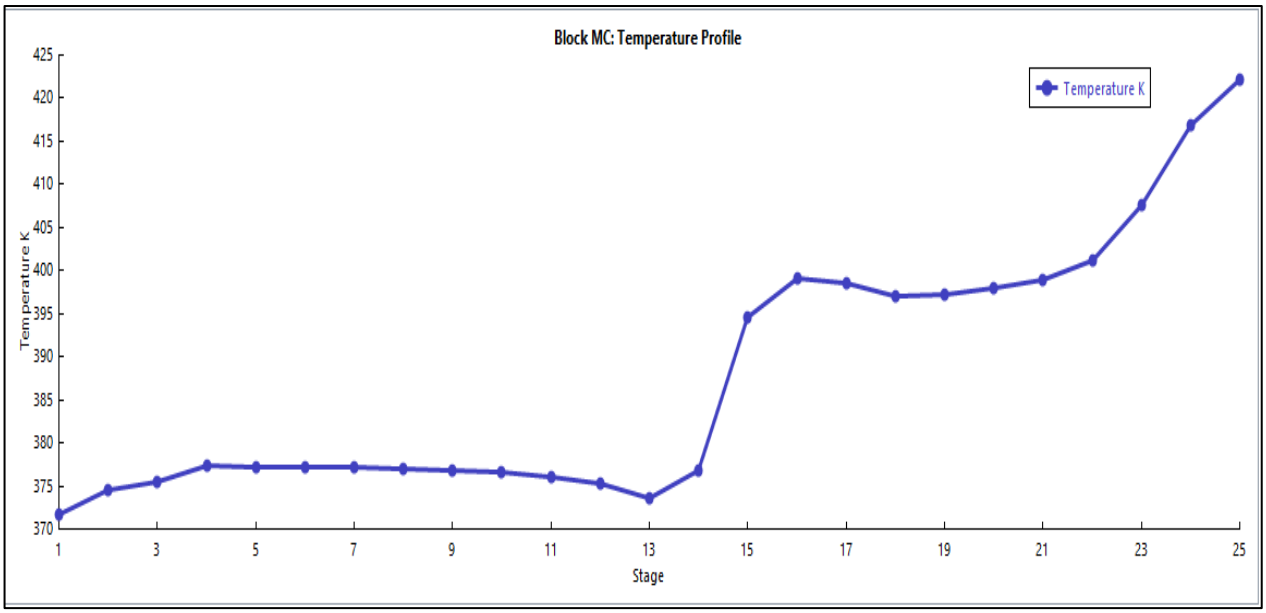

Fig.4.57 Temperature profile across RDWC LS (RDC)

4.5.2.4.2 Concentration profiles in the liquid phase:

Fig 4.58 and 4.59. shows composition profile of main column and side column respectively, propionic acid is fed at 5th stage and butanol fed at 18th stage. Both reactants react to give the product butyl propionate and water. From fig.4.58 it is clearly shown that, at bottom butyl propionate collected with 98.67% purity and the profile is similar to the standard RDC since the reaction is taking place in this column. However in Side column there is no any reaction, hence the concentration profile is almost constant throughout the column.

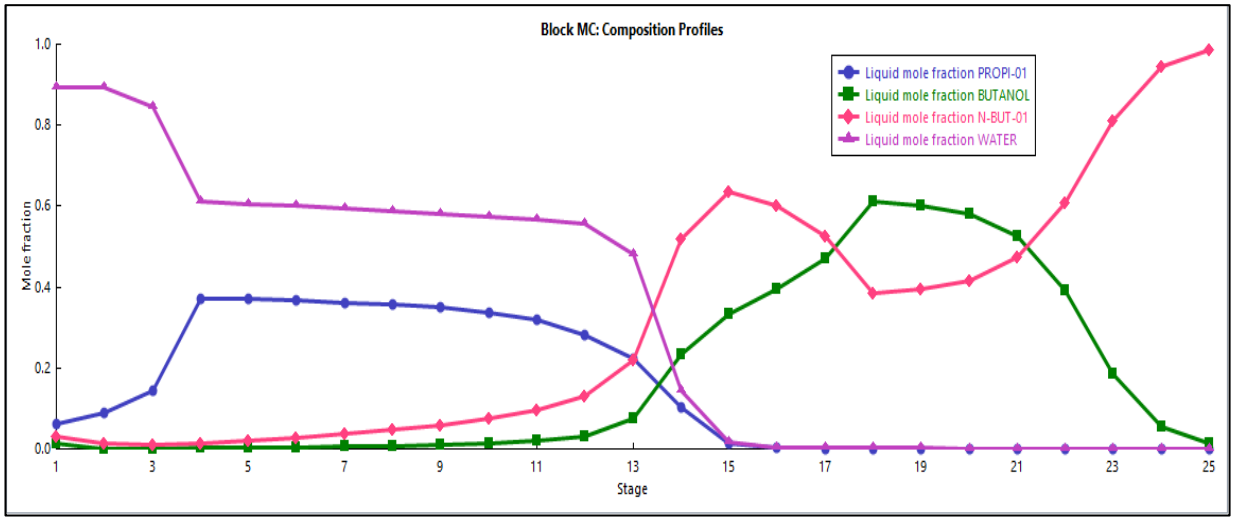

Fig.4.58 Composition profile across RDWC LS (RDC)

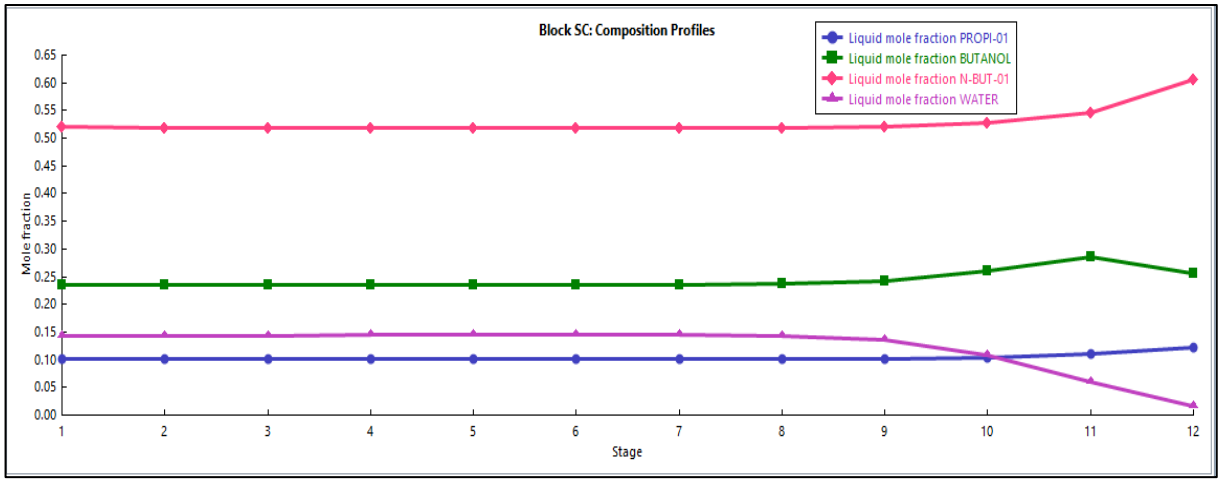

Fig.4.59 Composition profile across RDWC LS (RC)

4.5.2.4.3 Effect of reflux ratio on conversion of Propionic acid:

The change in product purity with respect to reflux ratio is shown in the Fig.4.60. As reflux ratio increases both butyl propionate and water purity increase. With the increase in reflux ratio it is observed that the water purity reduced after RR value 2.6 but for butyl propionate it's continues to increases until it reach to 3.7. but more reflux ratio leads to bigger diameter of the column and more capital cost.

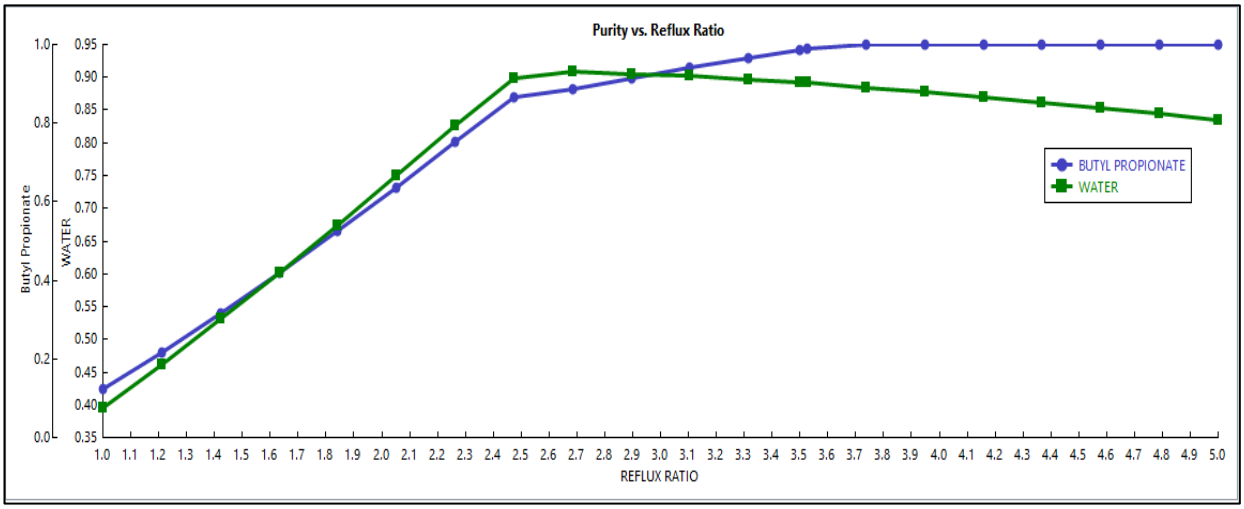

Fig.4.60 Effect of purity on Reflux Ratio

4.5.2.5. RDWC (Vapor Split) Process

Standard RD process is integrated into a single RDWC, with the reactive component on the RDWC's left side. At top of dividing wall, there is an internal Vapor split ratio (V), which is defined as proportion of Vs to V. In this equation, Vs represents flow rate of vapors supplied to right side of separating wall, and V represents total flow rate of vapors rising from rectifying section. Furthermore, V is generated automatically throughout simulation. Propionic acid and Butanol are provided at same flow rate of 25 Kmol/hr in MC in figure 4.64.

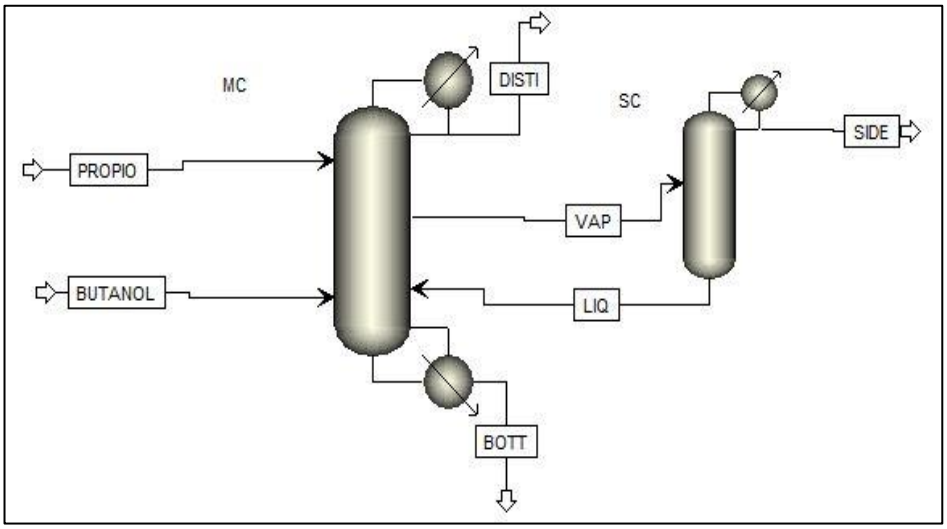

Fig.4.63 RDWC with Vapor Split

In presence of Sulfonated Ti SBA-15, reaction occurs. Following that, butyl propionate was extracted from bottom of RDC and RC, and water was extracted from top of the RDC column. Many elements, such as the number of stages and the reflux ratios, are changed to enhance the process.

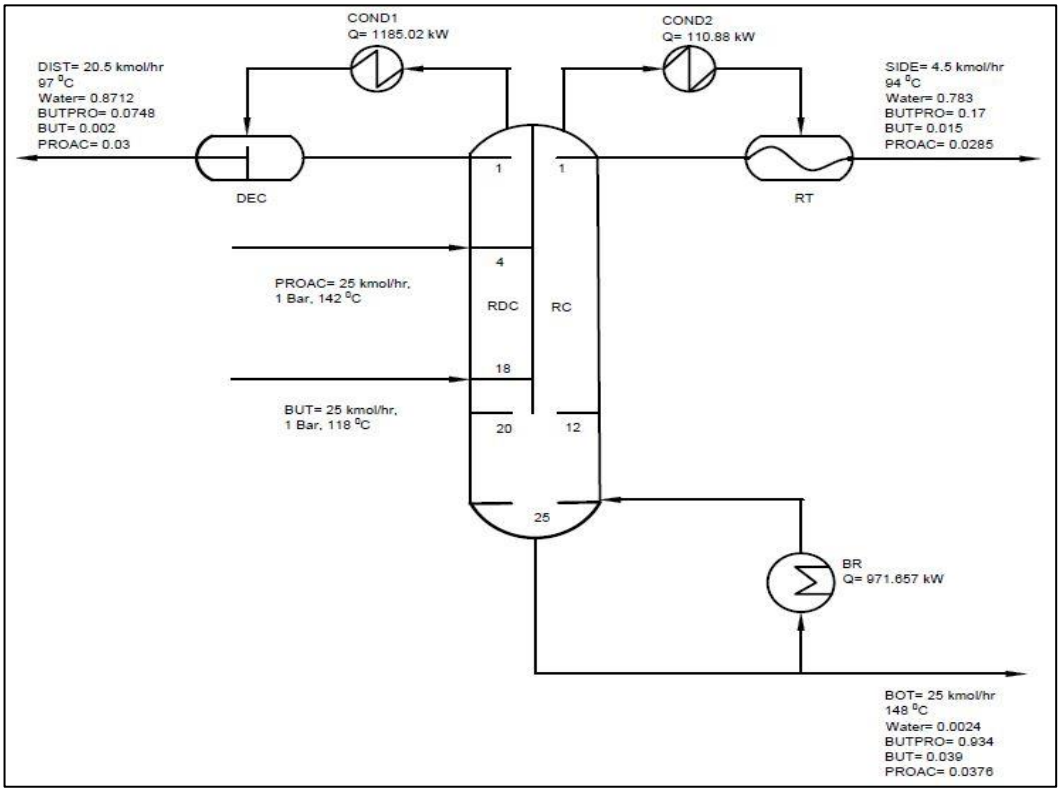

Fig.4.64 Schematic Representation of RDWC (VS) for N-Butyl Propionate

4.5.2.5.1 Temperature variation along the height of the column

The figure 4.65, shows temperature profile throughout the column per stage. Temperature at the top of the column is around 370 K and bottom at is around 420 K. While temperature inside the column ranges between these two values as shown in fig. 12. After 10th stage temperature suddenly increased indicates that reaction start at that stage. The profiles are similar to Liquid split and standard RDC.

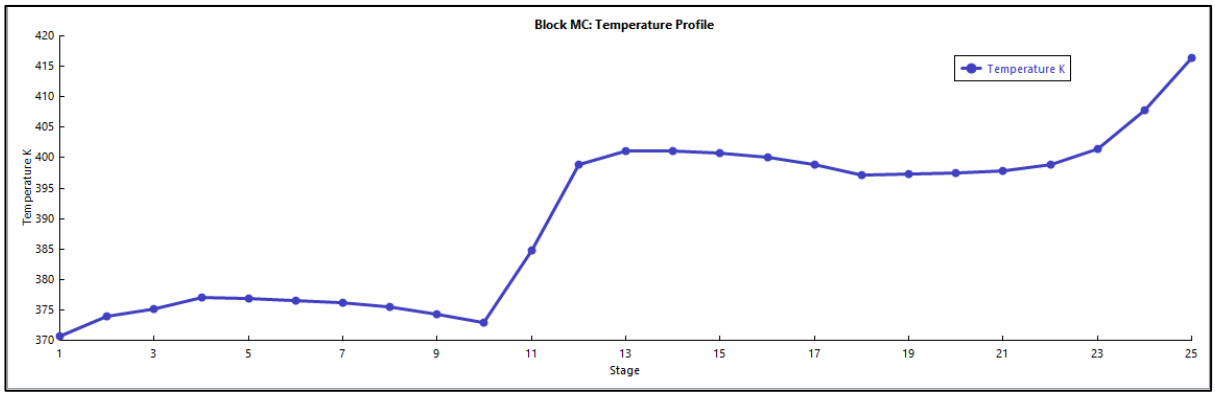

Fig.4.65 Temperature profile across RDWC VS (RDC)

4.5.2.5.2 Concentration profiles in the liquid phase:

Figure 4.66 and 4.67 shows the composition profile of components inside the column. As from the graph, Propionic acid and butanol reacts between 5 to 20 stages. Product butyl propionate is collected at the bottom at 93 mol% while water is obtained from the top at 86 mol%. The percentage of products obtained are less when compared to Liquid Split Scheme while the side

column shows no change in the compositions as there is no any reaction in the side column.

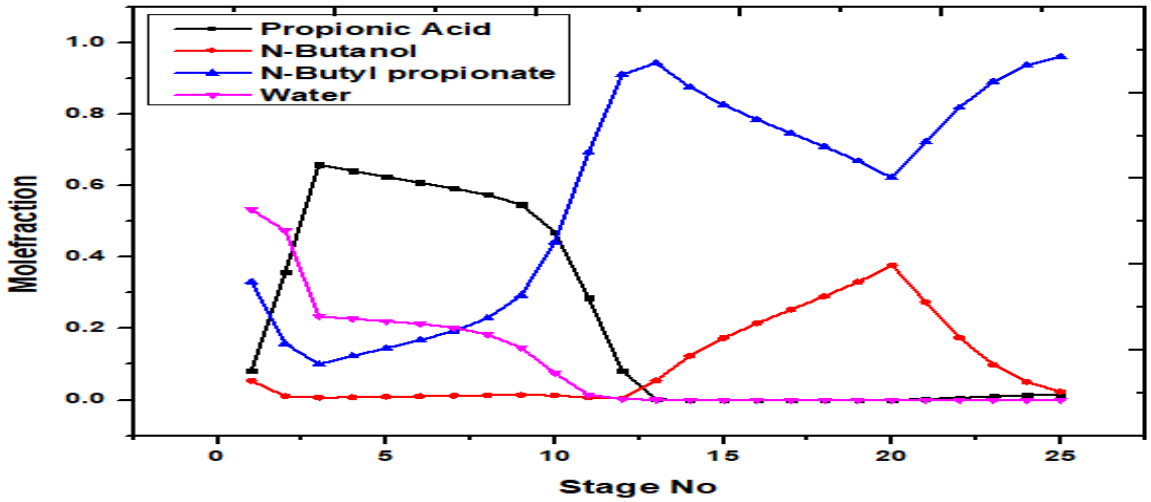

Fig.4.66 Composition profile across RDWC VS (RDC)

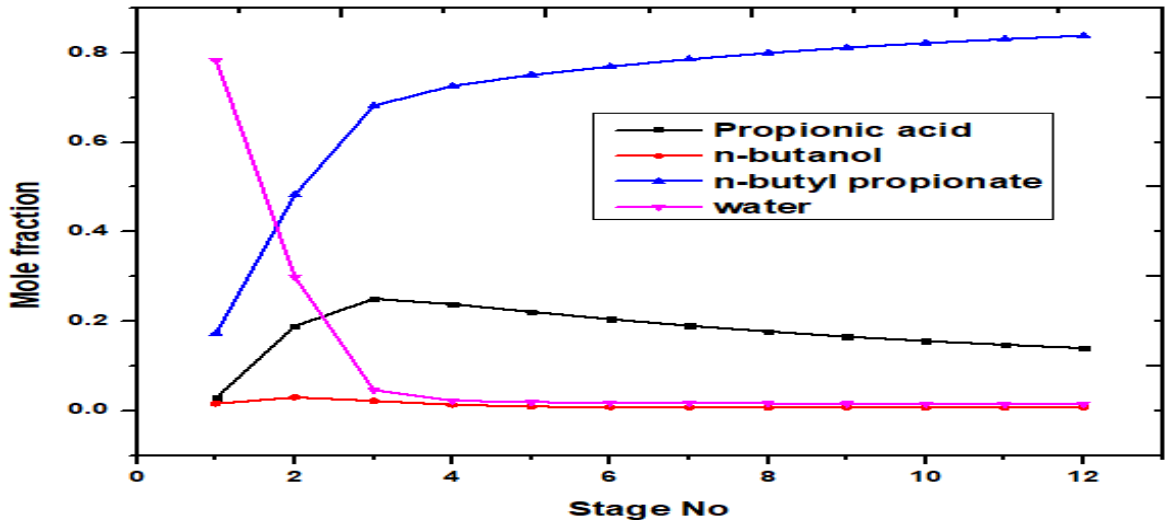

Fig.4.67 Effect of mole fraction on stages

4.5.2.5.3 Product purity as function of reflux ratio:

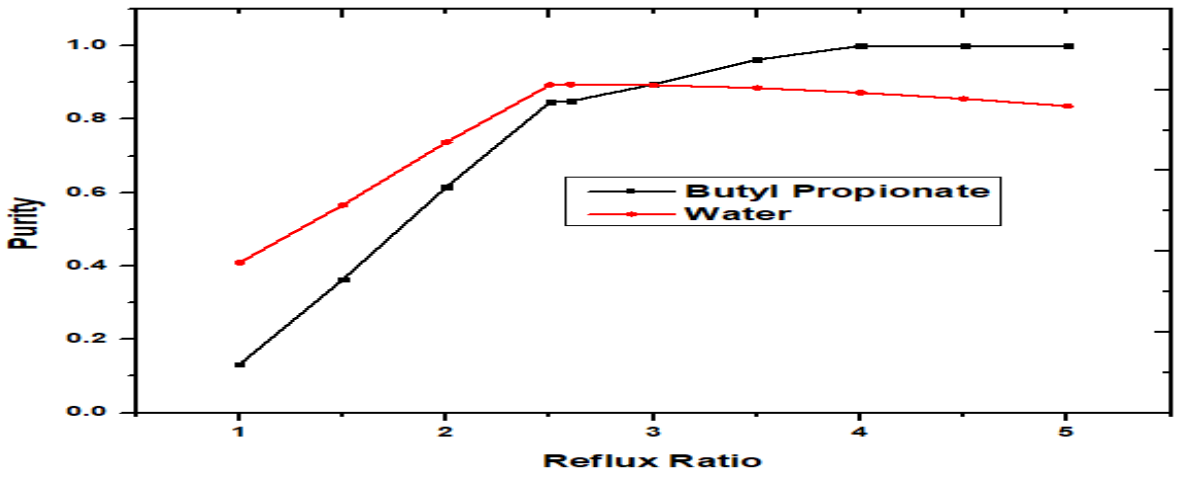

Fig.4.68 Effect of Reflux ratio on Purity of products

The change in purity of products with reflux ratio is shown in above fig 4.68. The profiles and the values are almost similar to the other scheme.

4.5.2.6 Thermodynamic and Exergy Analysis of Energy Integrated distillation Technologies

4.5.2.6.1 Method for Exergy Analysis:

The method of exergy analysis is considered well-established as it is based on the two main laws of thermodynamics. On the basis of the first law an energy balance can be applied to every energy system [138]. However, the second law states that not all the heat energy can be converted to useful work; thus, an exergy balance provides more adequate results. Exergy is the maximum available energy in datum conditions as it proceeds to a dead state; thus, it shows the quantity and quality of energy. In the case of distillation, exergy analysis shows how much of the invested heat can be transformed to separation work and how much irreversible loss is generated. In this study distillation technologies are compared by their heat demand and thermodynamic efficiencies. Enthalpy balances give information about the energy wastes while thermodynamic efficiencies show the rate of heat conversion and separation work. Thethermodynamic efficiency can be calculated with equations:

$$\eta = \frac{W_{sep}}{W_{sep} + EX_{Loss}} \quad (85)$$

Where W_{SEP} is separation work (kW) and Ex_{loss} is exergy loss (kW)

$$W_{sep} = \sum_{out} n_i . \dot{E}x - \sum_{in} n_i . \dot{E}x \quad (86)$$

Where n_i is no of moles per hour and

Ex is

$$Ex = H - T_O S \quad (87)$$

Where H is enthalpy (kJ/kMol), T_o is surrounding temp (K) and S is entropy (kJ/kMol.K)

And

$$Ex_{loss} = T_O \Delta S_{irr} \quad (88)$$

Where ΔS_{irr} is produced by exergy balance.

$$\Delta S_{irr} = \sum_{out} (\dot{n}_i S + \frac{Q_{Cond}}{T_{Cond}}) - \sum_{in} (\dot{n}_i S + \frac{Q_{reb}}{T_{reb}}) \quad (89)$$

Where Q_{cond} and Q_{reb} (kW) are heat flows and T_{cond} and T_{reb} (K) are the temperatures.

Recently exergy analysis has been applied for several technological improvements. Recent approach is the advanced exergy analysis. In advanced exergy analysis different forms of

inefficiencies are differed as avoidable and unavoidable ones.

4.5.2.7 Results for exergy analysis for CRD RDWC (LS) and RDWC (VS):

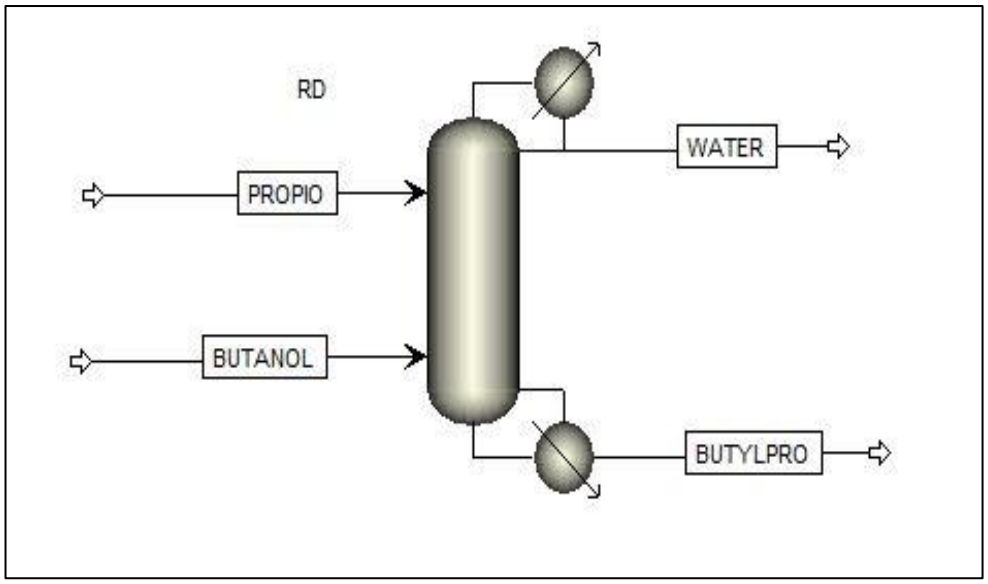

Fig.4.70 Reactive distillation

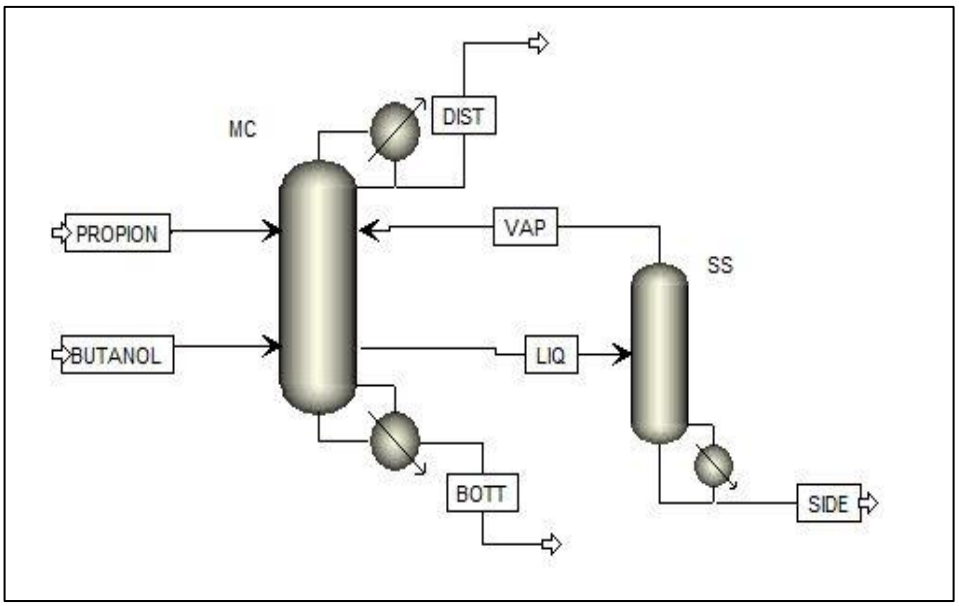

Fig.4.71 RDWC with Liquid Split

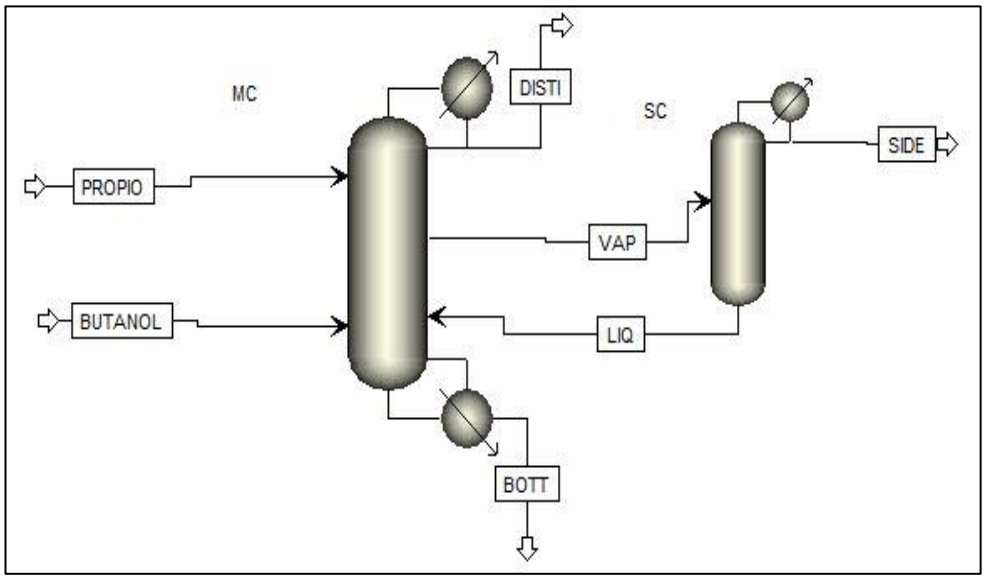

Fig.4.72 RDWC with Vapor Split

Figures given below contain the calculated thermodynamic efficiencies and heat demands of the studied systems.

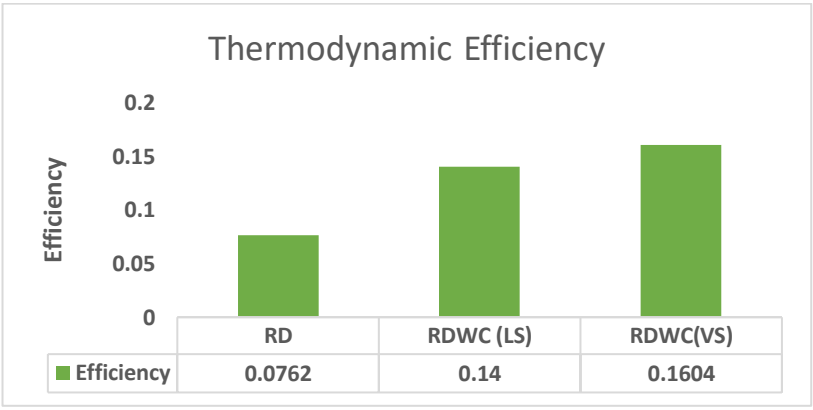

Fig.4.73 Thermodynamic efficiency for the case studies

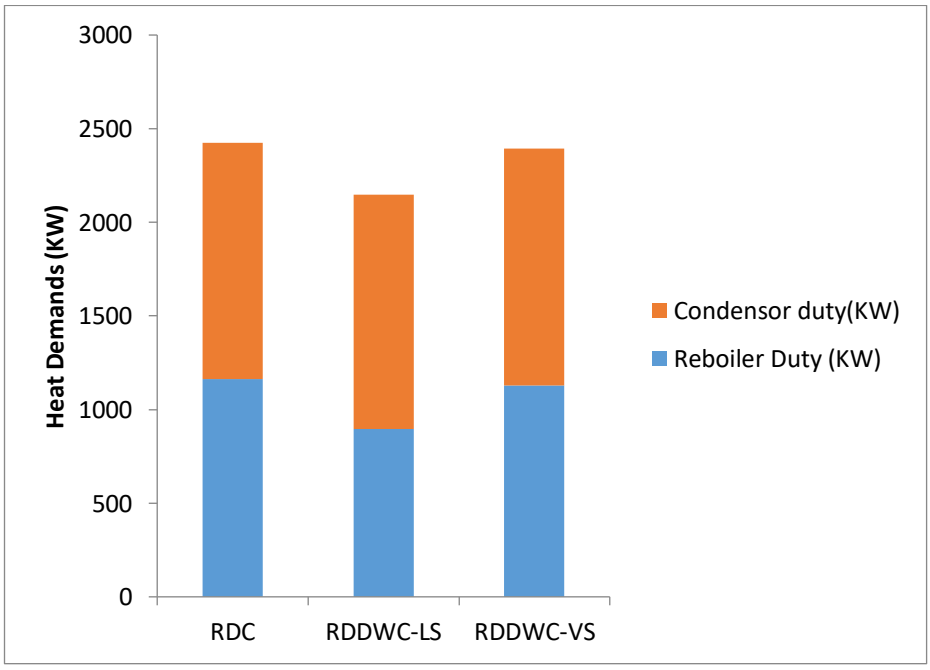

Fig.4.74 Heat Demands for the case studies

Results of the exergy analysis show that RDWC structures are thermodynamically more efficient than the corresponding conventional RD structures. While there is not much of a difference between the RDWC with liquid and vapor split. From the fig. 4.74 it is clearly visible that heat demand for RDDWC- LS is lower than vapor split and conventional RDC. Results show that heat-integration has the highest thermodynamic efficiency among the studied distillation technologies. RDWC-LS and RDWC-VS columns prove to be thermodynamically more efficient than the conventional RD system[144].

4.5.2.8 Cost Analysis for CRD, RDWC (LS) and RDWC (VS)

The basic economic foundation has been given by following equations, [1-3]

For column,

Column capital cost = $17640 * (Dia.)^{1.066} (Height)^{0.802}$ (1)

Dia. and Height in meter

Condensor,

Heat transfer coefficient = 0.852 kW/m^2K

Differential temperature = 13.9 K

Capital cost = $7296 *(Condensor area)^{0.65}$ (2)

Condensor area in m^2

Reboiler

Heat transfer coefficient = 0.568 kW/m^2K

Differential temperature = 34.8 K

Capital cost = $7296 *(reboiler area)^{0.65}$ (3)

Reboiler area in m^2

Energy,

Middle pressure steam (11bar, 457K) = $ 8.22 /GJ

Electricity = $ 16.8 / GJ

Refrigerant chilled water at 5°C = $ 4.43 /GJ

Payback period = 3 years

Capital cost = column capital cost + condensor cost + reboiler cost (4)

Total Annual Cost (TAC) = Capital cost / Payback period + Energy cost (5)

Table. 4.5 Butyl propionate purity and Total annual cost comparison of RDDWC VS & LS w.r.t. RDC

System	TAC ($/year)	% saving w.r.t. RDC	Butyl Propionate Purity
RDC	177939.9622	0	0.888318909
RDDWC_LS	164287.5042	7.672508083	0.986744418
RDDWC_VS	176457.5744	0.83308313	0.948251506

Where U=heat transfer coefficient
Dt-differential temperature
D=diameter of the column
H=height of the column
A_R= area of the reboiler in m^2
A_C=Area of the Condenser in m^2

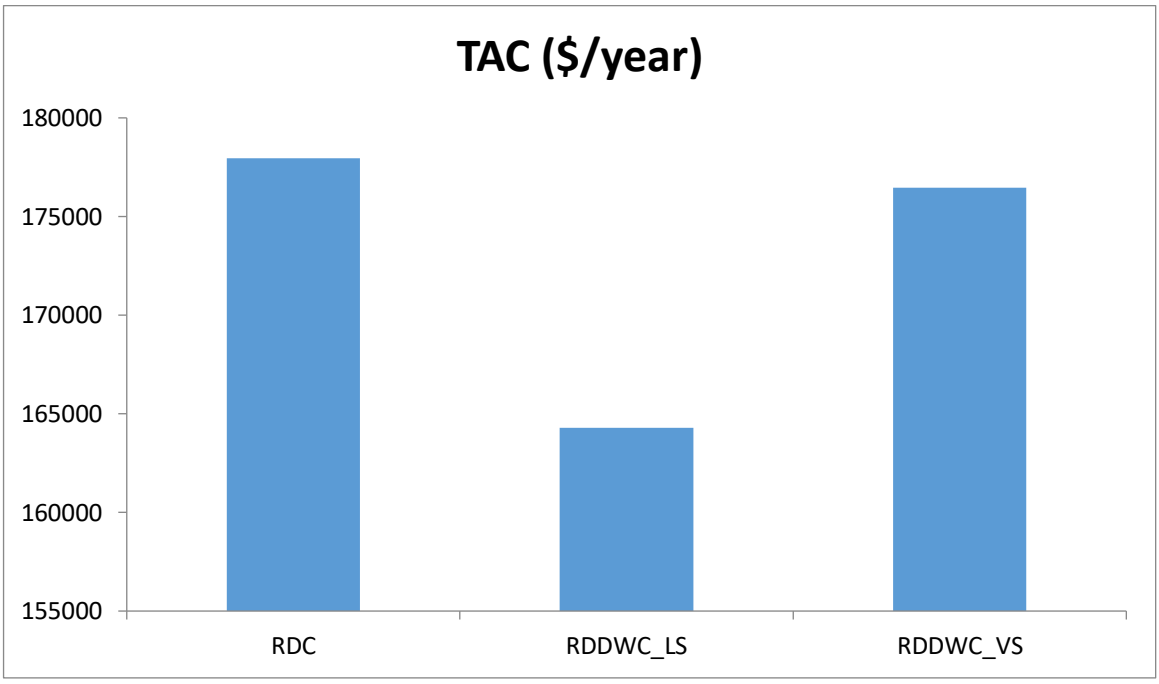

Fig.4.75 Total annual cost for the case studies

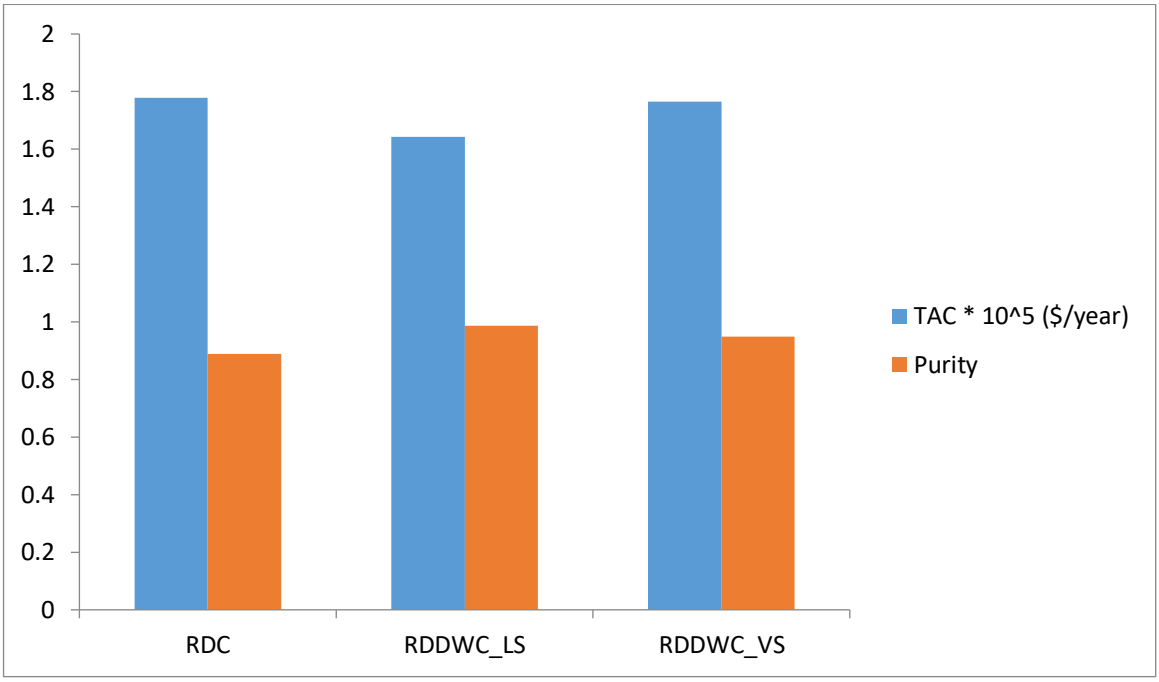

Fig.4.76 TAC and purity for the case studies

Fig. 4.76 gives clear picture about how RDDWC schemes are better than conventional reactive distillation system. RDDWC- LS scheme gives more purity with and reduction in Total annual cost when compared standard RDC. The new configuration proves that modification in the inside the column internals will facilitate high product purity at minimum total cost.

Conclusions and Future work

- The catalytic activities of commercially available liquid catalyst i.e P-Toluene Sulfonic acid and cation exchange resin catalysts i.e Indion 190, Indion180 and Amberlite IR-120 were evaluated for esterification of n-butanol with propionic acid in a stirred batch reactor.
- The experimental results shows that reaction rate increases with increase in temperature and catalyst concentration in the presence of all the studied catalysts.
- It is observed that the effect of the size of the catalyst particle is Minimal.
- The magnetic stirring beyond 240 rpm does not alter the reaction rate.
- Equilibrium conversion increases with the mole ratio of Propionic acid to N-Butanol 1:4>1:3>1:2>1:1
- Mole fraction of butyl propionate in reboiler is as high as 0.91 from RD in packed bed column with a reflux ratio of 2.0 for 1:2 reactant molar flow rate at 115 ºC of reboiler.
- High purity of Butyl propionate is obtained with Propionic acid at the bottom of the reaction zone and butanol at the top of the reaction zone.
- Kinetic models based on Pseudo homogeneous (ideal and non-ideal) approach and adsorption based models i.e Eley-Rideal (E-R) and Langmuir-Hinshel-Wood–Watson (LHHW) were used to find the kinetic parameters
- All the models are in good agreement with the experimental results, however the Pseudo homogeneous model is fitted well with the experimental results compared to adsorption based models for mesoporous catalyst.
- Temperature dependency of equilibrium constant for the reaction was calculated from Van't Hoff equation.
- The heat of reaction was found with mesoporous catalyst with Pseudo homogeneous model.
- A hybrid model for heterogeneous catalytic (Ti SBA-15@SO3H catalyst) esterification of Propionic acid and n-butanol is developed.
- The model predicts the kinetics of conversion accurately for various reaction conditions such as catalyst loading and temperature.
- Experimental results of Batch reactive distillation for the esterification of Propionic Acid and n-butanol to produce butyl propionate are in good agreement with the Mathematical developed based on evaporation based approach..

- Simulation results of continuous Reactive Distillation shows that at the reflux ratio 2 the conversion reached maximum.
- A new configured Reactive Distillation i.e Reactive Divided Wall column is simulated and established optimum parameter values for maximum purity with reduction energy
- The overall results thus have provided new insights into the catalytic reactive distillation process with new configurations.

Future work

1. Reactive distillation experiments by using the controllers in the reboiler and condenser To get high purity of the Butyl propionate.
2. Design and experimentation reactive divided wall column to validate the simulation results.
3. The hydrodynamic effects and separation efficiency of the packing material on the Column performance.

Publications:

1. Raju Kalakuntala, Srinath Suranani. **"Synthesis of environmental friendly Ti material Supported SBA-15 functionalized with Sulfonic acid and its application in esterification process"** published in **Journal of nanomaterial's (SCI).** Volume 2022, Article ID 6712464, 8 pages. https://doi.org/10.1155/2022/6712464
2. Raju Kalakuntala, Srinath Suranani. **"Kinetic Modelling and Optimizing of Butyl Propionate over a Synthesized Material (Tungsten Phosphoric Acid) Hetero-poly Catalyst Using Response Surface Technique"** published in **Annales de Chimie *(ESCI).*** Vol 45.no .4 Aug 2021 pp 273-280 .https://doi.org/10.18280/acsm.450402
3. Raju Kalakuntala, Srinath Suranani. "**Experimental studies on reactive distillation of propionic acid using n-butanol as Entrainer"** is published in **journal of engineering and technology International** (Scopus). Vol 7 (3.29) year (2018) pp no 46-48
4. Raju Kalakuntala, Srinath Suranani. **"Kinetics on propionic acid catalytic esterification with N-butanol over SBA-15(Santa Barbara amorphous-15) catalyst"** published in **Materials Today: Proceedings (Elsevier).** Volume 47, Part 14, 2021, Pages 4814-4819 https://doi.org/10.1016/j.matpr.2021.06.049
5. Raju Kalakuntala, Srinath Suranani. **"Kinetic studies for the esterification of propionic acid with 1-butanol process with ionic resin catalyst".**is published in **Environmental Science and Engineering (Springer publication).pp no 209-217.** https://doi.org/10.1007/978-3-030-96554-9_15. ISBN 978-3-030-96554-9
6. Raju Kalakuntala, Srinath Suranani. **"Kinetics and thermodynamic studies on Propionic Acid with N-butanol using Amberlite IR-120"**. (Accepted) for AIP proceedings

Conferences:

1. "Kinetic studies on propionic acid with N-Butanol using Heterogeneous Catalyst" 2nd international *conference* on. *Numerical heat transfer* and. *Fluid flow* (NHTFF) 2018 is organized by the department of mathematics National institute of technology Warangal(NITW)
2. "Kinetics of Catalytic Esterification of Propionic Acid with N-Butanol over Mesoporous Catalyst" International conference on "Recent advances in chemical engineering 2020" (RACE 2020) organized by University College of technology, Osmania University
3. "Kinetics and thermodynamic studies on Propionic Acid with N-butanol using Amberlite IR-120" 2nd international conference "Chemical, Bio and environmental engineering" (CHEMBION-2021) organized by Dr. B. R. Ambedkar National Institute of Technology Jalandhar, Punjab-144011, INDIA.
4. "Kinetic Modeling of Citrullus Lanatus (Watermelon) Peel Using Thermo Gravimetric Analysis" 2nd International Conference on New Frontiers in Chemical, Energy and Environmental Engineering (INCEEE 2019) organized by department of chemical engineering. National institute of technology Warangal(NITW)
5. "Kinetic modelling and simulations studies for propionic acid esterification process" Novel Materials and Technologies for Energy Applications 2022 organized by Bits Hyderabad

References:

[1] R. Taylor, R. Krishna, Modelling reactive distillation, Chem. Eng. Sci. 55 (2000) 5183–5229. https://doi.org/10.1016/S0009-2509(00)00120-2.

[2] P. Meena, R.K. Dohare, K. Singh, V.P. Singh, S. Upadhyaya, M. Agarwal, A review: control of reactive diviMeena, Priyanka, et al. “A Review: Control of Reactive Divided Wall Distillation Column.” International Journal of Advanced Technology and Engineering Exploration, vol. 4, no. 27, 2016, pp. 28–36, doi:10.19101/ijatee.2017, Int. J. Adv. Technol. Eng. Explor. 4 (2016) 28–36.

[3] B.A.N.N. Bamunusingha, E.C.L. de Silva, M.Y. Gunasekera, Performance of ion exchange resin as solid catalyst for the esterification of acetic acid with ethanol, J. Natl. Sci. Found. Sri Lanka. 44 (2016) 83–93. https://doi.org/10.4038/jnsfsr.v44i1.7985.

[4] S. Hernández, J.G. Segovia-Hernández, L. Juárez-Trujillo, J.E. Estrada-Pacheco, R. Maya-Yescas, Design study of the control of a reactive thermally coupled distillation sequence for the esterification of fatty organic acids, Chem. Eng. Commun. 198 (2011) 1–18. https://doi.org/10.1080/00986445.2010.493102.

[5] H. Sciences, 済無No Title No Title No Title, Chem. Eng. Sci. 4 (2016) 1–23.

[6] Y. Li, S. Han, L. Zhang, W. Li, W. Xing, Fabrication and modeling of catalytic membrane for removing water in esterification, J. Memb. Sci. 579 (2019) 120–130. https://doi.org/10.1016/j.memsci.2019.02.063.

[7] N. Redondo, M.L. Dieuzeide, N. Amadeo, ACID REMOVAL FROM CRUDE OILS BY CATALYTIC ESTERIFICATION NAPHTHENIC ACID CATALIZE BY Mg/Al HYDROTALCITE, Catal. Today. (2019) 0–1. https://doi.org/10.1016/j.cattod.2019.09.051.

[8] K. Raju, G.U.B. Babu, S. Surnanai, Heat and Mass Transfer Limitations in Esterification of Propionic Acid Over Ion Exchange Resin, Proc. Acad. 16th Int. Conf. (2018) 4–7.

[9] M. Banchero, R.D. Kusumaningtyas, G. Gozzelino, Reactive distillation in the intensification of oleic acid esterification with methanol - A simulation case-study, J. Ind. Eng. Chem. 20 (2014) 4242–4249. https://doi.org/10.1016/j.jiec.2014.01.027.

[10] M. Mallaiah, G.V. Reddy, Kinetic Study of Esterification of Acetic Acid with Methanol Over Indion 190 Acidic Solid Catalyst, Кинетика И Катализ. 56 (2015) 421–429. https://doi.org/10.7868/s0453881115040127.

[11] N. Asiedu, D. Hildebrandt, D. Glasser, Experimental Simulation of Three-Dimensional Attainable Region for the Synthesis of Exothermic Reversible Reaction: Ethyl Acetate Synthesis Case Study, Ind. Eng. Chem. Res. 54 (2015) 2619–2626.

https://doi.org/10.1021/ie503276s.

[12] V.S. Chandane, A.P. Rathod, K.L. Wasewar, P.G. Jadhav, Response Surface Methodology and Artificial Neural Networks for Optimization of Catalytic Esterification of Lactic Acid, Chem. Eng. Technol. 43 (2020) 2315–2324. https://doi.org/10.1002/ceat.202000041.

[13] Y. Cho, B. Kim, D. Kim, M. Han, [doi 10.1109_2Ficcas.2008.4694294] Youngmin Cho, _ Bokyung Kim, _ Dongpil Kim, _ Myungwan Han, -- [IEEE 2008 International Conference on Control, Automation and Systems (ICCAS) - Seoul, South Korea (2.pdf, (2008) 2596–2599.

[14] D. Seth, A. Sarkar, F.T.T. Ng, G.L. Rempel, Uncertainties in the simulation of catalytic distillation process: A systematic grid refinement study, Chem. Eng. Sci. 60 (2005) 5445–5457. https://doi.org/10.1016/j.ces.2005.04.036.

[15] F. Aiouache, S. Goto, Reactive distillation-pervaporation hybrid column for tert-amyl alcohol etherification with ethanol, Chem. Eng. Sci. 58 (2003) 2465–2477. https://doi.org/10.1016/S0009-2509(03)00116-7.

[16] S. Hernández, R. Sandoval-Vergara, F.O. Barroso-Muñoz, R. Murrieta-Dueñas, H. Hernández-Escoto, J.G. Segovia-Hernández, V. Rico-Ramirez, Reactive dividing wall distillation columns: Simulation and implementation in a pilot plant, Chem. Eng. Process. Process Intensif. 48 (2009) 250–258. https://doi.org/10.1016/j.cep.2008.03.015.

[17] P.A. Turhanen, J. Leppanen, J.J. Vepsalaïnen, Green and efficient esterification method using dried Dowex H+/NAI approach, ACS Omega. 4 (2019) 8974–8984. https://doi.org/10.1021/acsomega.9b00790.

[18] W.T. Liu, C.S. Tan, Liquid-phase esterification of propionic acid with n-butanol, Ind. Eng. Chem. Res. 40 (2001) 3281–3286. https://doi.org/10.1021/ie001059h.

[19] M.-J. Lee, J.-Y. Chiu, H. Lin, Kinetics of Catalytic Esterification of Propionic Acid and n -Butanol over Amberlyst 35 , Ind. Eng. Chem. Res. 41 (2002) 2882–2887. https://doi.org/10.1021/ie0105472.

[20] M. Mekala, V.R. Goli, Kinetics of esterification of methanol and acetic acid with mineral homogeneous acid catalyst, Chinese J. Chem. Eng. 23 (2015) 100–105. https://doi.org/10.1016/j.cjche.2013.08.002.

[21] A. Shahid, Y. Jamal, S.J. Khan, J.A. Khan, B. Boulanger, Esterification Reaction Kinetics of Acetic and Oleic Acids with Ethanol in the Presence of Amberlyst 15, Arab. J. Sci. Eng. 43 (2018) 5701–5709. https://doi.org/10.1007/s13369-017-2927-y.

[22] M. Weerasinghe, J. Wilkie, D.A. Mammant, A. Diez-Lazaro, M.L. Hitchman, Modelling and Simulation of a Laboratory Scale Esterification Process, IFAC Proc. Vol. 33 (2000) 1037–1042. https://doi.org/10.1016/s1474-6670(17)38677-9.

[23] C.E. Transactions, Simulation of Middle Vessel Batch Reactive Distillation Column : Application to Hydrolysis of Methyl Lactate Simulation of Middle Vessel Batch Reactive Distillation Column : Application to Hydrolysis of Methyl Lactate, (2015). https://doi.org/10.3303/CET1229100.

[24] D.Y. Aqar, N. Rahmanian, I.M. Mujtaba, Feasibility of integrated batch reactive distillation columns for the optimal synthesis of ethyl benzoate, Chem. Eng. Process. Process Intensif. 122 (2017) 10–20. https://doi.org/10.1016/j.cep.2017.08.012.

[25] A. Niesbach, N. Fink, P. Lutze, A. Górak, Design of reactive distillation processes for the production of butyl acrylate: Impact of bio-based raw materials, Chinese J. Chem. Eng. 23 (2015) 1840–1850. https://doi.org/10.1016/j.cjche.2015.08.019.

[26] I. Dejanović, L. Matijašević, Ž. Olujić, Dividing wall column-A breakthrough towards sustainable distilling, Chem. Eng. Process. Process Intensif. 49 (2010) 559–580. https://doi.org/10.1016/j.cep.2010.04.001.

[27] M.E. Pampulha, M.C. Loureiro-Dias, Energetics of the effect of acetic acid on growth of Saccharomyces cerevisiae, FEMS Microbiol. Lett. 184 (2000) 69–72. https://doi.org/10.1016/S0378-1097(00)00022-7.

[28] M. Zhang, L. Ni, J. Jiang, W. Zhang, Thermal runaway and shortstopping of esterification in batch stirred reactors, Process Saf. Environ. Prot. 111 (2017) 326–334. https://doi.org/10.1016/j.psep.2017.07.028.

[29] M. Arabi, M.M. Amini, M. Abedini, A. Nemati, M. Alizadeh, Esterification of phthalic anhydride with 1-butanol and 2-ethylhexanol catalyzed by heteropolyacids, J. Mol. Catal. A Chem. 200 (2003) 105–110. https://doi.org/10.1016/S1381-1169(03)00043-8.

[30] L.K. Rihktv, A.O.I. Krause, Kinetics of Heterogeneously Catalyzed tert-Amyl Methyl Ether Reactions in the Liquid Phase, Ind. Eng. Chem. Res. 34 (1995) 1172–1180. https://doi.org/10.1021/ie00043a020.

[31] Y. Li, S. Han, L. Zhang, W. Li, W. Xing, Fabrication and modeling of catalytic membrane for removing water in esterification, J. Memb. Sci. 579 (2019) 120–130. https://doi.org/10.1016/j.memsci.2019.02.063.

[32] L.U. Kreul, A. Górak, C. Dittrich, P.I. Barton, Dynamic catalytic distillation: Advanced simulation and experimental validation, Comput. Chem. Eng. 22 (1998) S371–S378. https://doi.org/10.1016/s0098-1354(98)00077-5.

[33] A. Shahid, Y. Jamal, S.J. Khan, J.A. Khan, B. Boulanger, Esterification Reaction Kinetics of Acetic and Oleic Acids with Ethanol in the Presence of Amberlyst 15, Arab. J. Sci. Eng. 43 (2018) 5701–5709. https://doi.org/10.1007/s13369-017-2927-y.

[34] M. Mekala, V.R. Goli, Kinetics of esterification of methanol and acetic acid with mineral

homogeneous acid catalyst, Chinese J. Chem. Eng. 23 (2015) 100–105. https://doi.org/10.1016/j.cjche.2013.08.002.

[35] K.N. Rao, A. Sridhar, A.F. Lee, S.J. Tavener, N.A. Young, K. Wilson, Zirconium phosphate supported tungsten oxide solid acid catalysts for the esterification of palmitic acid, Green Chem. 8 (2006) 790–797. https://doi.org/10.1039/b606088a.

[36] K. Raju, G.U.B. Babu, S. Surnanai, Heat and Mass Transfer Limitations in Esterification of Propionic Acid Over Ion Exchange Resin, Proc. Acad. 16th Int. Conf. (2018) 4–7.

[37] W.T. Liu, C.S. Tan, Liquid-phase esterification of propionic acid with n-butanol, Ind. Eng. Chem. Res. 40 (2001) 3281–3286. https://doi.org/10.1021/ie001059h.

[38] Y. Maralla, S. Sonawane, Process intensification using a spiral capillary microreactor for continuous flow synthesis of performic acid and it's kinetic study, Chem. Eng. Process. - Process Intensif. 125 (2018) 67–73. https://doi.org/10.1016/j.cep.2018.01.009.

[39] M. Mallaiah, G.V. Reddy, Kinetic study of esterification of acetic acid with methanol over Indion 190 acidic solid catalyst, Kinet. Catal. 56 (2015) 419–427. https://doi.org/10.1134/S0023158415040126.

[40] P. Botella, A. Corma, J.M. López-Nieto, The influence of textural and compositional characteristics of nafion/silica composites on isobutane/2-butene alkylation, J. Catal. 185 (1999) 371–377. https://doi.org/10.1006/jcat.1999.2502.

[41] S. Xiang, Y. Zhang, Q. Xin, C. Li, Enantioselective epoxidation of olefins catalyzed by Mn (salen)/MCM-41 synthesized with a new anchoring method, Chem. Commun. 2 (2002) 2696–2697. https://doi.org/10.1039/b206104j.

[42] A. Kara, B. Erdem, Synthesis, characterization and catalytic properties of sulfonic acid functionalized magnetic-poly(divinylbenzene-4-vinylpyridine) for esterification of propionic acid with methanol, J. Mol. Catal. A Chem. (2011). https://doi.org/10.1016/j.molcata.2011.08.016.

[43] A. Muftah Almagrbi, T. Hatami, S.B. Glisic, A.M. Orlović, Odredivanje kinetičkih parametara složene reakcije transesterifikacije primenom standardnih optimizacionih metoda, Hem. Ind. 68 (2014) 149–159. https://doi.org/10.2298/HEMIND130118037A.

[44] G.D. Yadav, P.H. Mehta, Heterogeneous Catalysis in Esterification Reactions: Preparation of Phenethyl Acetate and Cyclohexyl Acetate by Using a Variety of Solid Acidic Catalysts, Ind. Eng. Chem. Res. 33 (1994) 2198–2208. https://doi.org/10.1021/ie00033a025.

[45] J. Bedard, H. Chiang, A. Bhan, Kinetics and mechanism of acetic acid esterification with ethanol on zeolites, J. Catal. 290 (2012) 210–219. https://doi.org/10.1016/j.jcat.2012.03.020.

[46] M.I. Zubir, S.Y. Chin, Kinetics of modified Zirconia-catalyzed heterogeneous esterification

reaction for biodiesel production, J. Appl. Sci. 10 (2010) 2584–2589. https://doi.org/10.3923/jas.2010.2584.2589.

[47] M.B. Mandake, S. V Anekar, S. Walke, Kinetic Study of Catalyzed and Uncatalyzed Esterification Reaction of Acetic acid with Methanol, Am. Int. J. Res. Sci. Technol. Eng. Math. 3 (2013) 114–121.

[48] N. Singh, Raj kumar, P.K. Sachan, Kinetic Study of Catalytic Esterification of Butyric Acid and Ethanol over Amberlyst 15, ISRN Chem. Eng. 2013 (2013) 1–6. https://doi.org/10.1155/2013/520293.

[49] Y. Liu, E. Lotero, J.G. Goodwin, A comparison of the esterification of acetic acid with methanol using heterogeneous versus homogeneous acid catalysis, J. Catal. 242 (2006) 278–286. https://doi.org/10.1016/j.jcat.2006.05.026.

[50] K. Das, P. Sahoo, M.S.A.I. Baba, N. Murali, P. Swaminathan, Kinetic Studies on Saponification of Ethyl Acetate Using an Innovative Instrument with a Pulsating, Wiley Online Libr. 14 (2011) 1–6. https://doi.org/10.1002/kin.

[51] M. Trejda, A. Nurwita, D. Kryszak, Synthesis of solid acid catalysts for esterification with the assistance of elevated pressure, Microporous Mesoporous Mater. (2019). https://doi.org/10.1016/j.micromeso.2018.11.009.

[52] S. Karakus, E. Sert, D. Buluklu, F.S. Atalay, 4-Liquid Phase Esterification of Acrylic Acid with Isobutyl Alcohol.pdf, (2014).

[53] L. Gang, L. Xinzong, W. Eli, Solvent-free esterification catalyzed by surfactant-combined catalysts at room temperature, New J. Chem. 31 (2007) 348–351. https://doi.org/10.1039/b615448d.

[54] Y.K. Lin, V.H. Nguyen, J.C.C. Yu, C.W. Lee, Y.H. Deng, J.C.S. Wu, K.C.W. Wu, K.L. Tung, C.L. Chen, Biodiesel production by pervaporation-assisted esterification and pre-esterification using graphene oxide/chitosan composite membranes, J. Taiwan Inst. Chem. Eng. 79 (2017) 23–30. https://doi.org/10.1016/j.jtice.2017.06.031.

[55] F. Cunill, M. Iborra, C. Fité, J. Tejero, J.F. Izquierdo, Conversion, selectivity, and kinetics of the addition of isopropanol to isobutene catalyzed by a macroporous ion-exchange resin, Ind. Eng. Chem. Res. 39 (2000) 1235–1241. https://doi.org/10.1021/ie990315r.

[56] K. Neumann, K. Werth, A. Martín, A. Górak, Biodiesel production from waste cooking oils through esterification: Catalyst screening, chemical equilibrium and reaction kinetics, Chem. Eng. Res. Des. 107 (2016) 52–62. https://doi.org/10.1016/j.cherd.2015.11.008.

[57] M.T. Sanz, R. Murga, S. Beltrán, J.L. Cabezas, J. Coca, Autocatalyzed and ion-exchange-resin-catalyzed esterification kinetics of lactic acid with methanol, Ind. Eng. Chem. Res. 41 (2002) 512–517. https://doi.org/10.1021/ie010454k.

[58] E.C.L. De Silva, B.A.N.N. Bamunusingha, M.Y. Gunasekera, Heterogeneous Kinetic Study for Esterification of Acetic Acid with Ethanol, Eng. J. Inst. Eng. Sri Lanka. 47 (2014) 9. https://doi.org/10.4038/engineer.v47i1.6855.

[59] X. Wang, Q. Zhao, H. Wang, H. Zheng, Z. Sun, W. Shi, S. Wang, Z. Jiang, Acid-base bifunctional HPA nanocatalysts promoting heterogeneous transesterification and esterification reactions, Catal. Sci. Technol. 3 (2013) 2204–2209. https://doi.org/10.1039/c3cy20868k.

[60] W.M. Van Rhijn, D.E. De Vos, B.F. Sels, W.D. Bossaert, P.A. Jacobs, Sulfonic acid functionalised ordered mesoporous materials as catalysts for condensation and esterification reactions, Chem. Commun. (1998) 317–318. https://doi.org/10.1039/a707462j.

[61] E. Poli, J.M. Clacens, J. Barrault, Y. Pouilloux, Solvent-free selective epoxidation of fatty esters over a tungsten-based catalyst, Catal. Today. 140 (2009) 19–22. https://doi.org/10.1016/j.cattod.2008.07.004.

[62] M. Mekala, V.R. Goli, Kinetics of esterification of acetic acid and methanol using amberlyst 36 cation-exchange resin solid catalyst, Prog. React. Kinet. Mech. 40 (2015) 367–382. https://doi.org/10.3184/146867815X14413752286146.

[63] N. Redondo, M.L. Dieuzeide, N. Amadeo, ACID REMOVAL FROM CRUDE OILS BY CATALYTIC ESTERIFICATION NAPHTHENIC ACID CATALIZE BY Mg/Al HYDROTALCITE, Catal. Today. (2019) 0–1. https://doi.org/10.1016/j.cattod.2019.09.051.

[64] P.E. Jagadeeshbabu, K. Sandesh, M.B. Saidutta, Kinetics of esterification of acetic acid with methanol in the presence of ion exchange resin catalysts, Ind. Eng. Chem. Res. 50 (2011) 7155–7160. https://doi.org/10.1021/ie101755r.

[65] X. Lu, H. Yin, L. Shen, Y. Feng, A. Wang, Y. Shen, H. Hang, D. Mao, Reaction kinetics of the esterification reaction between ethanol and acetic acid catalyzed by Keggin heteropolyacids, React. Kinet. Mech. Catal. 111 (2014) 15–27. https://doi.org/10.1007/s11144-013-0641-7.

[66] M.-J. Lee, J.-Y. Chiu, H. Lin, Kinetics of Catalytic Esterification of Propionic Acid and n -Butanol over Amberlyst 35 , Ind. Eng. Chem. Res. (2002). https://doi.org/10.1021/ie0105472.

[67] S. Miao, B.H. Shanks, Mechanism of acetic acid esterification over sulfonic acid-functionalized mesoporous silica, J. Catal. 279 (2011) 136–143. https://doi.org/10.1016/j.jcat.2011.01.008.

[68] M. Mallaiah, G.V. Reddy, Optimization studies on a continuous catalytic reactive

distillation column for methyl acetate production with response surface methodology, J. Taiwan Inst. Chem. Eng. 69 (2016) 25–40. https://doi.org/10.1016/j.jtice.2016.10.007.

[69] L. Dai, Q. Zhao, M. Fang, R. Liu, M. Dong, T. Jiang, Catalytic activity comparison of Zr-SBA-15 immobilized by a Brønsted-Lewis acidic ionic liquid in different esterifications, RSC Adv. 7 (2017) 32427–32435. https://doi.org/10.1039/c7ra04950a.

[70] K.N.P. Rani, T.S.V.R. Neeharika, T.P. Kumar, B. Satyavathi, C. Sailu, R.B.N. Prasad, Kinetics of enzymatic esterification of oleic acid and decanol for wax ester and evaluation of its physico-chemical properties, J. Taiwan Inst. Chem. Eng. 55 (2015) 12–16. https://doi.org/10.1016/j.jtice.2015.04.011.

[71] L.T.A. Sofia, A. Krishnan, M. Sankar, N.K.K. Raj, P. Manikandan, P.R. Rajamohanan, T.G. Ajithkumar, Immobilization of phosphotungstic acid (PTA) on imidazole functionalized silica: Evidence for the nature of PTA binding by solid state NMR and reaction studies, J. Phys. Chem. C. 113 (2009) 21114–21122. https://doi.org/10.1021/jp906108e.

[72] N. Asiedu, D. Hildebrandt, D. Glasser, Modeling and Simulation of Temperature Profiles in a Reactive Distillation System for Esterification of Acetic Anhydride with Methanol, Chem. Process Eng. Res. 10 (2013) 51–94.

[73] Y.T. Tsai, H.M. Lin, M.J. Lee, Kinetics of catalytic esterification of propionic acid with methanol over amberlyst 36, Ind. Eng. Chem. Res. 50 (2011) 1171–1176. https://doi.org/10.1021/ie1001179.

[74] Y. Liu, E. Lotero, J.G. Goodwin, Effect of water on sulfuric acid catalyzed esterification, J. Mol. Catal. A Chem. 245 (2006) 132–140. https://doi.org/10.1016/j.molcata.2005.09.049.

[75] S.M.A. Rahman, A.S. Mujumdar, Leak detection of gas transport pipelines based on wigner distribution, 2011 Int. Symp. Adv. Control Ind. Process. (2011) 258–261. https://doi.org/10.1002/apj.

[76] M. Mallaiah, G.V. Reddy, Optimization studies on a continuous catalytic reactive distillation column for methyl acetate production with response surface methodology, J. Taiwan Inst. Chem. Eng. 69 (2016) 25–40. https://doi.org/10.1016/j.jtice.2016.10.007.

[77] F. Cunill, M. Iborra, C. Fité, J. Tejero, J.F. Izquierdo, Conversion, selectivity, and kinetics of the addition of isopropanol to isobutene catalyzed by a macroporous ion-exchange resin, Ind. Eng. Chem. Res. 39 (2000) 1235–1241. https://doi.org/10.1021/ie990315r.

[78] K. Neumann, K. Werth, A. Martín, A. Górak, Biodiesel production from waste cooking oils through esterification: Catalyst screening, chemical equilibrium and reaction kinetics, Chem. Eng. Res. Des. 107 (2016) 52–62. https://doi.org/10.1016/j.cherd.2015.11.008.

[79] M.T. Sanz, R. Murga, S. Beltrán, J.L. Cabezas, J. Coca, Autocatalyzed and ion-exchange-

resin-catalyzed esterification kinetics of lactic acid with methanol, Ind. Eng. Chem. Res. 41 (2002) 512–517. https://doi.org/10.1021/ie010454k.

[80] E.C.L. De Silva, B.A.N.N. Bamunusingha, M.Y. Gunasekera, Heterogeneous Kinetic Study for Esterification of Acetic Acid with Ethanol, Eng. J. Inst. Eng. Sri Lanka. 47 (2014) 9. https://doi.org/10.4038/engineer.v47i1.6855.

[81] X. Wang, Q. Zhao, H. Wang, H. Zheng, Z. Sun, W. Shi, S. Wang, Z. Jiang, Acid-base bifunctional HPA nanocatalysts promoting heterogeneous transesterification and esterification reactions, Catal. Sci. Technol. 3 (2013) 2204–2209. https://doi.org/10.1039/c3cy20868k.

[82] W.M. Van Rhijn, D.E. De Vos, B.F. Sels, W.D. Bossaert, P.A. Jacobs, Sulfonic acid functionalised ordered mesoporous materials as catalysts for condensation and esterification reactions, Chem. Commun. (1998) 317–318. https://doi.org/10.1039/a707462j.

[83] E. Poli, J.M. Clacens, J. Barrault, Y. Pouilloux, Solvent-free selective epoxidation of fatty esters over a tungsten-based catalyst, Catal. Today. 140 (2009) 19–22. https://doi.org/10.1016/j.cattod.2008.07.004.

[84] M. Mekala, V.R. Goli, Kinetics of esterification of acetic acid and methanol using amberlyst 36 cation-exchange resin solid catalyst, Prog. React. Kinet. Mech. 40 (2015) 367–382. https://doi.org/10.3184/146867815X14413752286146.

[85] N. Redondo, M.L. Dieuzeide, N. Amadeo, ACID REMOVAL FROM CRUDE OILS BY CATALYTIC ESTERIFICATION NAPHTHENIC ACID CATALIZE BY Mg/Al HYDROTALCITE, Catal. Today. (2019) 0–1. https://doi.org/10.1016/j.cattod.2019.09.051.

[86] M.E. Pampulha, M.C. Loureiro-Dias, Energetics of the effect of acetic acid on growth of Saccharomyces cerevisiae, FEMS Microbiol. Lett. 184 (2000) 69–72. https://doi.org/10.1016/S0378-1097(00)00022-7.

[87] M. Zhang, L. Ni, J. Jiang, W. Zhang, Thermal runaway and shortstopping of esterification in batch stirred reactors, Process Saf. Environ. Prot. 111 (2017) 326–334. https://doi.org/10.1016/j.psep.2017.07.028.

[88] M. Arabi, M.M. Amini, M. Abedini, A. Nemati, M. Alizadeh, Esterification of phthalic anhydride with 1-butanol and 2-ethylhexanol catalyzed by heteropolyacids, J. Mol. Catal. A Chem. 200 (2003) 105–110. https://doi.org/10.1016/S1381-1169(03)00043-8.

[89] M. Mekala, V.R. Goli, Kinetics of esterification of methanol and acetic acid with mineral homogeneous acid catalyst, Chinese J. Chem. Eng. 23 (2015) 100–105. https://doi.org/10.1016/j.cjche.2013.08.002.

[90] L.K. Rihktv, A.O.I. Krause, Kinetics of Heterogeneously Catalyzed tert-Amyl Methyl Ether Reactions in the Liquid Phase, Ind. Eng. Chem. Res. 34 (1995) 1172–1180. https://doi.org/10.1021/ie00043a020.

[91] Y. Li, S. Han, L. Zhang, W. Li, W. Xing, Fabrication and modeling of catalytic membrane for removing water in esterification, J. Memb. Sci. 579 (2019) 120–130. https://doi.org/10.1016/j.memsci.2019.02.063.

[92] L.U. Kreul, A. Górak, C. Dittrich, P.I. Barton, Dynamic catalytic distillation: Advanced simulation and experimental validation, Comput. Chem. Eng. 22 (1998) S371–S378. https://doi.org/10.1016/s0098-1354(98)00077-5.

[93] A. Shahid, Y. Jamal, S.J. Khan, J.A. Khan, B. Boulanger, Esterification Reaction Kinetics of Acetic and Oleic Acids with Ethanol in the Presence of Amberlyst 15, Arab. J. Sci. Eng. 43 (2018) 5701–5709. https://doi.org/10.1007/s13369-017-2927-y.

[94] K.N. Rao, A. Sridhar, A.F. Lee, S.J. Tavener, N.A. Young, K. Wilson, Zirconium phosphate supported tungsten oxide solid acid catalysts for the esterification of palmitic acid, Green Chem. 8 (2006) 790–797. https://doi.org/10.1039/b606088a.

[95] K. Raju, G.U.B. Babu, S. Surnanai, Heat and Mass Transfer Limitations in Esterification of Propionic Acid Over Ion Exchange Resin, Proc. Acad. 16th Int. Conf. (2018) 4–7.

[96] W.T. Liu, C.S. Tan, Liquid-phase esterification of propionic acid with n-butanol, Ind. Eng. Chem. Res. 40 (2001) 3281–3286. https://doi.org/10.1021/ie001059h.

[97] Y. Maralla, S. Sonawane, Process intensification using a spiral capillary microreactor for continuous flow synthesis of performic acid and it's kinetic study, Chem. Eng. Process. - Process Intensif. 125 (2018) 67–73. https://doi.org/10.1016/j.cep.2018.01.009.

[98] M. Mallaiah, G.V. Reddy, Kinetic study of esterification of acetic acid with methanol over Indion 190 acidic solid catalyst, Kinet. Catal. 56 (2015) 419–427. https://doi.org/10.1134/S0023158415040126.

[99] P. Botella, A. Corma, J.M. López-Nieto, The influence of textural and compositional characteristics of nafion/silica composites on isobutane/2-butene alkylation, J. Catal. 185 (1999) 371–377. https://doi.org/10.1006/jcat.1999.2502.

[100] S. Xiang, Y. Zhang, Q. Xin, C. Li, Enantioselective epoxidation of olefins catalyzed by Mn (salen)/MCM-41 synthesized with a new anchoring method, Chem. Commun. 2 (2002) 2696–2697. https://doi.org/10.1039/b206104j.

[101] A. Kara, B. Erdem, Synthesis, characterization and catalytic properties of sulfonic acid functionalized magnetic-poly(divinylbenzene-4-vinylpyridine) for esterification of propionic acid with methanol, J. Mol. Catal. A Chem. (2011). https://doi.org/10.1016/j.molcata.2011.08.016.

[102] A. Muftah Almagrbi, T. Hatami, S.B. Glisic, A.M. Orlović, Odredivanje kinetičkih parametara složene reakcije transesterifikacije primenom standardnih optimizacionih metoda, Hem. Ind. 68 (2014) 149–159. https://doi.org/10.2298/HEMIND130118037A.

[103] G.D. Yadav, P.H. Mehta, Heterogeneous Catalysis in Esterification Reactions: Preparation of Phenethyl Acetate and Cyclohexyl Acetate by Using a Variety of Solid Acidic Catalysts, Ind. Eng. Chem. Res. 33 (1994) 2198–2208. https://doi.org/10.1021/ie00033a025.

[104] M.I. Zubir, S.Y. Chin, Kinetics of modified Zirconia-catalyzed heterogeneous esterification reaction for biodiesel production, J. Appl. Sci. 10 (2010) 2584–2589. https://doi.org/10.3923/jas.2010.2584.2589.

[105] M.B. Mandake, S. V Anekar, S. Walke, Kinetic Study of Catalyzed and Uncatalyzed Esterification Reaction of Acetic acid with Methanol, Am. Int. J. Res. Sci. Technol. Eng. Math. 3 (2013) 114–121.

[106] N. Singh, Raj kumar, P.K. Sachan, Kinetic Study of Catalytic Esterification of Butyric Acid and Ethanol over Amberlyst 15, ISRN Chem. Eng. 2013 (2013) 1–6. https://doi.org/10.1155/2013/520293.

[107] Y. Liu, E. Lotero, J.G. Goodwin, A comparison of the esterification of acetic acid with methanol using heterogeneous versus homogeneous acid catalysis, J. Catal. 242 (2006) 278–286. https://doi.org/10.1016/j.jcat.2006.05.026.

[108] K. Das, P. Sahoo, M.S.A.I. Baba, N. Murali, P. Swaminathan, Kinetic Studies on Saponification of Ethyl Acetate Using an Innovative Instrument with a Pulsating, Wiley Online Libr. 14 (2011) 1–6. https://doi.org/10.1002/kin.

[109] M. Trejda, A. Nurwita, D. Kryszak, Synthesis of solid acid catalysts for esterification with the assistance of elevated pressure, Microporous Mesoporous Mater. (2019). https://doi.org/10.1016/j.micromeso.2018.11.009.

[110] S. Karakus, E. Sert, D. Buluklu, F.S. Atalay, 4-Liquid Phase Esterification of Acrylic Acid with Isobutyl Alcohol.pdf, (2014).

[111] L. Gang, L. Xinzong, W. Eli, Solvent-free esterification catalyzed by surfactant-combined catalysts at room temperature, New J. Chem. 31 (2007) 348–351. https://doi.org/10.1039/b615448d.

[112] Y.K. Lin, V.H. Nguyen, J.C.C. Yu, C.W. Lee, Y.H. Deng, J.C.S. Wu, K.C.W. Wu, K.L. Tung, C.L. Chen, Biodiesel production by pervaporation-assisted esterification and pre-esterification using graphene oxide/chitosan composite membranes, J. Taiwan Inst. Chem. Eng. 79 (2017) 23–30. https://doi.org/10.1016/j.jtice.2017.06.031.

[113] P.E. Jagadeeshbabu, K. Sandesh, M.B. Saidutta, Kinetics of esterification of acetic acid with methanol in the presence of ion exchange resin catalysts, Ind. Eng. Chem. Res. 50

(2011) 7155–7160. https://doi.org/10.1021/ie101755r.

[114] X. Lu, H. Yin, L. Shen, Y. Feng, A. Wang, Y. Shen, H. Hang, D. Mao, Reaction kinetics of the esterification reaction between ethanol and acetic acid catalyzed by Keggin heteropolyacids, React. Kinet. Mech. Catal. 111 (2014) 15–27. https://doi.org/10.1007/s11144-013-0641-7.

[115] M.-J. Lee, J.-Y. Chiu, H. Lin, Kinetics of Catalytic Esterification of Propionic Acid and n -Butanol over Amberlyst 35 , Ind. Eng. Chem. Res. (2002). https://doi.org/10.1021/ie0105472.

[116] S. Miao, B.H. Shanks, Mechanism of acetic acid esterification over sulfonic acid-functionalized mesoporous silica, J. Catal. 279 (2011) 136–143. https://doi.org/10.1016/j.jcat.2011.01.008.

[117] L. Dai, Q. Zhao, M. Fang, R. Liu, M. Dong, T. Jiang, Catalytic activity comparison of Zr-SBA-15 immobilized by a Brønsted-Lewis acidic ionic liquid in different esterifications, RSC Adv. 7 (2017) 32427–32435. https://doi.org/10.1039/c7ra04950a.

[118] K.N.P. Rani, T.S.V.R. Neeharika, T.P. Kumar, B. Satyavathi, C. Sailu, R.B.N. Prasad, Kinetics of enzymatic esterification of oleic acid and decanol for wax ester and evaluation of its physico-chemical properties, J. Taiwan Inst. Chem. Eng. 55 (2015) 12–16. https://doi.org/10.1016/j.jtice.2015.04.011.

[119] N. Asiedu, D. Hildebrandt, D. Glasser, Modeling and Simulation of Temperature Profiles in a Reactive Distillation System for Esterification of Acetic Anhydride with Methanol, Chem. Process Eng. Res. 10 (2013) 51–94.

[120] Y.T. Tsai, H.M. Lin, M.J. Lee, Kinetics of catalytic esterification of propionic acid with methanol over amberlyst 36, Ind. Eng. Chem. Res. 50 (2011) 1171–1176. https://doi.org/10.1021/ie1001179.

[121] Y. Liu, E. Lotero, J.G. Goodwin, Effect of water on sulfuric acid catalyzed esterification, J. Mol. Catal. A Chem. 245 (2006) 132–140. https://doi.org/10.1016/j.molcata.2005.09.049.

[122] S.M.A. Rahman, A.S. Mujumdar, Leak detection of gas transport pipelines based on wigner distribution, 2011 Int. Symp. Adv. Control Ind. Process. (2011) 258–261. https://doi.org/10.1002/apj.

[123] T. Pöpken, S. Steinigeweg, J. Gmehling, Synthesis and hydrolysis of methyl acetate by reactive distillation using structured catalytic packings: Experiments and simulation, Ind. Eng. Chem. Res. 40 (2001) 1566–1574. https://doi.org/10.1021/ie0007419.

[124] H. Zhang, Q. Ye, J. Qin, H. Xu, N. Li, Design and control of extractive dividing-wall

column for separating ethyl acetate-isopropyl alcohol mixture, Ind. Eng. Chem. Res. 53 (2014) 1189–1205. https://doi.org/10.1021/ie403618f.

[125] G. Fernholz, S. Engell, L.U. Kreul, A. Gorak, Optimal operation of a semi-batch reactive distillation column, Comput. Chem. Eng. 24 (2000) 1569–1575. https://doi.org/10.1016/S0098-1354(00)00553-6.

[126] K. Ouyang, Syn the sis of -Caprolactam from Cyclohexanone Oxime Using Zeolites H , HZSM-5 , and Alu mina Pil lared Mont mo ril lo nite, (2001) 137–144.

[127] B. Saha, H.T.R. Teo, A. Alqahtani, Iso-amyl acetate synthesis by catalytic distillation, Int. J. Chem. React. Eng. 3 (2005). https://doi.org/10.2202/1542-6580.1250.

[128] A.F. Martínez, C.A. Sánchez, A. Orjuela, I.D. Gil, G. Rodríguez, Isobutyl acetate by reactive distillation. Part II. Kinetic study, Chem. Eng. Res. Des. 160 (2020) 447–453. https://doi.org/10.1016/j.cherd.2020.06.023.

[129] S.P. Chopade, M.M. Sharma, Reaction of ethanol and formaldehyde: Use of versatile cation-exchange resins as catalyst in batch reactors and reactive distillation columns, React. Funct. Polym. 32 (1997) 53–65. https://doi.org/10.1016/S1381-5148(96)00069-7.

[130] J. Xie, C. Li, F. Peng, L. Dong, S. Ma, Experimental and simulation of the reactive dividing wall column based on ethyl acetate synthesis, Chinese J. Chem. Eng. 26 (2018) 1468–1476. https://doi.org/10.1016/j.cjche.2018.01.021.

[131] S. Hernández, R. Sandoval-Vergara, F.O. Barroso-Muñoz, R. Murrieta-Dueñas, H. Hernández-Escoto, J.G. Segovia-Hernández, V. Rico-Ramirez, Reactive dividing wall distillation columns: Simulation and implementation in a pilot plant, Chem. Eng. Process. Process Intensif. 48 (2009) 250–258. https://doi.org/10.1016/j.cep.2008.03.015.

[132] K. Khushalani, A. Maheshwari, N. Jain, Separation of mixture by divided wall column using Aspen Plus, Int. J. Emerg. Technol. Adv. Eng. 4 (2014) 563–571.

[133] D. Design, C.U. Aspen, DIVIDED-WALL (PETLYUK) COLUMNS, (n.d.).

[134] S. Lone, Modeling and Simulation of a Hybrid Process (Pervaporation+Distillation) using MATLAB, J. Chem. Eng. Process Technol. 06 (2015). https://doi.org/10.4172/2157-7048.1000234.

[135] B. Gheorghe, A. Ene, R. Isopescu, A. Torma, Process simulation of reactive distillation in dividing wall column for ETBE synthesis process, Chem. Eng. Trans. 18 (2009) 487–492. https://doi.org/10.3303/CET0918079.

[136] V.K. Sangal, V. Kumar, I.M. Mishra, Optimizacija kolone sa vertikalnom pregradom za razdvajanje smeše normalnih parafina C4-C6 pomoću Box-Behnkenovog plana, Chem. Ind. Chem. Eng. Q. 19 (2013) 107–119. https://doi.org/10.2298/CICEQ121019047S.

[137] L. Xu, M. Li, X. Yin, X. Yuan, New Intensified Heat Integration of Vapor Recompression Assisted Dividing Wall Column, Ind. Eng. Chem. Res. 56 (2017) 2188–2196. https://doi.org/10.1021/acs.iecr.6b03802.

[138] N. Gor, S.R. Satpute, ICSDEE-2017, (2017).

[139] S. Feng, X. Lyu, Q. Ye, H. Xia, R. Li, X. Suo, Performance Enhancement of Reactive Dividing-Wall Column via Vapor Recompression Heat Pump, Ind. Eng. Chem. Res. 55 (2016) 11305–11314. https://doi.org/10.1021/acs.iecr.6b02824.

[140] Y. Liu, J. Zhai, L. Li, L. Sun, C. Zhai, Heat pump assisted reactive and azeotropic distillations in dividing wall columns, Chem. Eng. Process. Process Intensif. 95 (2015) 289–301. https://doi.org/10.1016/j.cep.2015.07.001.

[141] A. Giwa, Steady-state modeling of n-butyl acetate transesterification process using aspen plus: Conventional versus integrated, ARPN J. Eng. Appl. Sci. 7 (2012) 1555–1564.

[142] L. Shi, S.J. Wang, K. Huang, D.S.H. Wong, Y. Yuan, H. Chen, L. Zhang, S. Wang, Intensifying reactive dividing-wall distillation processes via vapor recompression heat pump, J. Taiwan Inst. Chem. Eng. 78 (2017) 8–19. https://doi.org/10.1016/j.jtice.2017.05.013.

[143] J.A. Weinfeld, S.A. Owens, R.B. Eldridge, Reactive dividing wall columns: A comprehensive review, Chem. Eng. Process. Process Intensif. 123 (2018) 20–33. https://doi.org/10.1016/j.cep.2017.10.019.

[144] M. Schröder, G. Fieg, Influence of Reaction System Properties on the Energy Saving Potential of the Reactive Dividing-Wall Column: Separation Properties, Chem. Eng. Technol. 39 (2016) 2265–2272. https://doi.org/10.1002/ceat.201600134.

Appendix-A

Batch reactive distillation:

A. Mathematical model for the BRD operation

A.1. Condenser System and Accumulator Tank: j=1

▪ Accumulator Tank Mass Balance:

$$\frac{dH_a}{dt} = L_D$$

▪ Component Mass Balance:

a) Distillate Accumulator:

$$H_a \frac{dx_{ai}}{dt} = L_D(x_{Di} - x_{ai})$$

b) Condenser Holdup Tank:

$$H_c \frac{dx_{ci}}{dt} = V_C y_2 - (V_C + \Delta n_1 H_c)x_{Di} + r_{1i}H_c$$

▪ Energy Balance:

$$0 = V_C H_2^V - (V_C + \Delta n_1 H_c)H_1^L - Q_c$$

▪ Physical Properties and other equations:

$$H_1^L = H_1^L(x_{D1}, T_1, P)$$

$$T_1 = T_1(x_{D1}, P)$$

$$r_{1j} = r_{1j}(k_e, x_{Di})$$

$$\Delta n_1 = \sum r_{1j}$$

$$L_1 = R(V_C + \Delta n_1 H_c)$$

$$L_D = (1 - R)(V_C + \Delta n_1 H_c)$$

A.2. Internal trays: j=2 to N−1

▪ Total Mass Balance:

$$0 = L_{j-1} + V_{j+1} - L_j - V_j + \Delta n_j H_j$$

▪ Component balance:

$$H_j \frac{dx_j}{dt} = L_{j-1}x_{j-1} + V_{j+1}y_{j+1} - L_j x_j - V_j y_j + H_j r_{ji}$$

▪ Energy balance:

$$0 = L_{j-1}H_{j-1}^L + V_{j+1}H_{j+1}^V - L_j H_j^L - V_j H_j^V$$

▪ Equilibrium:

$$K_{j,i} = \frac{y_{j,i}}{x_{j,i}}$$

- Summation

$$\sum y_{j,i} = 1$$

▪ Relations Defining Physical Properties and Chemical Reactions:

$$K_{j,i} = K_{j,i}(y_{j,i}, x_{j,i}, T_j, P)$$

$$H_{j,i}^L = H_{j,i}^L(x_{j,i}, T_j, P)$$

$$H_{j,i}^V = H_{j,i}^V(y_{j,i}, T_j, P)$$

$$r_{j,i} = r_{j,i}(k_e, x_{j,i})$$

$$\Delta n_j = \sum r_{j,i}$$

.A.3. Pot Tank: j=N

▪ Total Mass Balance:

$$\frac{dH_n}{dt} = L_{n-1} - V_n + \Delta n_n H_n$$

▪ Component Mass Balance:

$$H_n \frac{dx_n}{dt} = L_{n-1}(x_{n-1} - x_n) - V_n(y_n - x_n) + H_n r_n$$

Energy balance:

$$0 = L_{n-1}(H_{n-1}^{L} - H_{n}^{L}) - V_{n}(H_{n}^{V} - H_{n}^{L}) + Q_{r}$$

B.1. Mathematical model for the BRD operation

▪ Reflux Ratio:

$$R = \frac{L_L + L_S}{V_C}$$

5.7.B.2. Pot Tank: j=N

▪ Total Mass Balance:

$$\frac{dH_n}{dt} = L_{n-1} - V_n + L_S + \Delta n_s H_n$$

▪ Component Mass Balance:

$$H_n \frac{dx_n}{dt} = L_{n-1}(x_{n-1} - x_n) - V_n(y_n - x_n) + L_S(x_{Di} - x_n) + H_n r_n$$

- Energy balance

$$0 = L_{n-1}(H_{n-1}^{L} - H_{n}^{L}) - V_{n}(h_{n}^{V} - H_{n}^{L}) + L_S(H_{1}^{L} - H_{n}^{L}) + Q_{r}$$